WPI

Fire Protection Engineering Department
Worcester Polytechnic Institute

Turf House Fire Safety

Full WPI Report for Hurstwic

Fernando Ebensperger (Ph.D. candidate): febensperger@wpi.edu

Navya Muniraj (Ph.D. candidate): nmuniraj@wpi.edu

Abhinandan Singh (Ph.D. candidate): asingh4@wpi.edu

Rayna Vreeland (Ph.D. candidate): rlvreeland@wpi.edu

Christian Vogt (MS. student): cavogt@wpi.edu

Jon Zimak (Ph.D. candidate): jzimak@wpi.edu

Professor James Urban (Faculty Advisor): jurban@wpi.edu

August 1, 2025

Abstract

The tenability of Viking-age turf houses exposed to a historically sized bonfire outside the door was investigated across three scales. A single laboratory scale experiment was conducted, consisting of a replica door, roof structure, and 1.2 m simulated entryway. Five door scale experiments, consisting of a replica door and roof structure attached to a shipping container to simulate the volume of a turf house, were conducted at Eiríksstaðir in Búðardalur, Iceland. A single full-scale replica Viking-age turf house was also built in Iceland. Gas concentration and temperature measurements were made throughout the structures to identify the limits of tenability and fire spread. Heat flux gauges measured the intensity of the bonfire used to ignite the door and roof structures of the replica Viking-age turf houses. Results of this experimental archaeology study indicate that the Viking-age combat tactic of burning turf houses was an effective way of defeating a defender within their house. Comments based on observations and experimental findings are made on the use of fire as a war tactic, and recommendations are made for the protection of contemporary replica turf houses.

Contents

List of Figures

1 Introduction

Turf houses, traditionally used across various cultures and notably in Iceland, represent a unique architectural heritage adapted to environmental and resource constraints. These structures, celebrated for their ecological sensitivity and historical value, have persisted through the centuries. Historical references indicate that elements of these households were often ignited during conflicts. A full study is required to better understand this Viking-age war tactic as historical records indicate why turf houses were burned, but provide very few details on how. In parallel to this study, a contemporary fire safety analysis will be performed to assist in safely reintroducing these structures today.

In modern times, while the usage of turf houses has diminished, they continue to serve as tourist attractions, educational sites, and cultural preservation projects [1]. Modern versions of turf houses, available for rent, tend to be wooden cabins with a turf roof or restored traditional turf houses. However, the lack of modern protections and regulations raises concerns regarding their structural behavior and safety [2].

The fire protection perspective establishes that doorframes and hallways often become critical ignition points due to the proximity of thermally thin materials easily ignited by common sources such as human activities. Despite this recognized risk, no established standards currently guide firefighting strategies or safety protocols for these heritage structures, which could be catastrophic in the event of a fire [3]. To address this gap, our research includes experiments on six full-scale doors and a full-scale compartment to investigate fire spread and tenability within these structures. These tests aim to provide a deeper understanding of how fires develop and propagate in turf houses and to develop guidelines that can enhance their safety and viability as modern accommodations.

Fires pose a significant threat to historical structures and have the potential to cause irreversible damage. The cultural significance of these structures amplifies the importance of protecting them from fire. Previous research on understanding how fire spreads in historical structures typically adopts one or more of the following approaches: analysis of building materials' properties and behavior [4, 5], burning of scaled model structures [6, 7], and analysis of the current state of historical structures [8]. However, the majority of these studies focus on timber structures due to the inherent flammability of the material [9].

Results from previous studies on historical structures are not conclusive or generalizable due to significant differences between all historical structures, including geometry and materials used. Examples of this are the studies comparing the thermal behavior of modern and historical timber, where findings vary widely [4, 5]. For this study, scaled model analysis and current state evaluations of existing turf structures were considered.

1.1 Turf Houses

The detailed construction methods of Viking-Age Turf Houses in Iceland are still speculative [10]. Usually, the only thing that survives to be excavated are postholes, foundation

stones, firepit stones, and fragments of turf. Since Viking-Age structures have not survived intact over time, their reconstruction relies on modern-era turf houses, based on the assumption that they followed similar construction techniques, and the Sagas, which are written histories of the Viking-age culture.

Viking-age turf houses in Iceland, typically longhouses, were 5 m to 7 m across and 15 m to 75 m long and made of turf walls over a wood frame on a stone foundation [11–13]. The layout would include one large main room where most of the activities occurred and smaller partitioned areas at the ends of the structure for storage or other special purposes. These partitioned areas would not have full-length walls and were open at the top. A fire pit would be placed in the center of the main room, and an opening in the roof would be made to exhaust smoke. Combining the written version of the sagas and the archaeological finds implies that there would have been very few doors or windows made of translucent animal skins.

The houses used as living spaces were often cramped as large families lived together; however, that does not mean that the structures were necessarily small. Storage was frequently optimized by utilizing the space above the beams to store items such as tables and other furniture, which could be retrieved for meals. Consequently, this design is believed to result in a significantly high fuel load.

The frame of the structure would be made of wooden posts and thick wooden beams, and rafters [12, 13]. Smaller sticks would be laid on top of the frame and rafters to form a stick roof visible from the inside of the structure. These sticks separate the rafters and the turf roof to prevent rot. On top of the sticks and against the wood frame, layers of turf or dense bog materials would be stacked to form the outer weatherproof shell of the house. In most houses, wooden wainscoting would cover the walls to keep out the dampness. This wainscoting consisted of wooden boards set slightly away from the turf walls, creating an air gap. The air gap played a crucial role in moisture control by allowing air circulation, which helped to reduce condensation and prevent the turf from rotting over time [13–16].

A current example of turf houses is the Viking-age turf house reconstruction can be found at Eiríksstaðir, Iceland. This historical reproduction of Eiríkr Þorvaldsson,'s house, who was known as Erik the Red and the father of Leif Eiríksson, was built to the best known standard of Viking-age construction. Figure 1 depicts the finished interior of this structure. Figure 2 depicts sketches of the floor plan and elevation views of the structure.

(a) Interior roof **(b)** Finished interior

Figure 1: Photos of the turf house interior at Eiríksstaðir (Photos: William R. Short)

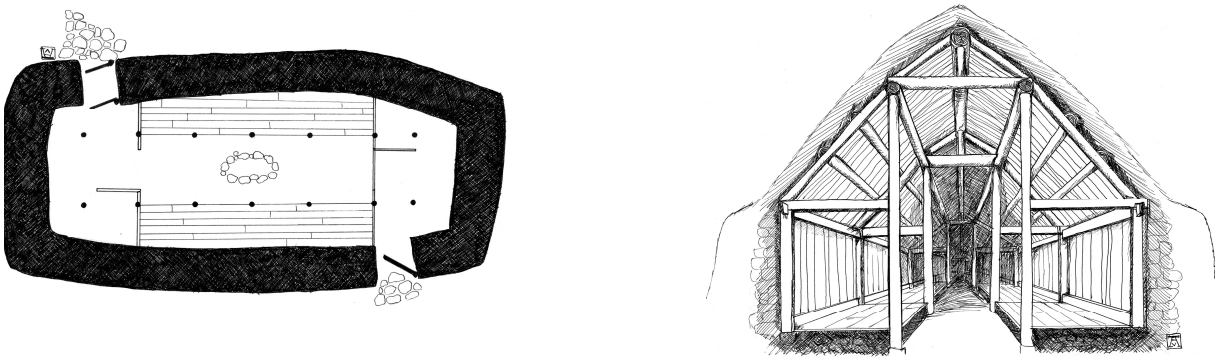

(a) Floor plan sketch

(b) Interior sketch

Figure 2: Floor and interior sketch of the turf house at Eiríksstaðir (Illustration: Andrew P. Volpe)

1.2 Viking-age Combat with Fire

Attacking a Viking in their home was a tactical choice often made to preserve combat power and mitigate losses of the attacking force [13]. One Viking could defend against a much larger attacking force if they were stationed at the door of the structure. Further, engaging in combat within the structure was highly difficult due to the weapons used and the construction of the structures. The interior was dark, and it would have been very hard to see, with many hiding places for defenders, obstacles, and the potential for shame in accidentally harming a non-combatant in the chaos. Current understanding suggests that turf houses were mostly fire-resistant from the outside, except for their wooden doors.

Historical records indicate that attackers would often light a bonfire at the base of the door, intending for the fire to ignite it and spread into the structure [13, 17–22]. Rather than burning houses indiscriminately, fires were set in a deliberate manner to control the damage and minimize unnecessary loss of life. Noncombatants were allowed to leave before or during the attack through the door. A negotiation between the attackers and defenders would typically occur, though the length of these negotiations is unknown [13]. While fire was used as a war tactic during the Viking-age, it was semi-regulated with rules and standards, as it was still forbidden in the honor code with harsh penalties [13, 23, 24]. Intentionally setting fire to a structure was regarded as a premeditated act and carried a harsher penalty [24]. Therefore, it is proposed that the bonfire would have been hastily made and ignited.

1.3 Fire Protection Practices for Historical Structures

Modern prescriptive standards for historic structures are sparse. The National Fire Protection Association (NFPA) has published standards 909 and 914 for cultural resources and historic structures, respectively [25, 26]. The International Existing Building Code (IEBC) also dedicates a chapter to building codes for historic buildings [27]. Additional resources and standards may be available depending on the region, the specific type of historic building, and local

preservation regulations. Local historic preservation officials may also impose specific standards [28]. The definition of a historic structure can vary widely between regions, cultures, and scales, complicating the use of codes for historic structures. Historic structures range from individual elements within buildings to entire towns, featuring diverse occupancies, construction types, and furnishings. Retrofitting historic structures to comply with modern codes may significantly impact or destroy the historic elements meant to be preserved. NFPA 909, NFPA 914, and IEBC Chapter 12 acknowledge the challenge of combining life safety and historic preservation by granting wide allowances to historic structures [29–31]. Ultimately, the authority having jurisdiction (AHJ) has the final approval. If compliance cannot be achieved through prescriptive elements, equivalent performance may be demonstrated through tailored fire safety concepts, such as limiting occupancy or providing fire safety training to staff.

1.4 Project Introduction

In January 2024, Dr. William R. Short of Hurstwic, LLC, an organization that researches Viking combat, approached the Worcester Polytechnic Institute (WPI) Fire Protection Engineering (FPE) Department to investigate the tenability for occupants of Viking-age turf houses intentionally set ablaze. This initiative led to a collaborative meeting in February 2024, marking the beginning of a partnership The team consisted of five Ph.D. students and one Master's student from the WPI FPE program: Fernando Ebensperger, Navya Muniraj, Abhinandan Singh, Rayna Vreeland, Christian Vogt, and Jon Zimak. The primary objective was to study the Viking-age combat technique of burning down a turf house door and to assess the tenability inside the turf house under these conditions. This report presents the fire dynamics and tenability findings derived from this collaboration.

The project was conducted in three main phases:

Phase 1: **Laboratory Experiments:** The first phase involved testing a standalone replica of a Viking-age door and door frame. This experiment was conducted at the WPI FPE Performance Laboratory on March 15, 2024. Data collected during this phase informed decisions about the instrumentation required for subsequent tests.

Phase 2: **Door-Scale Experiments in Iceland:** From July 2 to July 9, 2024, the WPI Hurstwic Team traveled alongside the Hurstwic Team to Iceland to perform five repeat experiments. These tests involved Viking-age replica doors, roof and frame structures attached to a shipping container, simulating a living space behind the door.

Phase 3: **Full-Scale House Testing:** The third phase included testing a full-scale replica of a Viking-age house entryway and the adjoining first room on July 7th, 2024, providing critical insights into the fire dynamics and tenability within a more realistic setup.

Hurstwic provided funding for the scientific equipment and construction materials needed to accomplish this work. The WPI Hurstwic Team took time away from their current studies and research to volunteer for this additional duty. WPI FPE program provided funding for transportation to and around Iceland for the WPI Hurstic Team. Hurstwic provided lodging

and the majority of the meals while in Iceland, with the balance supported by the WPI FPE laboratory.

A generalized view of the three scales can be observed in Fig. 3.

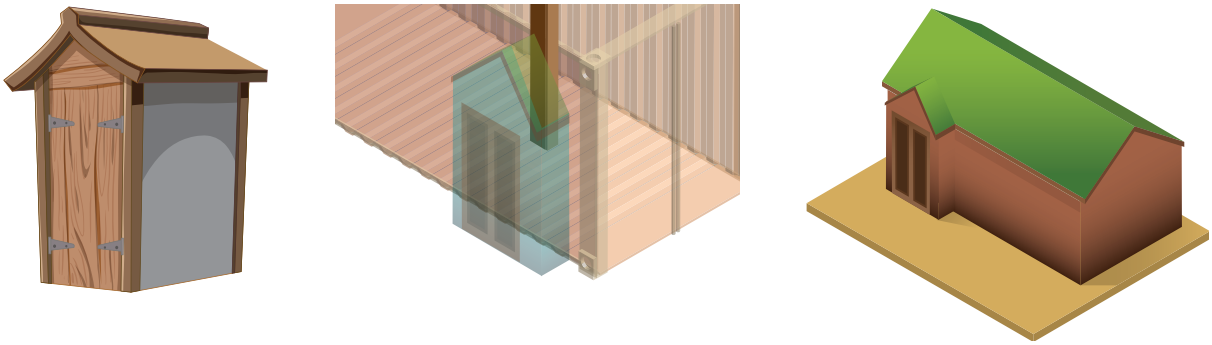

(a) Laboratory scale **(b) Door scale** **(c) Full scale**

Figure 3: Preliminary views of the scales

1.5 Project Summary

In general, the tenability of Viking-age turf houses exposed to a historically sized bonfire were investigated across three scales.

A single laboratory scale experiment consisting of a replica door, roof structure, and 1.2 m simulated entryway was conducted in the WPI Fire Protection Engineering Performance Laboratory. The bonfire was made by arranging bundles of pre-assembled branches. This preliminary test identified many valuable lessons and set the stage for the follow-on experiments conducted at Eiríksstaðir in Búðardalur, Iceland.

Five door scale experiments consisted of a replica door and roof structure attached to a shipping container, which simulated the volume of a turf house. These tests were conducted outside in Iceland using locally sourced materials. The dimensions of the door scale door and roof structure closely resembled the previous door scale. Bonfire sizes and intensity varied across experiments to understand the impact of bonfire size on the tenability outcomes.

A single full scale turf house replica was also conducted in Iceland. This Viking-age replica anddyri, a Norse equivalent of a mudroom, was constructed by the Hurstwic team over the course of one week. The internal structural members were made of logs with a diameter of 15 cm to 20 cm and the turf was laid in an overlapping, crosswise fashion with a thickness of about 1 m at the base. The dimensions of the turf house were similar to the interior volume of the container used for the door-scale experiments. This replica Viking-age structure was built to the best-known Viking-age construction standards and common practices.

In all scales, gas concentration and temperature measurements were made throughout the structure to identify the limit of tenability and the bonfire-style ignition intensity was measured with heat flux gauges.

Results of this experimental archaeology study indicate that the Viking-age combat tactic of burning turf houses was an effective way of defeating a defender within their house. Comments based on observations and experimental findings are made on the use of fire as a war tactic. Recommendations are made for protecting contemporary replica turf houses.

2 Project Definition

Given the novelty of the proposed fire safety measures and the lack of applicable fire protection standards, an abbreviated version of the SFPE Performance-Based Fire Protection design methodology was adopted, focusing specifically on protecting the structure from a fire threat, known as threat potential performance [32]. The SFPE Engineering Guide to Performance-Based Fire Protection defines performance-based design as:

> "An engineering approach to fire protection design based on
>
> 1. agreed-upon fire safety goals and objectives
> 2. deterministic and/or probabilistic analysis of fire scenarios
> 3. quantitative assessment of design alternatives against the fire safety goals and objectives using accepted engineering tools, methodologies, and performance criteria"

This methodology is used to guide the creation of the project scope through the design fires and experiments.

2.1 Scope, Goals, and Objectives

To simplify the experimental design and scope, only bonfire-style fires with locally sourced kindling ignited at the base of the doorway of Icelandic turf houses without suppression are considered. The structures are assumed to be empty with no furniture or wainscoting to simplify the test parameters. The use of extra materials in the structure to simulate additional fuel loads is also not considered. The only fuels included in the scope are the structural materials of the frame, roof assembly, stick layer between the frame and turf, the door, and turf.

The intent for the bonfire-style ignition of the structure is to recreate what Viking-age combatants may have done to ignite the door and roof assembly. The bonfire only used locally available sticks and branches. Historical firefighting methods such as using water, urine, or mysa, a sour whey, soaked animal skins are not considered to simplify the experimental scope [33–35]. The size of the bonfire is designed according to historical records and experimental needs.

The fire safety goals are:

- **Goal 1:** Occupant tenability
- **Goal 2:** Structural stability

The tenability goal can be further broken down into three objectives...

- **Objective 1.1:** Concerns the tenability based of thermal and atmospheric conditions for an occupant located within the hallway behind a closed door and directly relates to how Viking-age Icelanders would defend their livelihood.
- **Objective 1.2:** Concerns the atmospheric tenability of an occupant in the center of the structure, which represents an occupant sheltering within the turf house.
- **Objective 1.3:** is to characterize the fires rate of spread through the entryway and into the main enclosure.

All Goal 1 Objectives better seek to better understand historical accounts and quantify the available safe egress time.

Goal 2, structural stability, is comprised of two objectives.

- **Objective 2.1:** Partial collapse of the structure that does not prohibit the egress of occupants within the structure but renders the structure unsafe to enter.
- **Objective 2.2:** Total structural collapse defined as destruction to greater than 50% of the structure.

Partial or total structural collapse is further defined as visual observations of any gross movement in the organic structure as a result of fire damage that dislodges structural material. The movement of any structural components would also likely increase the ventilation and change the fire dynamics of the structure for the worse.

Adjacent to understanding the historical context, basic recommendations for protecting or responding to fires in turf houses will be made in support of the local fire department and for future testing based on the experimental observations and findings.

Three experimental designs are studied: a laboratory scale consisting of a door and roof structure, a field door scale consisting of a door and roof assembly connected to a closed shipping container, and a partial full-scale turf house. In each experiment, the construction methods and building materials are chosen based on the current understanding and interpretation of the specifications for Viking-age turf houses as found in historical sources. The variety of scales allows for an iterative study to best understand the fire dynamics factors at play when assessing tenability and structural integrity.

2.2 Performance Criteria

The tenability time is the time after ignition that the structure becomes untenable. The structure will be deemed untenable when at least one of the following criteria is reached [36, 37]:

- **Thermal Tenability: Radiation.** Compartment upper layer temperature reaches 200 °C, where the thermal radiation from the hot gases to the occupants reaches the tenability limit for exposure of skin to radiant heat.

- **Thermal Tenability: Convection.** Compartment gas temperatures at an occupant height reach 70 °C, which is the tenability limit for skin burns.
- **Incapacitation.** The fractional effective dose (FED) for incapacitation due to asphyxiation, (F_{IN}), reaches 1.
- **Structural Collapse.** Partial structural failure of any portion of the structure that prohibits the egress of occupants.

The F_{IN} was calculated using the method described by [36] using the following equations:

$$F_{\mathrm{IN}} = (F_{\mathrm{I_{CO}}} + F_{\mathrm{I_{CN}}} + F_{\mathrm{I_{NOx}}} + FLD_{\mathrm{irr}}) \times V_{\mathrm{CO_2}} + F_{\mathrm{I_O}} \tag{1}$$

Where $F_{\mathrm{I_{CO}}}$ is the fractional effective dose for incapacitation by carbon monoxide (CO) and is calculated as

$$F_{\mathrm{I_{CO}}} = 3.317 \times 10^{-5} \cdot [\%\mathrm{CO}]^{1.036} \frac{(V)(t)}{D} \tag{2}$$

Where [%CO] is the concentration of the species in (ppm), V is the volume of air breathed (25 lpm), t is time in minutes, and D is the exposure dose for incapacitation (taken to be a constant of 30% carbon monoxide in the blood expressed as percentage carboxyhemoglobin (COBH)) [36]. $F_{\mathrm{I_{CN}}}$ is the fractional effective dose for incapacitation by hydrogen cyanide (HCN). $F_{I_{NO_x}}$ are the fractional effective doses for incapacitation by nitrogen oxides (NOx). FLD_{irr} is the fractional lethal dose for irritants. $V_{\mathrm{CO_2}}$ is the multiplicative effect of inhaled carbon dioxide (CO_2) and is calculated through Eq. 3.

$$V_{\mathrm{CO_2}} = \exp\left(\frac{[\%\mathrm{CO_2}]}{5}\right) \tag{3}$$

$F_{\mathrm{I_O}}$ is the fractional effective dose for incapacitation by low-oxygen and is calculated through Eq. 4.

$$F_{\mathrm{I_O}} = \frac{t}{\exp\left(8.13 - 0.54 \cdot (20.9 - [\%\mathrm{O_2}])\right)} \tag{4}$$

The contribution of HCN, NOx, and irritants ($F_{\mathrm{I_{CN}}}$, $F_{\mathrm{I_{NOx}}}$, and FLD_{irr}) was neglected in this analysis due to difficulty in obtaining accurate measurements and the expected low generation of these trace gases from the burning organic materials.

The F_{IN} is calculated in 10-second increments, by inputting the average measured concentrations for each species during the time into Eqs. (1-4) and adding the result to the previous F_{IN} to capture the cumulative effects of the asphyxiants.

2.3 Fire and Ignition Scenarios

While it is known that the historical ignition of the structure was accomplished through a bonfire-style fire ignited at the structure door, little else is known about the fire's size or duration [13, 17–22]. The term bonfire-style is intended to represent a fire made of sticks and deadfall wood arranged in a semi-organized manner, see Figs. 13, 17, and 19a presented later in this report.

Much of what is known today comes from the translated Sagas, which only mention that combat with fire occurred, but not specifically how it was accomplished. From historical accounts, it is known that kindling and other combustibles were placed in front of the door and ignited. There would be a dialogue between occupants inside the turf house and those outside the house, and there would be an opportunity for occupants to leave through the door and fire to the outside. Additionally, occupants of the turf house look to utilize preplanned escape tunnels, which would require some effort to find, clear, transit, and exit through [13]. The time required to utilize the secondary escape is also not well-known or defined.

Because of the lack of clear details, several fire sizes were selected in order to provide a spectrum of possible fire threats. Additionally, the variety will help provide context for modern fire safety recommendations. All bonfire-style fires were made from locally sourced deadfall arranged in a manner that would promote fire growth and duration while also maximizing the speed of task completion. Care was taken to balance the hastiness required to replicate a war tactic with the careful execution needed for scientific repeatability.

3 Methodology

It was decided by the project sponsor, Hurstwic, that the structures for all the testing would have the same dimensions as the turf house at Eiríksstaðir, Iceland. This house was constructed based on a National Museum of Iceland archaeologist's report of a nearby turf house excavation and is thought to be a very typical, modest house from Viking-age Iceland. The report is available in Icelandic [38]. Many aspects of Viking construction methods remain unknown, requiring informed assumptions when reconstructing certain elements. One such example is door thickness, which was estimated using a combination of sources: a post-Viking-age church door from the National Museum of Icelands collection and Viking-age planks used for other purposes, gathered from various museums [10]. Additionally, experimental archaeology conducted by the Hurstwic team provided valuable insights that supported several design choices.

3.1 Experiment Locations

The laboratory scale experiment was conducted in the Performance Laboratory of the Department of Fire Protection Engineering at Worcester Polytechnic Institute in Worcester, Massachusetts. The door scale and full scale burns were conducted at Eiríksstaðir in Búðardalur, approximately 100 km north of Reykjavík, Iceland, (65°03'28.4"N 21°32'08.1"W). The experimental site was collocated with a historical reproduction of Eiríkr Þorvaldsson,'s house. This proximity to the historical reproduction house allowed the team to constantly confirm design or construction choices with the best historical evidence available.

The field experiments in Iceland were conducted on a dry portion of the river bed between two mountain ranges. The river provided easy containment of the fire and access to water if needed for suppression efforts. The mountain ranges restricted the wind to typically be either easterly or westerly. All experiments faced north to maximize viewing for the public and project sponsors, alongside improving repeatability. Further details regarding the experimental site are shown below in Fig. 4, which exhibits the relative location on the Iceland Geography, a zoom view of the specific location, and the location of the Historical Turf House and the Experimental Site.

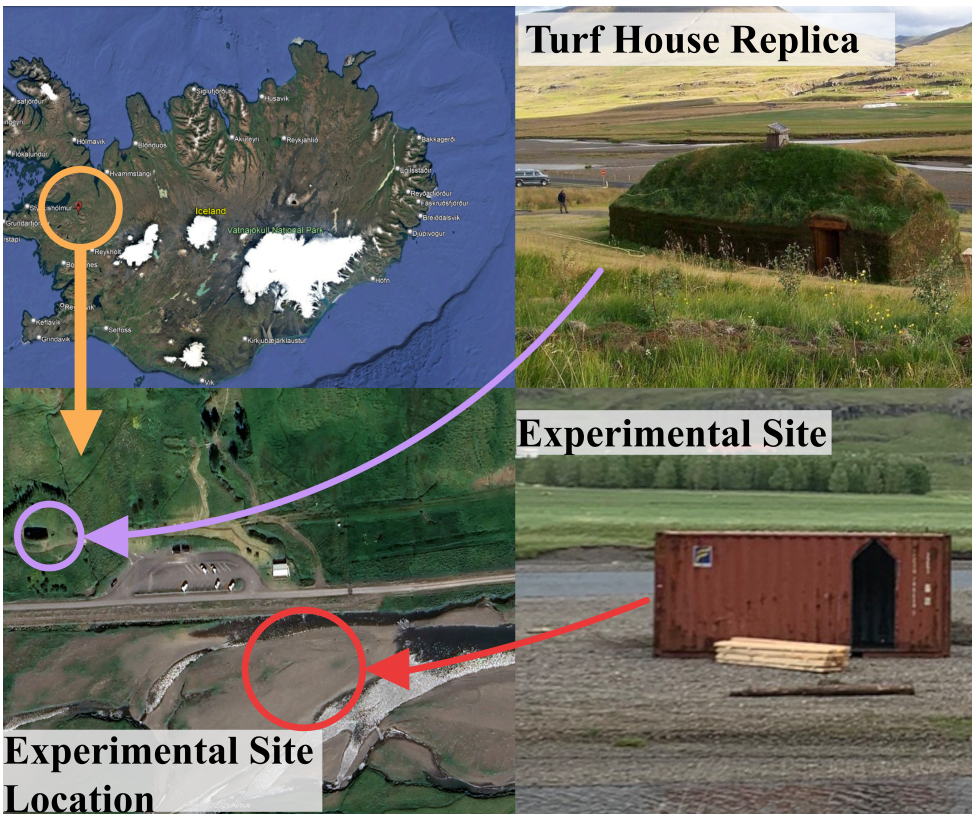

Figure 4: Experimental site

3.2 Instrumentation Overview

- **Heat Flux Gauges (HFG):** HFG's are instruments designed to measure the rate of heat transfer per unit area or heat flux. According to the model, it can be classified depending on the type of heat they measure and are referred to as either a total HFG (convective and radiative flux) or a radiative HFG. Shown below is a picture of a RHFG, Fig. 5b [39, 40].

(a) Radiative heat flux gauge

(b) Radiative heat flux gauge mounted on the stand

Figure 5: Radiative heat flux gauge instrumentation

- **Thermocouples (TC):** Temperature measurement devices that operate based on the Seebeck effect [41,42], which generates a voltage when two dissimilar metals that are joined at one end and exposed to a temperature difference between the joined end (hot junction) and the other end (cold junction). The voltage produced is proportional to the temperature difference, allowing accurate temperature readings. Thermocouples were pre-mounted onto metal wire meshes that could be easily screwed into the doors or roof members, as shown in Fig. 6.

Figure 6: Thermocouples preassembled on metal meshes mounted to the door

- **Gas Sensors:** Time-resolved oxygen concentration measurements were made with electrochemical oxygen sensors calibrated to have an average delay time of 4 ± 0.1 s with

7.6 m of 0.32 cm internal diameter tubing and a resolution of 0.1% O_2 by volume. The lengths of the tubing were increased depending on the experimental scale. Steel refrigeration tubing probes were used to sample the gasses near the fire or structure. The steel tubes terminated in a cool area and connected to polyvinyl chloride (PVC) tubing leading to the gas analyzers. A course particulate filter, HEPA filter, and desiccant tube were used to condition the sample before the sensor. Desiccant tubes were changed daily. CO, CO_2, and methane (CH_4) concentrations were made by infrared gas sensors with onboard temperature and pressure sensors for real-time concentration corrections. A single sampling probe used for O_2, CO, CO_2, and CH_4 with a water-fed chiller to further cool the sampled gases, depicted below in Fig. 7. While the sensor measures CH_4, this value approximates the amount of unburnt hydrocarbons (UHC) in the products of combustion.

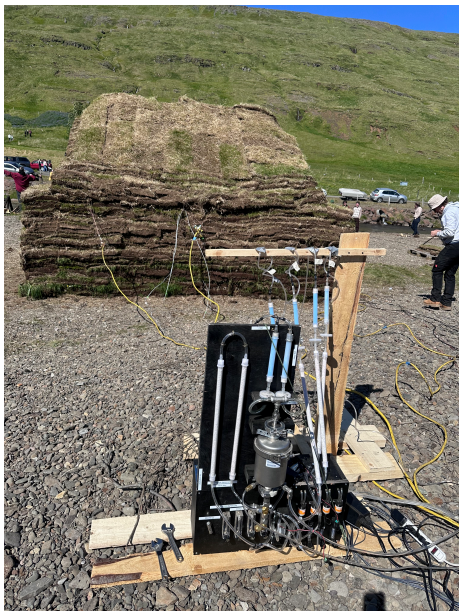

Figure 7: Gas sampling setup installed for the full scale test

- **Cool water supply:** Cooling water required for the heat flux gauges and the gas sampling chiller was provided by a submersible pump fed by locally sourced water from the nearby river, as shown in Fig. 8. The water was allowed to settle in a 15-gallon tub for 20 h before being used to remove any sediment. The system was set up in a closed loop and topped daily as needed.

Figure 8: Cooling water reservoir and pump system

3.3 Laboratory Scale

3.3.1 Experimental Setup

A single experiment with a Viking-age turf house door, roof section, and simulated corridor was conducted in the FPE Performance lab at WPI in Worcester, Massachusetts. The experimental setup for the laboratory scale fire was informed by literary sources and measurements from the example house at Eiríksstaðir. Due to constraints in cost and size, various simplifying assumptions were made. Since fire behavior inside the turf house was not the subject of study, it was decided to only construct the door frame and the adjacent corridor. It was assumed that for the relevant timescale, the turf walls, though prone to smoldering combustion, would not significantly contribute to the fire spread along the corridor. For this reason, the corridor walls were constructed of a 2x6 in whitewood stud frame and covered on the inside with 1.3 cm thick gypsum board.

The door was handcrafted from 30 mm Canadian Sitka, spruce, planks joined using hand-smithed iron nails and wooden pegs. The door was inset 1.3 cm into a handmade square frame made of 10.2 cm thick square cross-sectional beams, such that the backside of the door was flush with the back of the frame. Two wooden planks were attached to the back of the door horizontally to prevent the door slats from moving. The door was screwed into place on the corridor stands, flush with the door frame members as shown in Fig. 9 .

In addition to the fire spreading through the door, the fire propagation along the roof structure was of particular interest to this study. For this reason, the roof was framed using reclaimed eastern red cedar fence rails, with a diameter of about 15 cm. The frame was covered with small diameter sticks, approx 1 cm, that were arranged perpendicular to the joists and served as support for the turf mats used as roof shingles, as shown in Fig. 10a. In accordance with what is known about Viking-age construction, the structural members under the ceiling were left exposed. The roof frame was screwed directly into the top of the corridor studs. Four layers of overlapping locally sourced sod were used as a stand-in for turf.

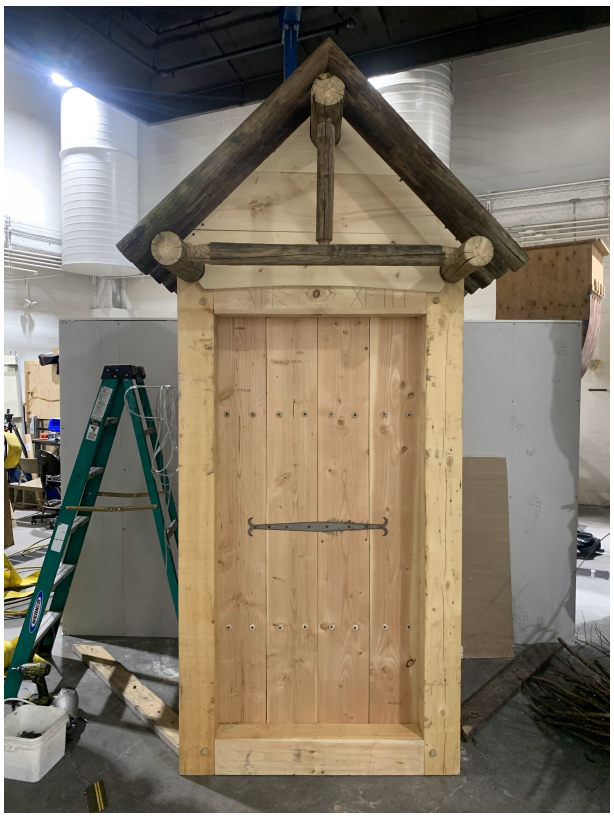

Figure 9: Lab scale door and roof assembly without turf

(a) Lab scale finished roof from below

(b) Lab scale roof beams from above

Figure 10: Lab scale roof structure

The gable above the door was framed with 1 cm wooden boards. The ceiling covered the length of the corridor and extended about 50 cm out from over the door and was finished with additional boards.

3.3.2 Instrumentation

The Lab scale door and roof were instrumented with thermocouples as shown in Fig. 12a. Thermocouples were affixed to the back side of the door and on the top side of the beams, but under the layer of sticks and turf. Oxygen sensors were located at the open back face of the assembly at various locations with the intent of measuring the oxygen concentration entering and exiting the doorway assembly, as shown in Figs. 11 and 12b.

Figure 11: Lab scale experimental setup with instrumentation from behind

The distribution of the instrumentation is observed in Fig. 12, in terms of the thermocouples, gas sensor cameras, and the dimensions of the setup. For the Fig. 12c note that EXFC stands for external front camera and HFGF for heat flux gauge front, both used to understand the radiative heat release rate of the flame; on the same figure Cam 0 and Cam 1 corresponds to the interior or ”sacrificial” cameras used to record the experiment from the inside.

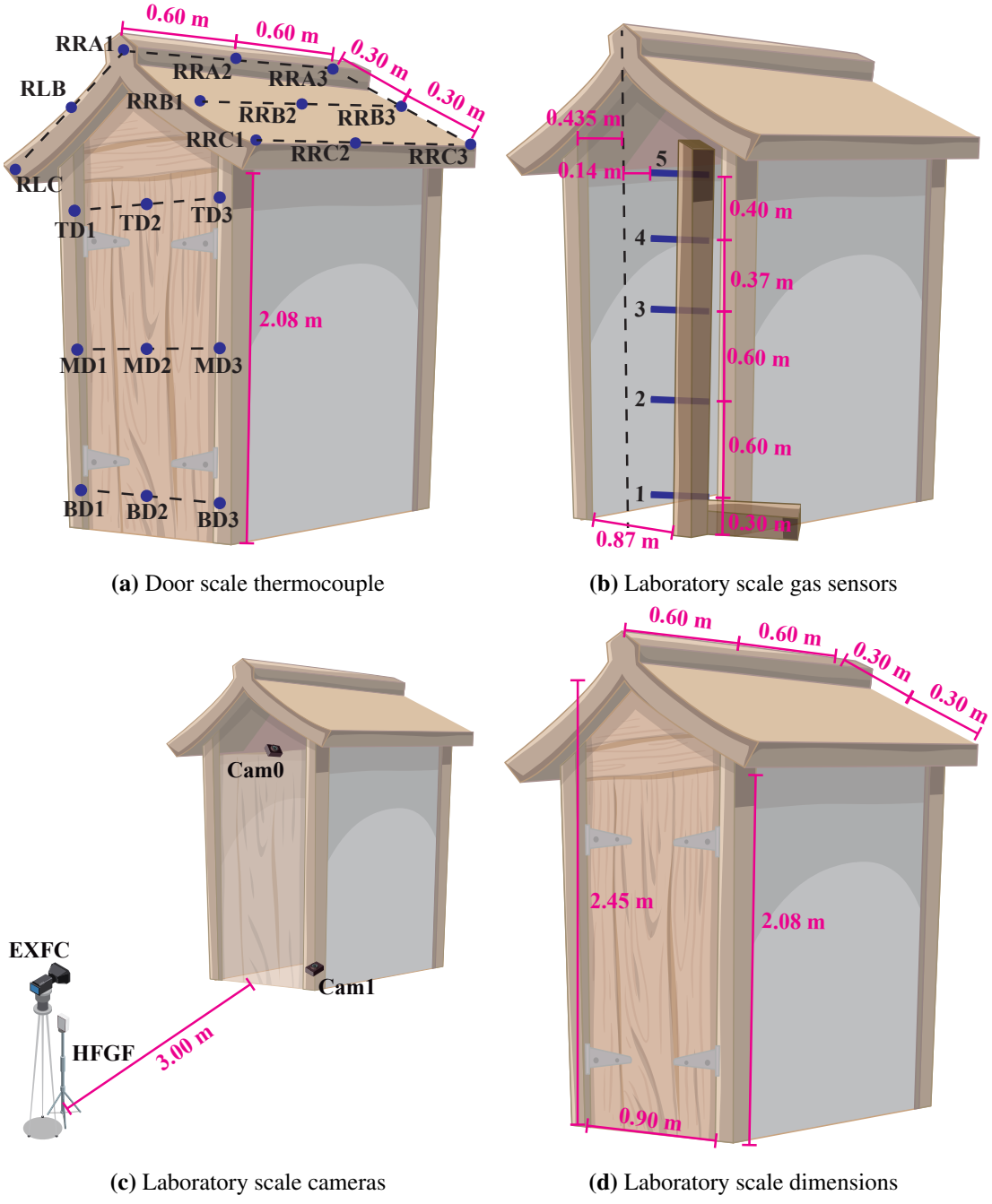

(a) Door scale thermocouple

(b) Laboratory scale gas sensors

(c) Laboratory scale cameras

(d) Laboratory scale dimensions

Figure 12: Instrumentation location laboratory scale

3.3.3 Ignition

For the laboratory-scale experiment, a bonfire was constructed on the outside of the door from locally sourced deadfall and sticks ranging in length from 70 to 150 cm, with diameters from 1 cm to 2.5 cm. This material was collected near Worcester, MA, and stored in a dry area. Without specific guidance as to how the Vikings would have ignited the door, the decision was made to arrange easily carried bundles of sticks against the door. Smaller diameter sticks or

kindling were used at the base of the bonfire, and larger diameter sticks were stacked on top as shown in Fig.13. The fire was ignited using a handful of organic fire-starting material placed at the base of the door by the lab director, wearing full personal protective equipment (PPE).

Figure 13: Lab scale bonfire ignition setup

3.3.4 Suppression

Once the fire had spread through the door and flames were extending out of the rear of the corridor, the lab director terminated the experiment. Sensitive Data Acquisition (DAQ) equipment was shut off to prevent water damage before the fire was extinguished using water delivered via a hand line. The turf mats from the roof were removed systematically, and the structure was wet down. The remains were left in place overnight to ensure any smoldering reaction was quenched.

3.4 Door Scale

The door-scale experiments had two main purposes. First, they served as repeat tests for the lab-scale experiment, conducted under more environmentally realistic conditions to better reflect full-scale scenarios while incorporating lessons learned from the lab-scale experiment. Second, they aimed to enhance the understanding of fire dynamics within the entryway, with a particular focus on assessing tenability within the large main room (see Fig. 1) of the turf house. This was achieved by attaching the door and roof assembly to a shipping container to emulate a compartment without the need to construct multiple full-scale structures. These experiments were conducted over three days on-site at Eiríksstaðir in Iceland.

3.4.1 Experimental Setup

The door scale experimental setup consisted of a replica door, a replica roof assembly, and a noncombustible entryway made by attaching gypsum boards on wooden studs. The entryway was secured to a shipping container, as shown in Fig. 14. During the lab-scale experiment, the door frame did not significantly contribute to the fire. Therefore, a non-combustible door frame was used in the door-scale experiments to conserve resources and achieve a short turnaround between experiments. The non-combustible door frame was constructed in a similar manner to the entryway, with wooden studs covered in gypsum board. This allowed for a quick change of the replica door and the replica roof assembly between experiments.

The door and fascia were made of 25 mm thick planks of Canadian Sitka, a type of spruce, which was sourced from the Icelandic Forest Service. Similar to the lab-scale experiment, the roof assembly consisted of numerous thin sticks attached to a frame of wooden logs of around 15 cm diameter. The turf was placed over the thin sticks. The outer edges of the door were screwed directly into the non-combustible frame, while the roof assembly was screwed to the entryway.

Figure 14: Door scale replica door and roof assembly attached to shipping container

The construction of the replica door and roof assembly for the door-scale experiments largely mirrored the lab-scale approach, but with changes based on the lab-scale experiment lessons learned and the visit to the longhouse replica at Eiríksstaðir. The soffit was shortened considerably to about 25 cm. This more closely matched the longhouse replica and prevented the soffit from redirecting much of the fire plume, as observed during the lab-scale experiment. While a longer soffit can be aesthetically pleasing, it can also lead to the redirection of the hot plume and cause a rapid flame intrusion, something the Vikings would have wanted to avoid. Additionally, any open spaces between the twigs or the gable and the turf roof were filled with turf offcuts. At the lab-scale, it had been observed that these gaps were the main avenue of flame intrusion.

It is unknown whether doing so is in line with historical practices. However, considering the cold temperatures in Iceland, it is plausible that any open spaces were filled with turf or other insulating materials to maintain comfortable temperatures for the occupants.

The main room of the longhouse acts as a compartment and can experience the accumulation of combustion products from the fire at the entryway. To allow for this accumulation, a shipping container of dimensions $2.4 \times 2.4 \times 3.9$ m^3 was used during the door-scale experiments. The door and roof assembly was attached to the shipping container by cutting a rectangular hole of size 2.3×0.9 m^2 into its side wall. A 0.30×0.28 m^2 opening was cut in the center of the container's ceiling to replicate the presence of a fireplace exhaust, consistent with the fireplace in the longhouse replica. In the first two door-scale experiments, this opening was left flush with the container's ceiling. However, this resulted in the combustion products being pushed back into the compartment. This was avoided in the subsequent experiments by building a chimney of height 0.1 m above the ceiling. The use of the chimney is speculated to be consistent with the Viking-age design. Throughout the experimental duration, the container doors were closed to maintain a fixed control volume and allow for the accumulation of the combustion products.

A total of five instrumented experiments were conducted. Two on July 5, 2024, two on July 6, 2024, and one on July 7, 2024. Between each burn, any damaged gypsum boards were replaced, a new roof assembly and door were installed, and all defective instruments were fixed.

An additional door-scale experiment was conducted on July 7, 2024, without instrumentation. The purpose of this burn was to investigate the feasibility of using goat skin soaked in mysa to extinguish and prevent fire intrusion through the door. For this burn, no roof was used in the entryway, and the container doors were left open. One person used the goat skin and a bucket of mysa to extinguish the fire on the inside of the door, while a group slowly added kindling to the fire on the outside of the door. A firefighter and a safety officer monitored conditions and terminated the experiment when smoke accumulated behind the door. No scientific measurements were taken during this experiment.

3.4.2 Instrumentation

A schematic of the instrumentation used during the door-scale experiments is shown in Fig. 15. Various thermocouples, gas sensors, and cameras were used to measure and observe the fire behavior. In Fig. 15c, EXFC stands for the external front camera, HFGF for the heat flux gauge front, EXFS for the external side camera, and HFGS for the heat flux gauge side. The cameras and the heat flux gauges were used to estimate the heat release rate of the bonfire during the experiment. In the same figure, Cam0 and Cam1 represent the "sacrificial" cameras that record the experiment from the inside.

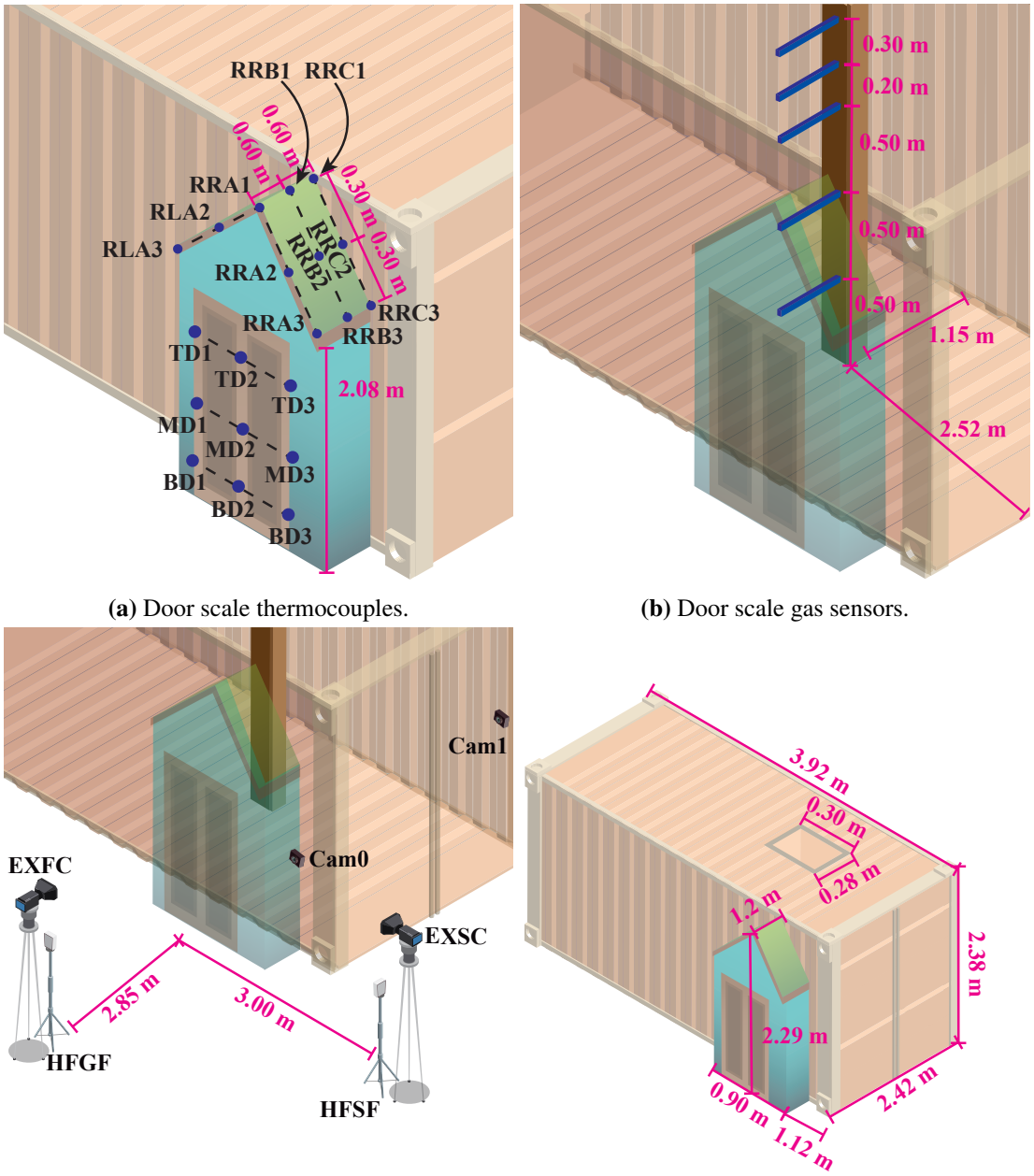

(a) Door scale thermocouples.

(b) Door scale gas sensors.

(c) Door scale cameras and HFGs.

(d) Door scale dimensions of the setup.

Figure 15: Instrumentation Location Laboratory Scale

3.4.3 Ignition

The wood sticks used in the bonfire for the door-scale experiments were provided by the local farmers and the Icelandic Forest Service. The bonfire was built in front of the door by the WPI Hurstwic team by creating a base of split logs to level the surface, keep the bonfire materials dry, and assist with heat retention. A small array of stacked sticks, referred to as a crib, was used to establish a sustained fire under windy conditions. Larger branches were bundled and stacked on top of the crib to provide the bulk of the fuel load. The branches ranged between

61 cm and 122 cm in length, with diameters between 0.5 cm to 6 cm. The logs used to build the base had diameters up to 20 cm and did not significantly contribute to the fire. Additionally, some off-cuts from the construction were added to the bonfire. Newspaper and locally sourced wood shavings were embedded in the crib and ignited using a gas lighter.

In the case of the first burn, the bonfire was constructed on a scale and confined by chicken wire to allow for mass loss measurements. Subsequent experiments were performed without the scale due to the loss of equipment from fire damage. In these burns, the fire was built on a mound of gravel in front of the door.

A wind block in the form of a plywood panel or stacked pallets was placed on the upwind side of the bonfire to shield it from the wind. This panel was removed once the fire was deemed able to sustain itself under the influence of the wind. If the wind caused a failed ignition of the bonfire, defined as a partial or full blow-off, the crib was reloaded with kindling and fire-starting materials and reignited. The ignition time referred to in this document refers to the last successful ignition.

Efforts were made to construct various bonfire sizes while minimizing the need for additional fuel. However, due to the fuel-controlled nature of the fires, additional kindling was periodically added during each burn.

3.4.4 Weather

On July 5, 2024, the weather for the nearest weather station in Búðardalur, within 20 km of the experimental site, was cloudy with a high of 8 °C and a low of 6 °C. Winds were generally NE at 1 to 3 m/s. On July 6, 2024, there were generally clear skies, a NE wind between 4 and 8 m/s, a high of 4 °C, and a low of 2 °C. Detailed wind measurements taken adjacent to the experiments are presented in Appendix A.

3.4.5 Suppression

Suppression was provided by the local fire department using a brush truck with a water tank. Once the burn coordinator determined the burn was complete, suppression efforts began. Typical experiments were called off once the bonfire burned through the available fuel or the door became thoroughly degraded.

The sensitive DAQ equipment was first shut off to prevent water damage. Following this, firefighters with PPE, including the Self-Contained Breathing Apparatus (SCBA), used hand lines to extinguish any externally visible fire. The firefighters were instructed to use water sparingly to ensure that there was as little water damage to the door frame as possible. Once the exterior fire had been extinguished, the compartment was opened and ventilated. The firefighters then entered the compartment and extinguished any fire found inside.

The turf on the roof was removed piece by piece using hand tools. Many of the mid-layer turf pieces that were removed were found to be smoldering. For this reason, any piece of turf that

was warm to the touch or appeared to be smoking was soaked in a nearby river. In some cases, the fire continued to burn behind the gypsum board along the entryway. In these cases, it was necessary to remove the gypsum board to fully extinguish the fire.

3.4.6 Overhaul

Once all of the fire was extinguished, overhaul efforts began to prepare the door frame for the next experiment. Any gypsum board found to have been damaged by fire or water was replaced to ensure that all exposed structural members were covered. Simultaneously, a roof frame was created on the ground. Once the frame was completed, it was hoisted onto the entryway walls, reattached with screws to the entryway studs, and covered with a layer of sticks and turf to complete the roof. Holes between the framing and the ceiling were stuffed with turf to form a seal. Once the roof was installed, the door was screwed into place from the inside. Finally, the instrumentation was reset and/or reinstalled. The thermocouples were placed on the door and corridor ceiling, while cameras, gas sensors, and the instrumentation tree were inspected for functionality. In cases where cables or wiring were exposed or at risk, they were buried below dirt or covered with turf. Upon completion of the overhaul, the next burn would be conducted.

3.5 Full Scale

3.5.1 Experimental Setup

The full-scale experiment took place on July 7, 2024, on-site at Eiríksstaðir and was conducted in a replica anddyri, the Viking-age equivalent of a mudroom. The turf structure was constructed by the Hurstwic team[1] over the course of the week, while the door scale burns were conducted. The turf was sourced from a local farm.

The internal structural members were made from Fir trees provided by the Icelandic Forest Service and consisted of logs with a diameter of $15 - 20$ cm, joined with metal hardware and nails. The use of metal hardware does not represent the construction practices of the Viking Age, but allows for a safe and efficient building process that does not affect the fire dynamics.

The structure's skeleton was assembled, and the turf was laid in an overlapping, crosswise fashion with a thickness of about 1 m at the base. Cables and tubing for instrumentation were placed through the walls as they were being constructed. A schematic of the full-scale setup is shown in Fig. 16a. The dimensions of the turf house were similar to the interior volume of the container used for the door-scale experiments. The construction of the full-scale roof was done similarly to the roofs for the door- and lab-scale experiments. It used thick joists topped with sticks and approximately 50 cm thick turf. A chimney opening to the interior volume of the structure was created at the center of the turf house's roof.

The entryway was incorporated into the North side of the structure with dimensions matching

[1] Comprised of experts in Viking-age history, experienced turf house builders, general construction experts, and local volunteers

those of the door-scale burns. The door was screwed into the wooden doorframe from the inside. The gable of the turf house was finished with wooden boards, and a small soffit extended beyond the door, adorned with a wooden panel inscribed with Viking runes. The door and fascia were made of 25 mm thick planks of Canadian Sitka, sourced from the Icelandic Forest Service.

3.5.2 Instrumentation

The distribution of the instrumentation and the dimensions of the structure are presented in Fig. 16. Like the door-scale experiments, thermocouples, gas sensors, and cameras were used for the full-scale. In Fig. 16c, EXFC stands for the external front camera, HFGF stands for the heat flux gauge front, EXFS stands for the external side camera, and HFGS stands for the heat flux gauge side. In the same figure, Cam2, Cam4, Cam6, and Cam8 correspond to the "sacrificial" cameras used to record the experiment from the inside.

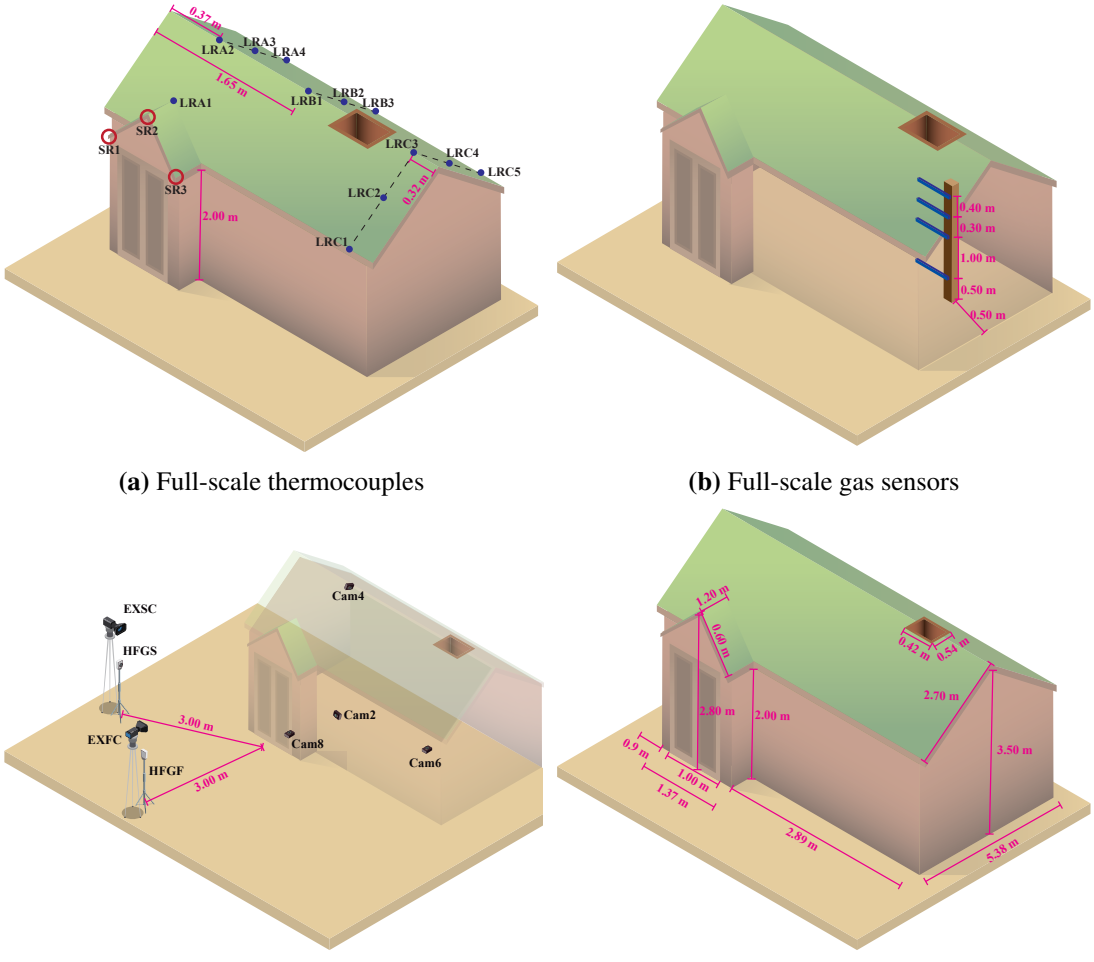

(a) Full-scale thermocouples

(b) Full-scale gas sensors

(c) Full-scale cameras

(d) Full-scale dimensions

Figure 16: Instrumentation location full scale

3.5.3 Ignition

The full-scale burn was ignited, similar to the door-scale burns, using a bonfire placed in front of the door. The fuel was locally sourced deadfall. A detailed depiction of the bonfire and its construction is shown in Fig. 17.

(a) Base layer and crib **(b)** Second layer **(c)** Top layer

Figure 17: Full scale bonfire construction

Since there was only one opportunity to conduct the full-scale experiment, extra care was taken to ensure there was enough fuel to sustain a fire for an extended period in case the structure began to collapse, and refueling the bonfire was no longer an option.

Ignition was achieved by striking a traditional fire-steel against flint and catching the resulting spark in a bed of wood shavings. Once the wood shaving bundle was ignited, it was placed into the bonfire.

3.5.4 Weather

On July 7, 2024, the weather for the nearest weather station in Búðardalur, within 20 km of the experimental site, was cloudy with a high of 12 °C and a low of 8 °C. Winds were generally NE at 4 to 8 mph. Detailed wind measurements taken adjacent to the experiments are presented in Appendix A.

3.5.5 Suppression

After burning for over two hours, the experiment was terminated, and suppression began. The first step was to shut down any sensitive DAQ systems, and then the fire department was cleared to extinguish the structure.

The fire department extinguished the structure using water from a tanker truck mixed with biodegradable class A foam concentrate (KnockDown Class A Foam Concentrate) using a compressed air foam system. Firefighters under full SCBA performed the initial fire attack with a

fog nozzle through the doorway. Due to concerns over structural integrity, firefighters did not mount an aggressive interior attack to knock down the fire in the turf house. Instead, the firefighters used a lance attachment for the fog nozzle to pierce through the turf walls of the structure to extinguish the fire in the interior. The use of foam in this situation was chosen to allow firefighters to train using the foam system rather than an operational necessity. Nonetheless, the foam proved to be an effective firefighting agent.

Once the bulk of the fire was extinguished, the roof of the turf house was torn down with hand tools to ensure all of the flammable structural members were extinguished. Despite the use of 8000 L of water (the capacity of the tanker truck), widespread smoldering combustion in the turf was still occurring. For this reason, most of the turf walls were disassembled by hand, and the pieces of turf were individually soaked. Nonetheless, some turf was still found to be smoldering the next morning, more than 15 hours after the fire.

The next day, some of the damaged remains of the instrumentation, such as several of the sacrificial cameras and some metal tubing from the gas sensors, were recovered for failure analysis.

4 Results and Discussion

Results for each of the three scales (laboratory, door, and full) are presented in this chapter, grouped by the type of result: qualitative, ignition of the structure and heat release rate (HRR) of the bonfire, flame spread within the structure, gas measurements within the structure, and tenability.

4.1 Qualitative Results

Qualitative results in this sub-section are derived mainly from the video cameras within and around the structure. These qualitative results are presented first to establish a foundation for understanding the test results by providing a physical understanding of the data collected, and are presented in later sub-sections. Tables showing the observed phenomena can be found in appendix C.

4.1.1 Laboratory Scale

The laboratory test was characterized by a very rapidly growing, intense, quick fire. Firebrands are observed entering the structure through the void spaces between the door and roof structure at 155 s after ignition and through the door slats at 191 s. Flame intrusion at the top of the door occurs at 198 s. Flames are observed to be sustained at the gable at 202 s, and the fire becomes sustained at the ceiling at 204 s. Heavy smoke exits the enclosure at 215 s, and a ceiling jet develops at 230 s. The fire spreads rapidly across the ceiling, and at 639 s the gable begins to degrade and vent the roof structure. The structure continues to deteriorate until suppression begins at 939 s.

The construction and assembly of the door, roof, and simulated entryway allowed hot gases from the bonfire to easily enter the roof assembly, which quickly ignited the stick layer and wooden beams. This flame intrusion led to rapid fire spread and a quick deterioration of the conditions within the entryway.

After suppression, the turf was removed carefully from the roof. The exterior layers of the turf were visibly burned and waterlogged, but deeper layers continued to smolder and reignite when exposed to ambient air.

The consensus was that the fire initially ignited the exterior roof overhang, propagated through the gable, and ignited the interior of the roof structure. Simultaneously, the bonfire ignited the exterior of the door, which thermally degraded the door and created gaps between the door boards. These gaps allowed for hot gases to enter the structure and ignite the rear of the door. Therefore, fire propagation into the structure can be thought of as a one-dimensional problem of the bonfire thermally degrading the door and gable material, which creates gaps for hot gases from the bonfire to enter the enclosure. These gases can ignite the underside of the roof structure and increase the concentration of the products of combustion within the structure. The fire can

then spread along the underside of the entryway roof to the main structure and ignite it. Both the products of combustion from the bonfire entering the structure through the gable and door gaps and the combustion products from the entryway roof fire decrease tenability.

The results of the laboratory-scale test led to several changes that were adapted for future testing.

- The overhang was shortened to minimize the collection of hot gases, which quickly ignited the gable and preceded the fire intrusion to the main structure. Gaps around the gable and roof overhang would allow an easy pathway for hot gases to enter the structure. While these gaps can be controlled slightly with tighter construction, reducing the collection of these gases will also reduce the ability for hot gasses to enter the structure. It should be noted that the original selection of the overhang length was speculative as dimensions are not defined in literary sources.
- Air pockets were sealed around the door, roof structure, and entryway structure with turf such that the main avenue for hot gases to enter the structure was through the gaps made from the thermal degradation of the door and gable.
- The door frame, which was not observed to contribute to the overall fire, was covered with a noncombustible layer of gypsum board at the door scale to mitigate the need to change the frame for each test. The frame was solid wood for the full-scale test.

4.1.2 Door Scale

Much of the fire damage to the door and roof structure was on the exterior North face, closest to the bonfire, as shown in Figs. 17-22.

Burn 1 of the door-scale experiments was characterized by significantly less fire intensity than the laboratory scale experiments. The bonfire outside the door was pushed by the wind, which reduced fire exposure to the ceiling. Nonetheless, some flame intrusion and fire spread were observed inside the corridor, though it was mostly intermittent in nature. First firebrands were visible inside the structure 547 s after ignition, and first flames appeared at 642 s. Sustained fire spread to the corridor ceiling was noted at 679 s, almost 13 minutes after ignition. 733 s into the experiment, the visibility inside the structure was reduced to a level that which no more fire behavior could be observed. The bonfire was tended to by placing a windscreen (974 s), compressing the fuel (1266 s), and adding more fuel (1293 and 1430 s). The fire was finally suppressed at 1878 s, about 32 minutes after ignition.

After suppression, the turf was removed from the roof. Several mats were smoldering and needed to be wet down further.

It is notable that the fire intensity and rate of spread deviated from what was seen in the laboratory scale experiment. There may be several reasons for this. The wind appeared to have a great effect on the fire's spread to the ceiling by reducing the chances of direct flame contact. Figure 18b shows that the right side of the door and roof shows more scorch marks than the left.

(The wind was blowing from left to right in this image, see Fig. 62a). The reduced overhang of the ceiling and the fact that many void spaces were filled in with turf reduced the avenues that facilitated rapid fire spread in the laboratory experiment. Finally, the fact that different wood and turf species were used for fuel and construction, with variations in moisture content, may have impacted the outcome of the experiments in a manner that is hard to quantify.

In order to compensate for the slower fire spread, a bonfire with a higher fuel load was used in subsequent tests.

(a) Start **(b)** End

Figure 18: Photos of door scale Burn 1

Burn 2 showed significantly faster fire spread than its predecessor. The interior cameras captured significant fire spread inside the corridor as well. The first firebrands could be seen entering the structure at 105 s. Shortly afterwards, at 117 s, the first flame contact of the gable was observed. Flame intrusion was seen through gaps in the door at 144 s. The interior ceiling finally ignites at 152 s, less than 2.5 minutes into the experiment. New fuel was added to the bonfire at 367 s. The smoke condition continues to deteriorate over the next minutes, making ceiling observations difficult by 510 s into the experiment. The experiment was terminated and the fire extinguished about 1000 s after ignition.

Post suppression, significant damage to the door was noted. The bottom of the door had burned through completely, and charring was noted in the exterior of the gable. Smoldering in the turf was also found.

While most of the environmental variables were similar to the first burn, fire intrusion was achieved notably faster. The consensus was that the primary factor for this was the increased initial fuel load of the bonfire. The larger fuel bundle shielded the incipient fire from the wind and led to higher flame heights, which consequently led to a greater flame impingement on the gable. It should be noted that while a significant smoke condition did develop inside the compartment for both the first and the second burn, the visibility was merely reduced, not eliminated entirely, in both cases. It was also observed on the interior camera that the wind blowing over the flat ventilation opening on the ceiling of the container contributed to the mixing

of the smoke layer by causing eddies.

Improvements for the future burns also focused on the bonfire, which was stacked more methodically to ensure that it contained a good mix of small kindling that would increase the fire size quickly, and large fuels that would keep the fire burning at a high intensity for longer.

(a) Start **(b)** End

Figure 19: Photos of door scale Burn 2

Burn 3 was the first burn that came close to emulating the results from the laboratory scale. This burn showed rapid fire spread inside the corridor and achieved blackout smoke conditions inside the compartment. The ignition of this fire was hampered by wind, requiring two ignition attempts. Post ignition, the fire was suppressed by the wind, necessitating the use of a windscreen which was placed at 232 s and removed at 273 s. The bonfire grew rapidly after the use of the windscreen, and the first firebrands were visible inside the structure at 300 s. The first flame intrusion and subsequent intermittent flame spread were noted at 351 s. This matches the external observations, which saw smoke emanating from the eaves at 478 s. Sustained fire spread in the ceiling was observed at 550 s, shortly after the bonfire was consolidated at 538 s. By 663 s, the fire in the corridor ceiling had spread away from the ceiling adjacent to the door and was extending into the corridor. A large amount of new fuel was added at 734 s, which was arranged with a shovel to be in contact with the door. Subsequent footage showed heavy fire in the gable at 856 s and a piece of turf falling from the roof at 909 s. Inside the compartment, a blackout smoke condition occurred at 961 s. More fuel was added at 1003 s. Further minor structural collapse was observed on the exterior cameras starting at 1259 s when a soffit panel and a turf mat fell from the roof within a minute of each other. At 1706 s, the interior cameras show that the corridor ceiling is fully involved. The fire was finally suppressed at 1979 s.

Post suppression, it was found that the door had burned through the gaps between the wooden boards. Furthermore, the bottom of the door had burned through completely. The gable had also burned through with significant charring in the structural members of the ceiling. There was widespread smoldering found in the lower layers of the turf, and most of the small branches that acted as supports for the turf had burned away.

This burn started off slowly due to difficulties with ignition, which were primarily caused by the intense wind that was blowing that day. (See Fig. 62c) However, once the fire had grown, the intensity of the fire behavior was notable. Again, the path of intrusion was observed to be via void spaces above the door, showing first firebrands, then intermittent fire spread before showing sustained spread along the ceiling. While previous burns had shown a significant smoke condition inside the structure, this burn was the first to have developed a true zero-visibility condition. Towards the end of this experiment, the smoke condition lightens, revealing heavy fire on the ceiling. This indicates that even while the ceiling was obscured by smoke, significant fire spread was still taking place. Furthermore, the lightning of the smoke condition indicates that the ventilation of the compartment improved, which may be a result of the collapse of roof components and the associated increase in ventilation that was seen several minutes prior.

Following this burn, we erected a wind break upwind of the door by leaning two pallets against each other. Furthermore, a makeshift chimney was constructed out of some scrap wood to shield the flat vent opening from the wind and reduce mixing of the gas layers in the compartment.

(a) Start **(b)** End

Figure 20: Photos of door scale Burn 3

Burn 4 showed many similarities to burn 3 and was also characterized by significant fire intensity inside the compartment. Ignition was facilitated with a windscreen, which was removed 24 s after ignition. The first firebrands in the structure were visible 45 s after ignition. Flames were in contact with the gable at 98 s, and the first flame intrusion in the ceiling was seen at 111 s. Sustained fire spread occurred at 176 s inside the corridor. The external gable and door were fully involved at 243 s, and occlusion of the ceiling inside the corridor by smoke occurred at 328 s, at which time the glow of flames was still visible. A zero visibility smoke condition occurred 507 s into the experiment, about 8 minutes and 20 seconds after ignition. The bonfire was consolidated with a shovel at 490 and 771 s. While the external footage showed that the fire intensity had dropped by 853 s, the fire inside the corridor appears to be severe, with a significant glow indicating a possible ceiling jet of flame extending beyond the corridor into

the container at around 994 s. Significant intensification of the fire inside the corridor occurred at 1014 s, and direct observation of a ceiling jet was possible. This jet burned out at 1056 s. Another moment of dramatic intensification of the fire inside the ceiling was seen at 1171 s with a piece of turf falling from the ceiling into the corridor at 1180 s. Six seconds later, at 1186 s, one of the interior cameras failed after prolonged exposure to elevated gas temperatures.

After the burn, the door showed similar damage patterns to the previous burns. The door had burned through on the bottom and in between the gaps of the boards. The gable showed significant charring and failure of the facade. Main structural members in the corridor ceiling were charred, while the smaller branches had burned through.

Burn 4 showed great similarities to the laboratory scale in terms of fire intensity, fire behavior, and the spread profile. This burn also allowed observation of phenomena that had not been observed in previous burns, such as the collapse of the turf from the underside of the ceiling, and the ceiling jet extending into the container.[2] Nonetheless, the burn also showed paths of fire intrusion that had been seen in previous burns.

Based on the results of Burn 4, it was the goal of Burn 5 to attempt a close replica of this burn.

(a) Start **(b)** End

Figure 21: Photos of door scale Burn 4

Burn 5 was very similar to the previous burn, although there were some differences in the environmental configuration, particularly the wind direction. Furthermore, due to the failure of one of the cameras, Burn 5 was conducted with only one interior camera. This burn was ignited using a traditional fire steel and flint, which was used to ignite a bundle of locally sourced tinder, which was then inserted into the bonfire. This also served as a practice run for the full-scale fire, which was ignited in the same manner. The fire progression was similar to the previous burns, with the first firebrands inside the structure being observed at 90 s after ignition. Shortly afterwards, the eaves experienced intermittent flame contact at 97 s. Fire intrusion into the ceiling was observed at 113 s. Unfortunately, the sunlight that was passing through the vent opening scattered off the smoke in the compartment, making further observations of the fire behavior in the corridor challenging; however, deterioration of the smoke condition was noted at 170 s. Smoke was observed leaving the compartment from under the eaves and gaps between the corridor and the container. True occlusion of the interior camera occurred at 398 s, although

[2] Although these phenomena may have occurred in other burns, obscured by smoke.

a glow was still visible through the smoke, indicating the presence of significant fire. The fire was consolidated with a shovel at 418 s, and new fuel was added at 566 s. By 462 s, there was a zero visibility smoke condition in the compartment. However, a glow and thermal damage artifacts in the camera indicated the presence of severe fire in the corridor. The fire was again rearranged and refueled at 1215 s and 1244, respectively. The camera footage ended at 1515 s, after which fire suppression began.

The damage pattern showed that the door had burned through at the bottom and in between the gaps of the boards. Likewise, the boards of the gable had almost burnt through completely. The structural members in the corridor ceiling showed significant char, and the branches that supported the turf had burned away.

This burn appears to have behaved fairly similarly to Burn 4 in terms of fire behavior and intensity, despite a completely different wind pattern. Unfortunately, the camera system inside the compartment was limited in the fire phenomena it was able to observe. Nonetheless, the footage gives indications as to what fire phenomena might have occurred. Verification of such phenomena may be possible using other instrumentation.

(a) Start **(b)** End with Turf removed

Figure 22: Photos of door scale Burn 5

Burn 6 did not contain any instrumentation and varied significantly in its configuration. It was characterized by a large bonfire that was refueled frequently. As the roof assembly was missing for safety reasons in this test, no comments can be made about the fire spread into the corridor. However, the fire soon began burning on the door and charred through a significant portion of it. The inside of the door remained relatively intact, due to the steady application of mysa.

Due to safety concerns, this burn was not able to recreate the same conditions as the other door-scale burns. Nonetheless, the burn allowed for an investigation into the efficacy of firefighting methods. It is difficult to say what impact firefighting efforts using a mysa-soaked goat skin could have had, especially in combating the intrusion of the products of combustion. However,

this experiment showed that it would be plausible that the occupants could have prevented the intrusion of fire through the door.

(a) Start **(b)** End

Figure 23: Photos of door scale Burn 6

Summary

Overall, the repetitions of the door-scale burns showed many similarities. In all burns, the basic sequence of fire intrusion (firebrands, intermittent flames, sustained fire spread, significant smoke, intense fire, and possible ceiling jet) occurred in the same order. The time of occurrence of these phenomena tended to be related to several factors, such as the prevailing wind and the size of the fire. Collapse of some elements was seen in Burns 3 and 4, both of which also showed a significant increase in fire intensity shortly before or after such a collapse.

It is the consensus that the reduction of the overhanging roof and the improved filling of void spaces appeared to have extended the time it took for the fire to move into the structure. It also appears that the presence of an enclosed volume, rather than an open back, as in the case of the laboratory scale, may have slowed the development of a flow path along the roof into the compartment. Such a flow path did develop once the fire had grown enough, as was observed in Burns 3 and 4. Finally, the development of a descending smoke layer and later complete blackout conditions was an aspect that was impossible to recreate in the laboratory scale environment.

4.1.3 Full Scale

The full scale burn can be divided into several characteristic stages, also commonly found in traditional compartment fires. The first is the incipient stage, beginning with ignition and ending with flashover. This stage is characterized by a growing fire, fire intrusion into the compartment, subsequent zero-visibility conditions, and initial fire spread to some of the structural members of the structure. In the full-scale experiment, this incipient stage lasted from 0 s (ignition) to 928 s, at which point a ceiling jet developed in the corridor ceiling, which extended into the compartment. The next stage was fully developed burning. This stage was characterized by fire burning both inside and outside of the structure, facilitated by self-ventilation and the burning of structural members themselves. This stage is followed by the decay stage, in which

fire intensity decreases as the available fuel is used up. Separating these stages is challenging because new fuel was added periodically, leading to periodic increases and decreases in fire intensity as the fuel was added and used up. Nonetheless, a clear separation can be made. The fully developed stage began with the first onset of the ceiling jet at 928 s and lasted through the first flashover at 2010 s. The decay phase was characterized by decreased fire intensity, only interrupted by the addition of new fuel, as well as decreasing structural integrity, as the supporting members lost their strength. This phase lasted from the end of the first flashover at 2010 s until fire suppression occurred. This phase saw minor collapses of members in the doorway, as well as a section of the ceiling that opened up, but no further structural collapse was noted. Notably, this phase also saw an incidence of flashover occur after a large bundle of fuel was added into the doorway. This occurred at 3758 s. Throughout the entire experiment, the fire was fuel-controlled. For this reason, certain compartment fire dynamics could not be observed, or only occurred after significant amounts of new fuel were added (e.g. Flashover).

Following the fire suppression, most of the turf had to be disassembled and soaked to ensure that it was completely extinguished. The structural members of the compartment, away from the corridor, appeared to have accumulated a char layer, but had retained most of their diameter in pristine condition below the char layer. One explanation for the lack of structural collapse, despite prolonged fire exposure, is the fact that the fire dried the turf, which subsequently reduced the load on the members.

In the incipient stage, the fire behavior in the full-scale burn mirrored the behavior that had been seen in the door-scale burns, particularly with respect to the fire intrusion pathway. In the later stages, the fire behavior highly depended on the bonfire. The fire intensity inside increased when fuel was added and decreased if the fire in the doorway had died down. One explanation for this was the fact that, besides the structural members of the turf hut itself, there was no further fuel (i.e. furniture) inside the structure. The presence of such contents would likely have led to a clearer delineation of the different stages, especially the fully developed and decay phases.

(a) Start **(b)** End

Figure 24: Photos of full-scale burn

4.2 Heat Release Rate of bonfire

The heat release rate (HRR) of a fire is defined as the rate of thermal energy released by a burning material. The total HRR can be divided into two components: convective HRR and

radiative HRR. It is based on the heat dissipation mode from the fire, which can be either convection, i.e., movement of hot gases, or radiation. In fire safety, HRR is a critical parameter, as it quantifies the intensity and growth of a fire. Therefore, to understand the fire risk posed by the bonfire, its HRR for each experiment was evaluated. The Radiative HRR is presented in this report. To translate the radiative HRR to a total HRR, a radiative fraction could be applied to the measurements.

4.2.1 Laboratory Scale

The radiative HRR of the bonfire was estimated from the incident radiative heat flux measured by the HFGF as shown in Fig. 12c. The incident radiative heat flux measurements ($\dot{q}''_{inc,\,s}$) were converted to radiative heat flux emitted by the flame ($\dot{q}''_{flame}$) by estimating a view factor between the flame and the heat flux gauge ($F_{fl \rightarrow HFGF}$):

$$\dot{q}''_{inc,\,s} = \dot{q}''_{flame} \times F_{fl \rightarrow HFGF} \tag{5}$$

For simplification, the bonfire flame was assumed to have a half-conical shape, and the length and diameter of the cone were acquired from image analysis of the video captured by EXFC. The view factor was calculated following the approach presented in Pinto et al. [43]. Once the emitted radiative heat flux was available, it was converted into radiative HRR by multiplying it with the flame area (A_{fl}):

$$\dot{Q}_{rad} = \dot{q}''_{flame} \times A_{fl} \tag{6}$$

In the lab-scale experiment, both total and radiative heat flux gauges were placed adjacent to each other, and the temporal variation in the heat flux measurements by the two gauges is shown in Fig. 25a. The radiative heat flux emitted by the flame is presented in Fig. 25b, which is around 100 times greater than the incident radiative heat flux measured by HFGF. Figure 25c shows the temporal variation of radiative HRR, which peaks at around 700 kW.

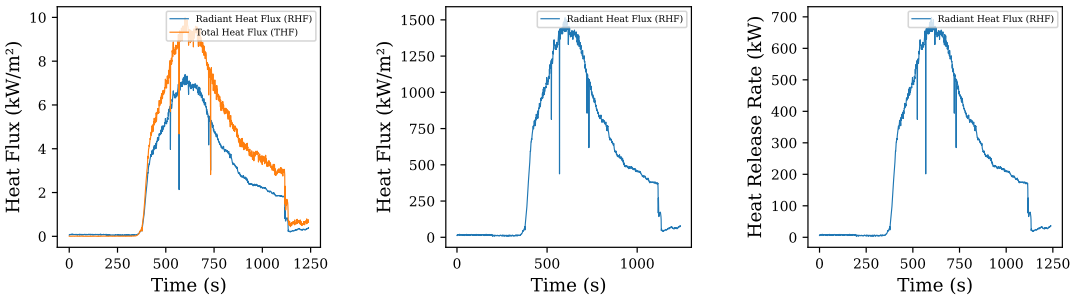

(a) Incident radiative heat flux measured by HFGF

(b) Radiative heat flux emitted by the bonfire

(c) Radiative heat release rate of the bonfire

Figure 25: Lab scale radiative heat results

4.2.2 Door Scale

For the door-scale experiments performed in Iceland, two radiative HFGs were used to measure the radiative heat flux, as shown in Fig. 15c. The temporal variation in the radiative heat flux measured by both the gauges for the five experiments is shown in Fig. 26. It is observed that the measurements from the two gauges are generally the same, with some misalignments due to the tilting of the flame under the wind. This suggested that either the side or the front HFGs could be used to estimate the flame HRR.

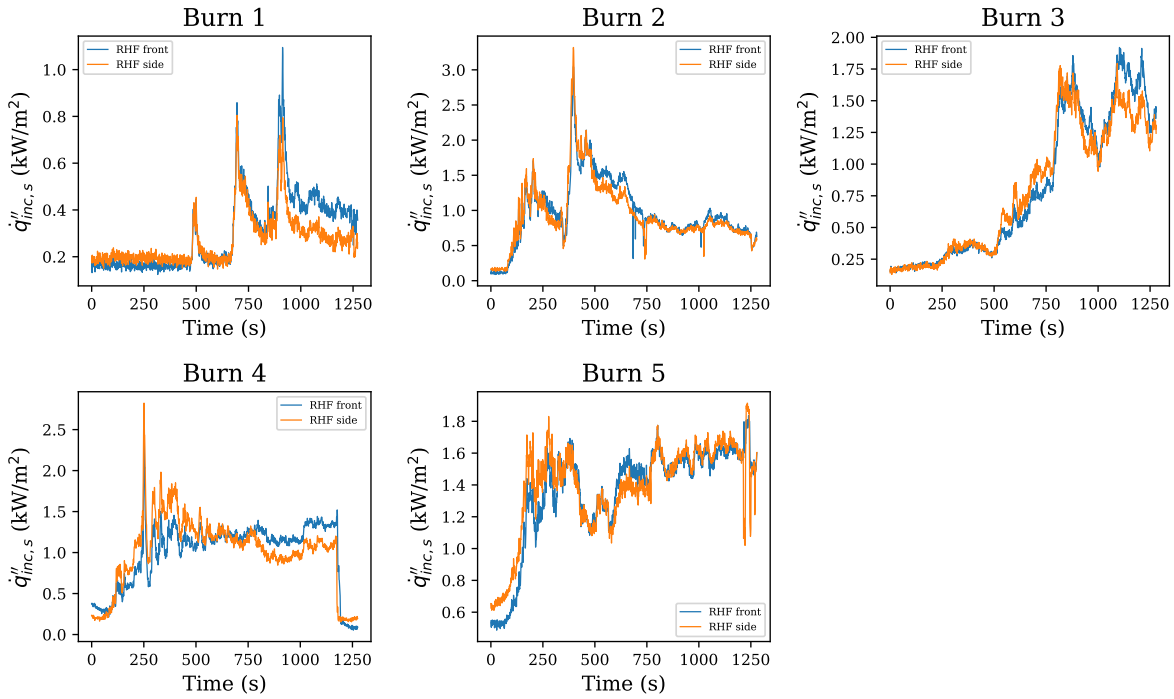

Figure 26: Temporal variation in the radiative heat flux measurements by side and front radiative heat flux gauges

The view factor calculations were carried out by assuming a half-cone geometry for the flame for both the front and side measurements. The flame geometry was measured using the videos acquired by the side and front cameras. The videos were acquired at 30 frames per second, but the flame geometry was measured for only 1 frame per minute. Based on the view factor calculations, the radiative heat flux emitted by the bonfire flame was evaluated and is presented for the 5 door-scale burns in Fig. 27. Generally, the emitted values were around 100 times greater than the measured radiation, except for Burn 5, where the emitted radiation was approximately 300 times the measured values.

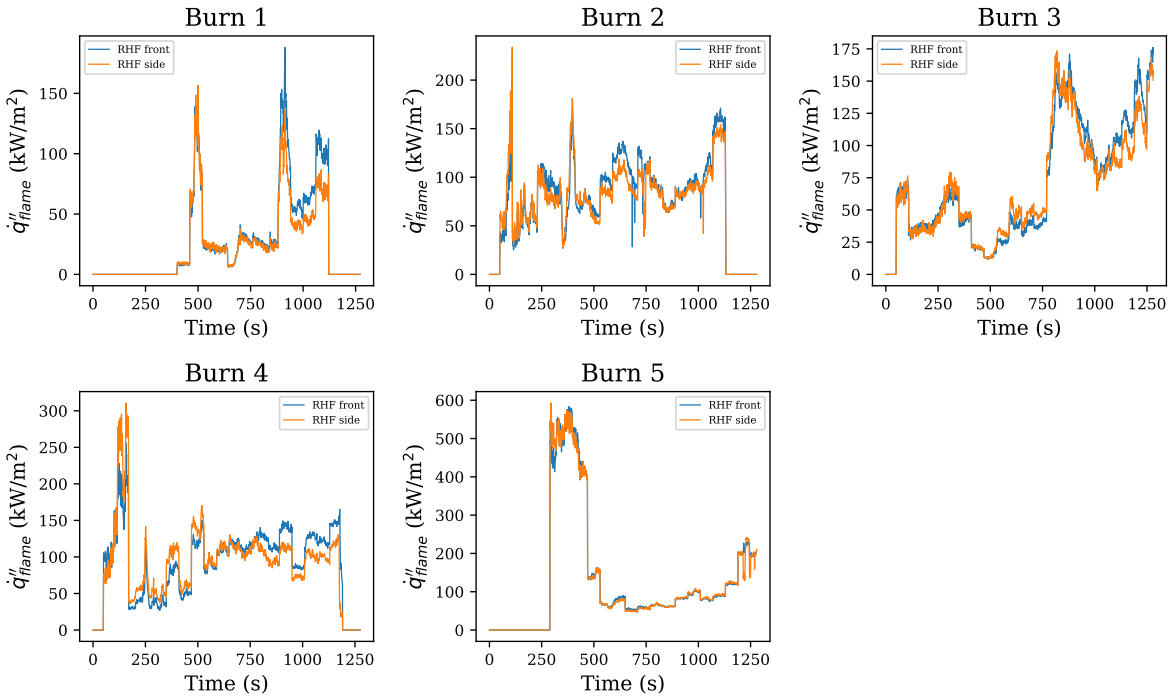

Figure 27: Temporal variation in the radiative heat flux emitted by the bonfire flame based on the side and front measurements

The emitted radiative heat flux values were converted to radiative HRR by multiplying the values by the flame area. These values are presented in Fig. 28. The different peaks present in the HRR plots occur due to the addition of kindling after the initial ignition.

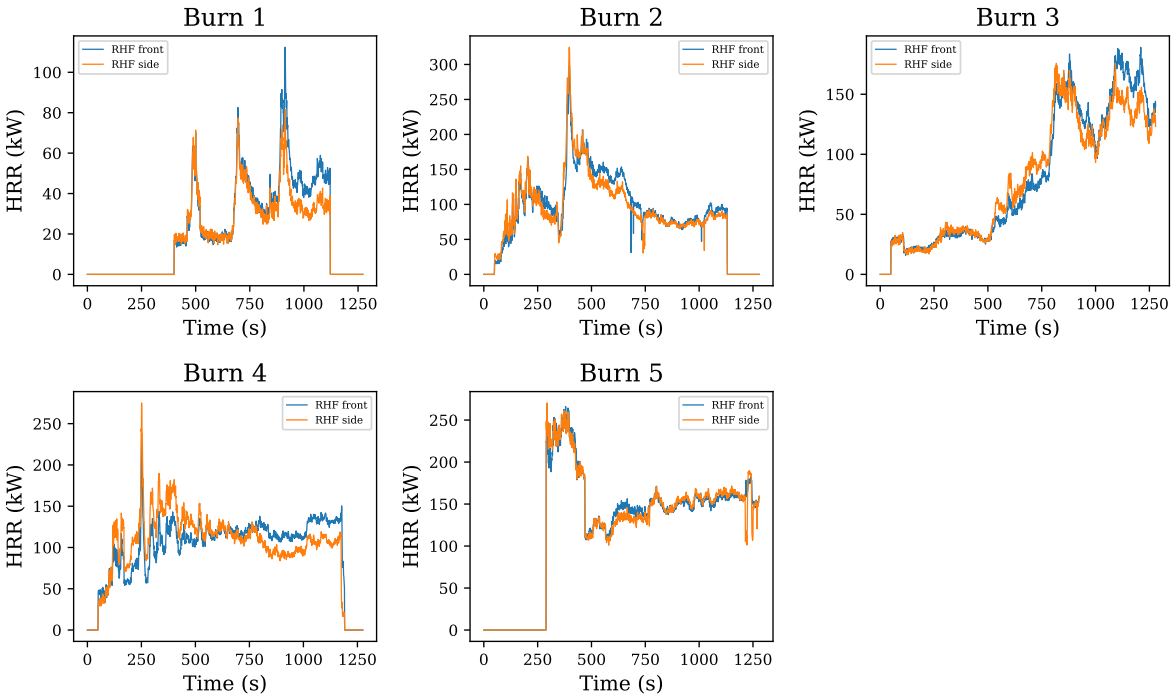

Figure 28: The radiative heat release rate of the bonfire for the 5 door-scale burns

4.2.3 Full Scale

The front and side radiative heat flux gauges were also used during the full-scale experiments. The same approach was used to calculate the radiative HRR for the bonfire. The incident radiative heat flux, the radiative heat flux emitted by the flame, and the radiative HRR are presented in Fig. 29. Similar to previous cases, the emitted radiation is around 100 times greater than the heat flux measured by the gauges. The heat flux measurements show sudden reductions due to the obstruction caused by the presence of authorized personnel moving to either add kindling to the bonfire or investigate the structural integrity of the turf house. The radiative HRR of the bonfire remained higher than 100 kW, with a peak value of greater than 300 kW.

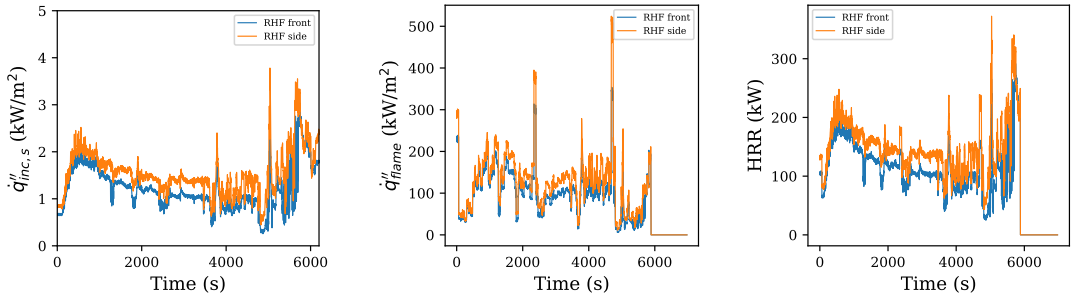

(a) Incident radiative heat flux measurements **(b)** Radiative heat flux emitted by the bonfire **(c)** Radiative heat release rate of the bonfire

Figure 29: Full scale radiative heat results from front and side heat flux gauges

4.3 Flame spread

The bonfire was ignited outside the door to evaluate the door's resistance to flame penetration. The temperature on the opposite side of the door was measured using an array of thermocouples, and a reference temperature of 300 °C was used as the criterion for determining flame penetration. The thermocouple array provided a comprehensive assessment of the door's thermal performance and potential failure points. The door was instrumented only for the laboratory and the door scale experiments.

4.3.1 Laboratory Scale

The severity and the corresponding risk associated with a fire can be understood by estimating its rate of spread. For a turf house exposed to a bonfire at its doorway, the flame can spread either through the door or it can ignite the roof and then spread along it. The thermocouples were placed on the roof and the door to capture the initiation of the fire inside the entryway. The temporal and spatial variation of temperature (in °C) at the overhang of the roof is presented in Fig. 30. The flame enters the roof at the TC 2 location and engulfs the overhang, with the flame stabilizing faster in the middle, which appears to lead to higher fuel consumption as the temperature reduces quickly along the middle. The flame spreads to the roof around 200 s after the bonfire ignition. In comparison, the thermocouples placed on the door observe the flame around 330 s after the roof. Only the top thermocouples of the door experience the flame, while the temperature of the thermocouples in the middle and the bottom of the door never exceeds 150 °C. This suggests that the flame ignites the roof and spreads along it, while the door only experiences charring on the outside and spreads on the inside because of the flames moving from the roof to the door.

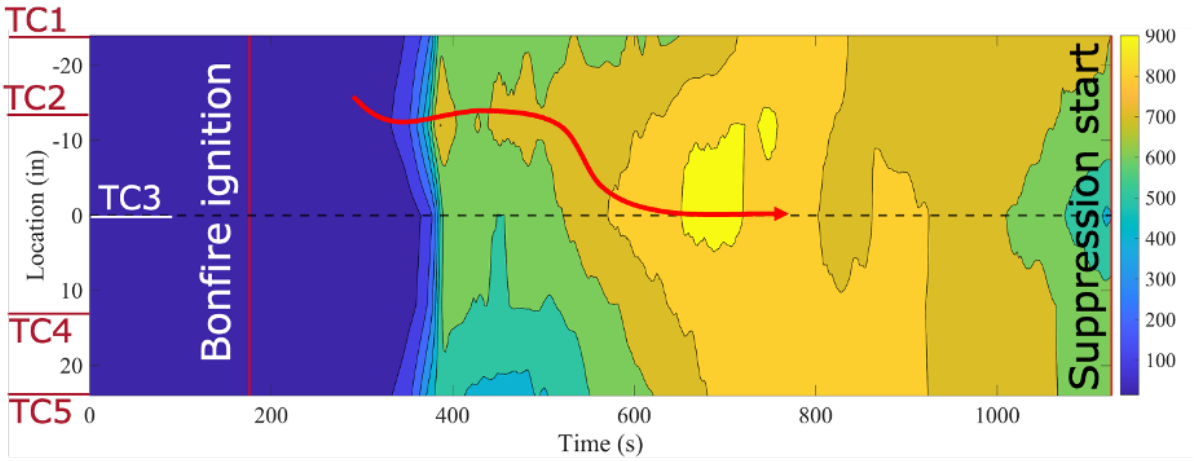

Figure 30: Temporal variation of temperature at the start of the roof

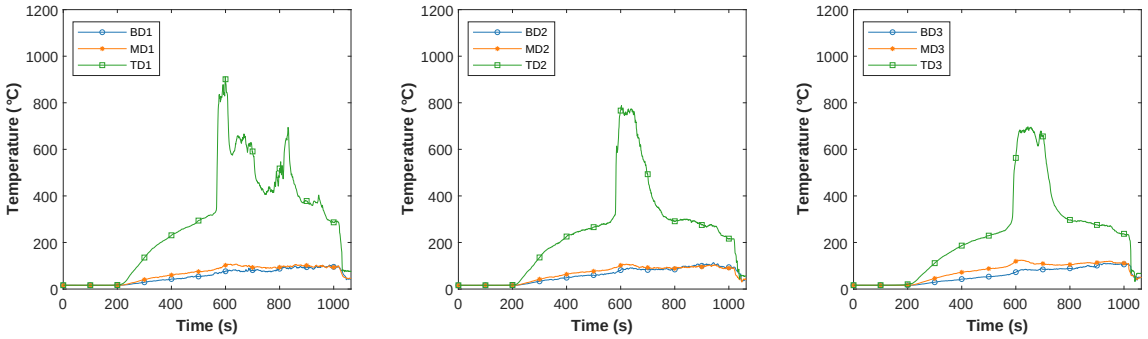

(a) Left **(b)** Center **(c)** Right

Figure 31: Temperature profiles along the inside of the door for the lab scale experiment

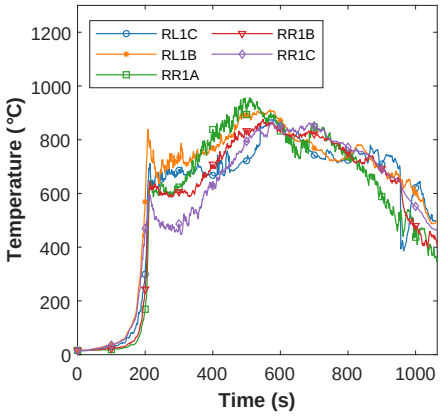

Figure 32: Temperature variation at the front of the roof for Lab scale

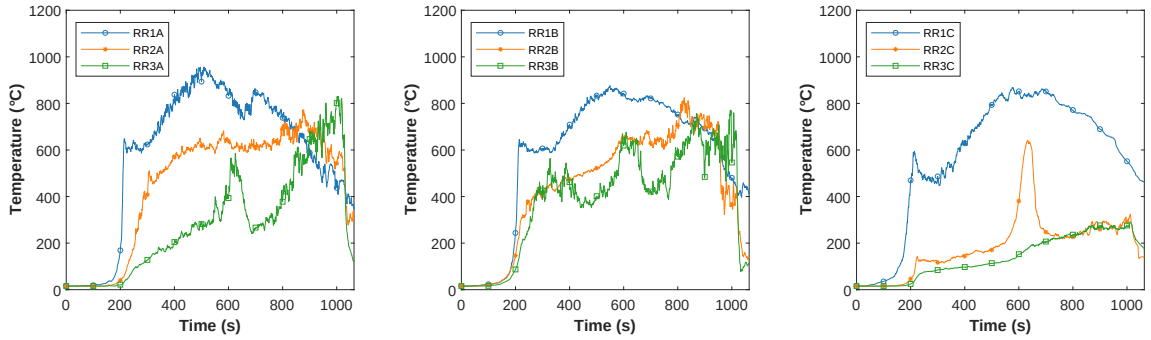

(a) Crest **(b)** Middle **(c)** Edge

Figure 33: Temperature profiles along the roof for Lab scale

Since the flame spreads along the roof, the rate of spread can be quantified using the thermocouples placed along the length of the roof. Out of the nine thermocouples on one side of the roof, only six were inside the entryway, while the remaining three were outside. The flame spread rate is calculated by finding the time of ignition at different thermocouple locations and using the distance between these thermocouples. The reference temperature of $300\,^{\circ}\mathrm{C}$ is used to evaluate the time of ignition. This temperature falls in the range of vegetation pyrolysis temperature $280-350\,^{\circ}\mathrm{C}$ and can be assumed to correspond to its ignition temperature [44]. The fire spread rate along the middle of the roof (i.e., along the TC 3 location in Fig. 30) is slower than the fire spread rate along the TC 4 location. Moreover, the rate of spread decreases as the flame moves along the roof. This reduction is higher for the TC 3 location (74%) than the TC 4 location (57%). The primary reason behind this reduction is the reduced influence of the bonfire. For the initial spread, the bonfire interacts with the fire in the roof and assists its spread to the next thermocouple 61 cm away from the overhang. Since the roof was completely engulfed in the fire, suppression was initiated before the fire could propagate through the door.

4.3.2 Door Scale

The temperature measurements and flame spread behavior of the five door-scale experiments are presented and discussed here.

- **Burn 1:** The temperature measurements at the door are presented in Fig. 34, and the values remained below the ignition temperature throughout the experiment. The low temperature indicates that the door did not fail. However, some high values with a peak close to $200\,^{\circ}\mathrm{C}$ were present for the bottom thermocouple at the center of the door. This occurred because of some flame penetration through the gaps present in the door. This penetration was not enough to ignite the door or cause failure.

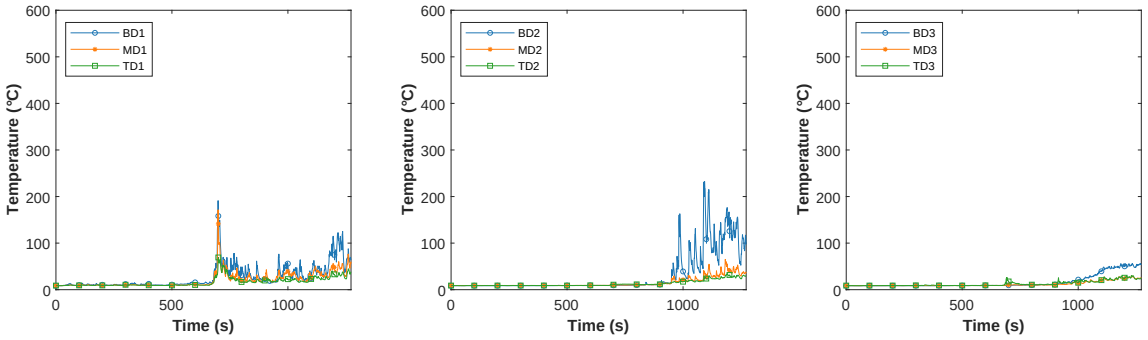

(a) Left **(b)** Center **(c)** Right

Figure 34: Temperature profiles along the inside of the door for Burn 1

The temperature measurements at the front of the roof and along the roof are presented in Figs. 35 and 36, respectively. Temperatures exceeding ignition were observed at the front and center of the roof (RLB, RR1B, and RR1A). These high temperatures existed briefly and did not lead to a sustained flame presence. These temperature peaks occurred because of the bonfire's impingement on the front of the roof. The temperature peaks correspond to the peaks in the measured radiative heat flux Fig. 26. A higher peak heat flux occurs at around 900 s but causes a lower temperature increase at the roof due to the wind, which tilts the flame away from the center. The flame did not spread past the front of the roof.

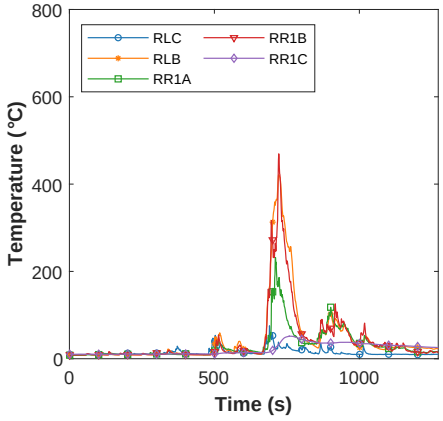

Figure 35: Temperature variation at the front of the roof for Burn 1

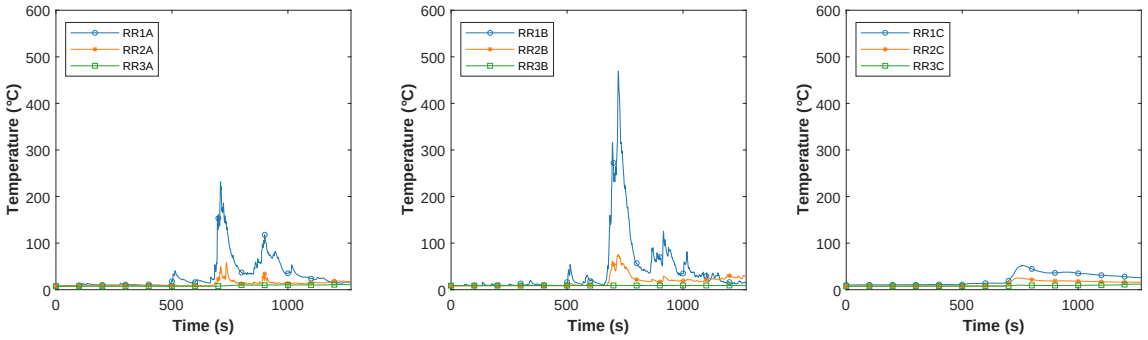

(a) Crest **(b)** Middle **(c)** Edge

Figure 36: Temperature profiles along the roof for Burn 1

- **Burn 2:** The door temperature is shown in Fig. 37, and it was intermittently higher than the ignition temperature at the bottom measurement location. This meant that the flame penetrated the door at the bottom while the door did not fail at any higher location as the temperature remained lower than the ignition temperature.

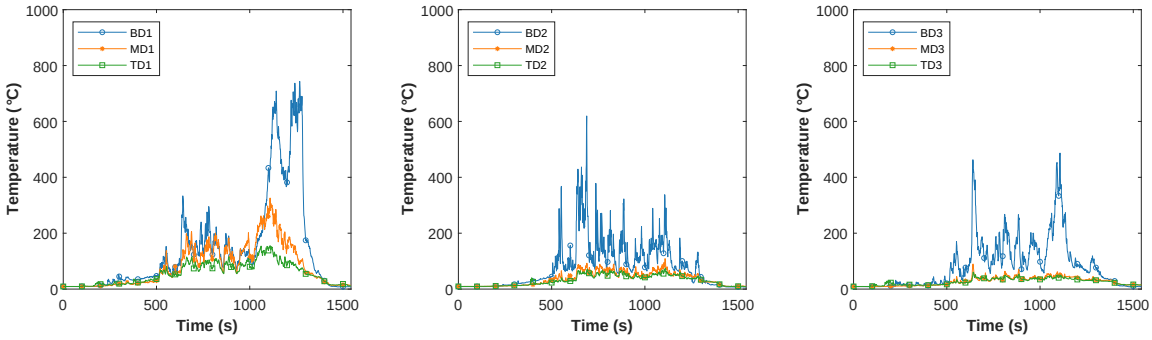

(a) Left **(b)** Center **(c)** Right

Figure 37: Temperature profiles along the inside of the door for Burn 2

Similar to Burn 1, high temperatures were observed at the front and center of the roof, particularly at RLB and RR1B locations, as shown in Fig. 38. Fig. 39 shows the temperature variation at various locations on the roof. No definitive flame spread was observed along the roof from the temperature measurements.

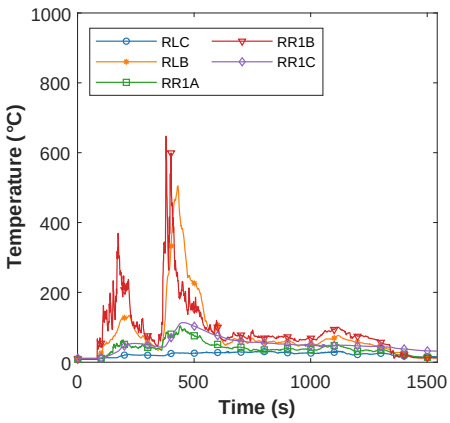

Figure 38: Temperature variation at the front of the roof for Burn 2

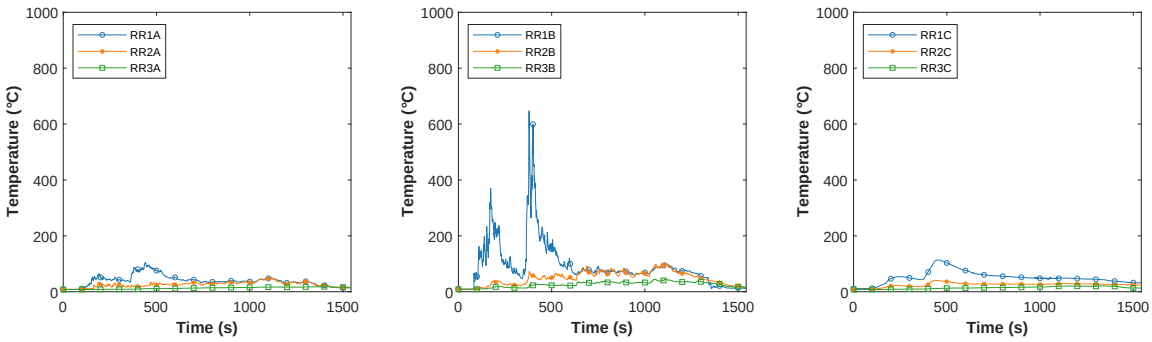

(a) Crest **(b)** Middle **(c)** Edge

Figure 39: Temperature profiles along the roof for Burn 2

- **Burn 3:** The temperature along the door is presented in Fig. 40. In this case, flame penetration is observed in the bottom and the middle. It is non-uniform as only two thermocouples (MD1 and BD3) record a temperature greater than ignition, and these thermocouples are located on the two edges of the door.

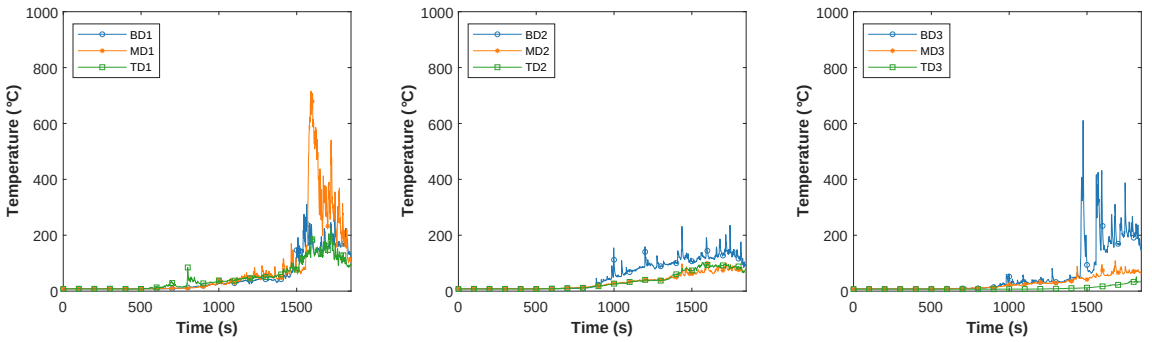

(a) Left **(b)** Center **(c)** Right

Figure 40: Temperature profiles along the inside of the door for Burn 3

In contrast to Burns 1 and 2, flame spread was observed along the roof in this burn. It is observed from Fig. 41 that a stable flame presence occurred at the front of the roof with faster ignition close to the edges, i.e., thermocouples along rows B and C. In addition, flame spread from column 1 to column 2 along the roof, but no ignition was observed along column 3, which was the closest to the container. The roof ignition occurred because of the sustained heat release from the bonfire in Burn 3 (as shown in Fig. 28) compared to the other burns, where the HRR decreased before ignition could occur.

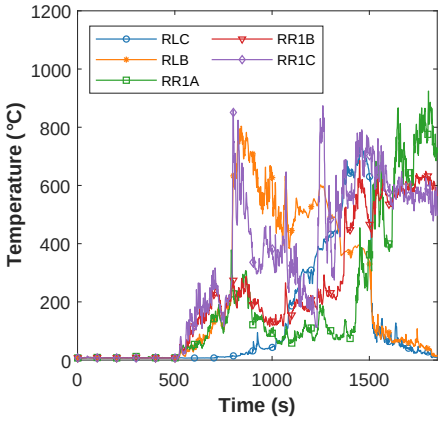

Figure 41: Temperature variation at the front of the roof for Burn 3

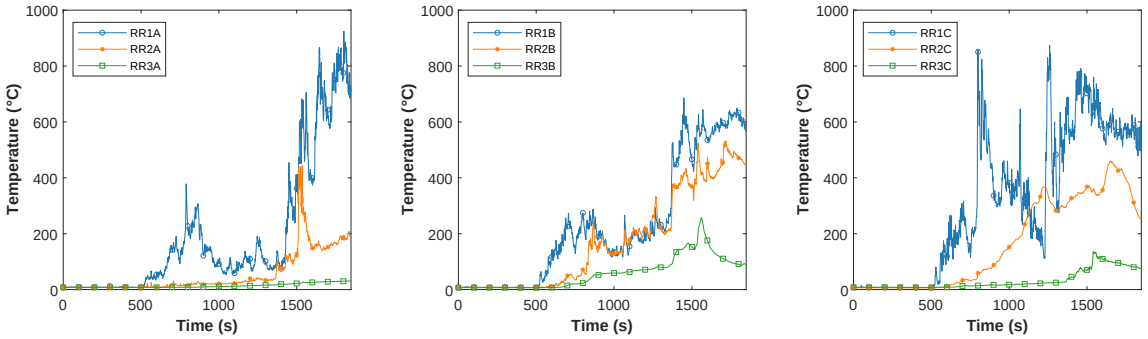

(a) Crest **(b)** Middle **(c)** Edge

Figure 42: Temperature profiles along the roof for Burn 3

- **Burn 4:** This was the first burn that experienced a complete door failure. The temperature on the inside of the door reached values greater than 300°C as seen in Fig. 43. The first flame penetration occurred in the middle and along the center of the door, MD2 location, while a consistent temperature increase was observed at other locations. After around 900 s the complete door was engulfed in flames. This door failure can be understood from the bonfire HRR Fig. 28 evolution. A fast increase followed by steady high HRR values of around 150 kW consumed the door and caused its failure.

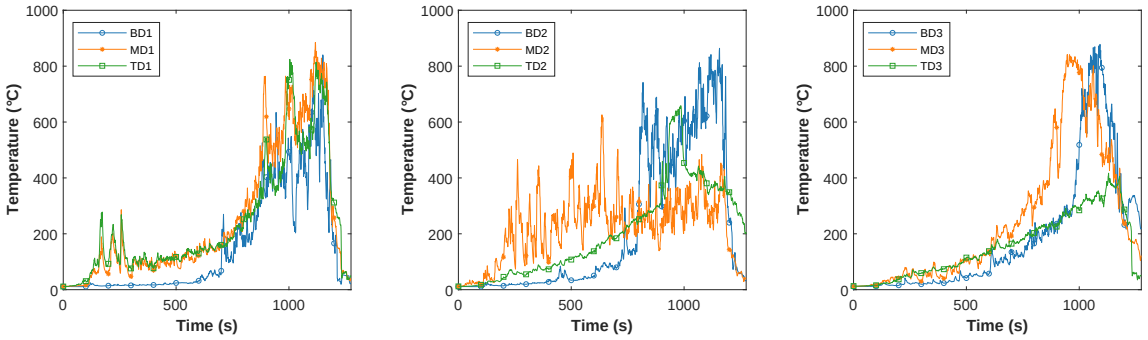

(a) Left **(b)** Center **(c)** Right

Figure 43: Temperature profiles along the inside of the door for Burn 4

The fast growth rate of HRR also led to faster and sustained ignition at the front of the roof. Similar to previous burns, the fire occurred at rows B and C, as seen in Fig. 44. The ignition was non-uniform along the roof front, as RLC always recorded temperatures below 300°C. The presence of wind at the test site tilted the flame and caused non-uniform heating of the roof structure. Fig. 45 shows the flame spread along the roof. It is observed that the flame spread occurred only along the middle and edge rows (B and C) of the roof, while hot gases were present along the crest (row A) with intermittent flame presence. The temperature measurements at RR2A and RR2B suggest that the thermocouple did not interact with the flame, while flames might be present around that location. This is a common occurrence in fire science because thermocouples are point measurement devices and can miss the flame presence if slightly misaligned. Therefore, cameras were used to provide additional observation.

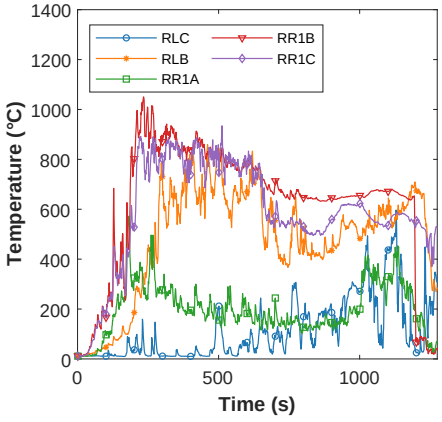

Figure 44: Temperature variation at the front of the roof for Burn 4

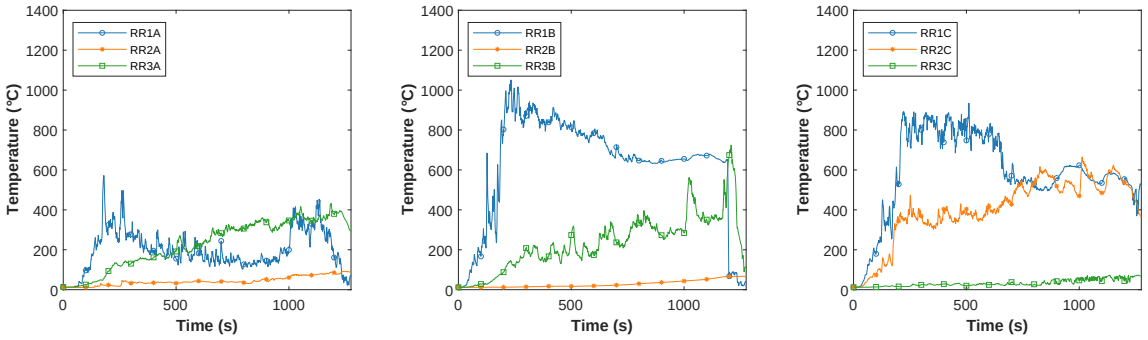

(a) Crest **(b)** Middle **(c)** Edge

Figure 45: Temperature profiles along the roof for Burn 4

- **Burn 5:** Similar to Burn 4, fast and sustained high HRR values were used for this burn. However, these high HRR values did not lead to a complete door failure because of the ambient wind pushing the flames away from the door. However, intermittent flame presence was observed at the bottom of the door, as shown in Fig. 46.

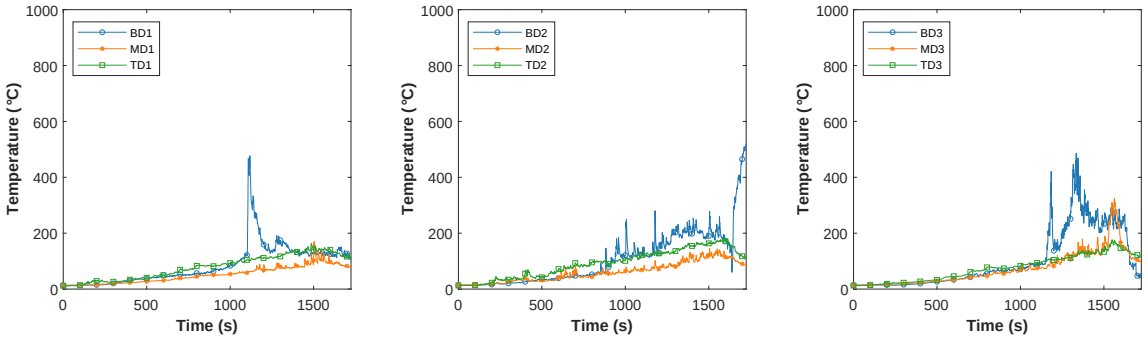

(a) Left **(b)** Center **(c)** Right

Figure 46: Temperature profiles along the inside of the door for Burn 5

The flame was present non-uniformly at the front of the roof where RLC did not experience temperatures greater than 200 °C, but the other locations at rows B and C experienced sustained flame presence throughout the experiment. Limited flame spread occurred along the roof crest (row A), but fast flame spread occurred along the middle and edge of the roof (rows B and C). The thermocouple at RR3C failed to capture the flame, probably due to its orientation.

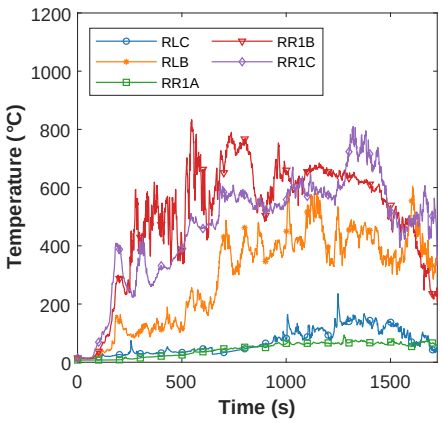

Figure 47: Temperature variation at the front of the roof for Burn 5

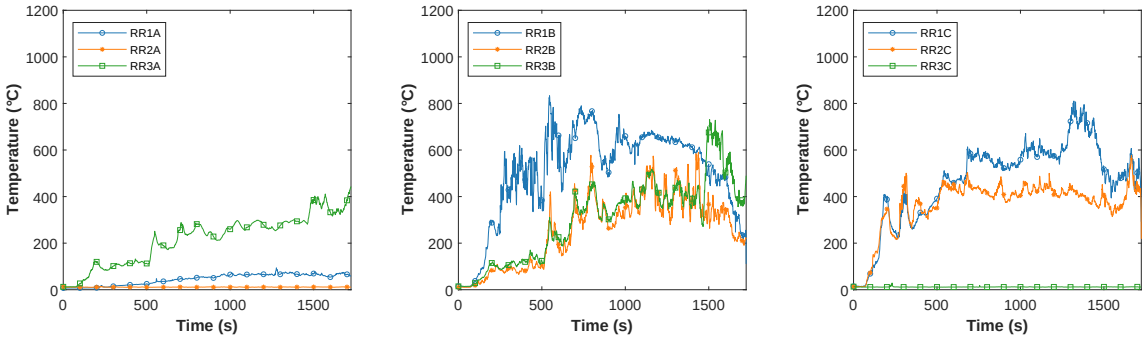

(a) Crest **(b)** Middle **(c)** Edge

Figure 48: Temperature profiles along the roof for Burn 5

4.3.3 Full Scale

Figure 49 presents the temperature measurements along the entryway and main structure roof, providing insights into flame spread behavior in the full-scale burn. After ignition, the temperature variation from the entryway to the main roof did not exhibit a clear gradient, likely due to the substantial size of the bonfire and continuous addition of fuel. Both roofs experienced elevated temperatures, indicating high fire intensity.

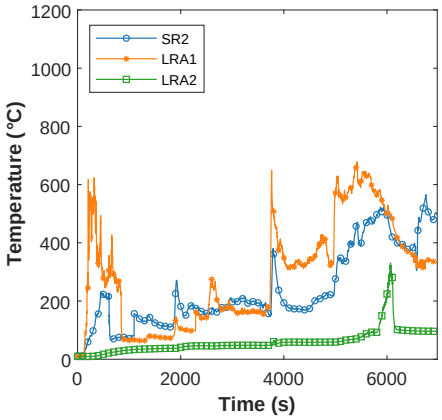

Figure 49: Temperature profiles along the small roof and large roof

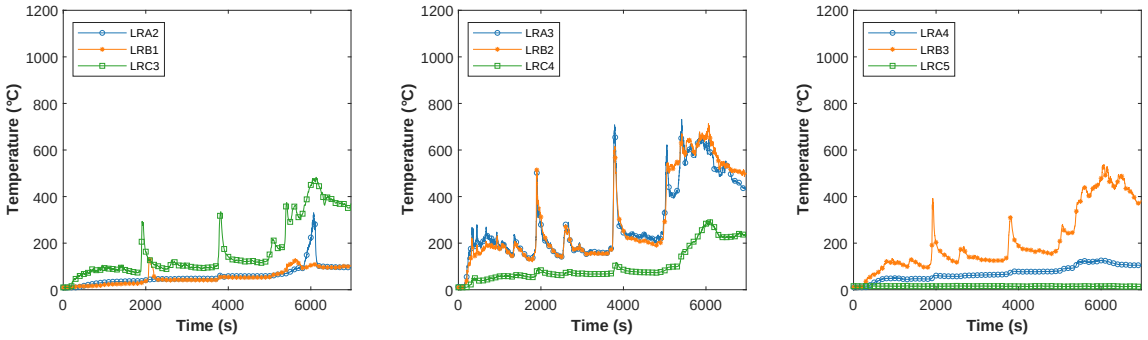

(a) Crest **(b)** Back middle **(c)** Back Edge

Figure 50: Temperature profiles along the main roof for full scale

During the entire burning process, flashover was observed to occur in two distinct instances, each marked by a significant spike in the temperature readings. These sharp temperature increases are evident in the plots and highlight the transition of the fire to a fully developed stage at these moments. The data suggest that the heat release rate and the fire dynamics intensified dramatically during these flashover events, further emphasizing their critical impact on the overall burning behavior.

4.3.4 Flame spread rate

The spread rate was determined based on thermocouple observations. $300\,^{\circ}\mathrm{C}$ was assumed to be reference temperature [44].

- **Lab scale:**

  Row B (RR1B - RR2B - RR3B) exhibited the most significant fire spread compared to other areas on the roof. The table below presents the fire spread rate and corresponding

time recorded between thermocouple locations RR1 - RR2, RR2 - RR3, and RR1 - RR3 in Row B of the roof.

Table 1: Rate of spread for lab scale

Location Row(RR1-RR2-RR3)B	Rate of spread, cm/s	Time, s
RR1-RR2	3.5859	17
RR2-RR3	1.7929	34
RR1-RR3	1.1953	51

The highest spread rate occurred between RR1 and RR2, with the fire taking 17 s, while the spread rate decreased between RR2 and RR3, taking 34 s. The overall spread from RR1 to RR3 was the slowest.

- **Door scale:**

Table 2: Rate of spread for door scale

Burn	Location Row(RR1-RR2-RR3)B	Location Row(RR1-RR2-RR3)C	Rate of spread, cm/s	Time, s
1	-	-	No spread	-
2	-	-	No spread	-
3	-	RR1C-RR2C	0.1343	454
4	-	RR1C-RR2C	1.1084	55
5	RR1B-RR2B	-	0.20595	296

Table 2 provides details on the fire spread rate. Temperature data analysis indicates that no significant fire spread was observed along the roof in Burn 1 and Burn 2. However, in Burn 3, fire spread was detected on the right side of the roof along Row C (RR1C-RR2C-RR3C), with a rate of 0.1343 cm/s from RR1C to RR2C over 454 s, while no spread occurred between RR2C and RR3C. Similarly, Burn 4 exhibited fire spread along Row C, where the rate between RR1C and RR2C was 1.1084 cm/s over 55 s. In Burn 5, fire spread was observed along Row B (RR1B-RR2B-RR3B), with a rate of 0.20595 cm/s from RR1B to RR2B, taking 296 seconds. Among all burns, Burn 3 recorded the slowest spread rate at 0.1343 cm/s.

- **Full scale:**

Table 3: Rate of spread for full scale

Location Row(LRA3-LRB2-LRC4)	Rate of spread, cm/s	Time, s
LRA3-LRB2	-	-
LRB3-LRC4	0.032725	4217
LRA3-LRC4	0.032779	4210

Analysis of the temperature data revealed that the fire spread rapidly from the entryway to the main roof. This was primarily due to the continuous addition of fuel to the bonfire during the burn, making it large enough to reach the larger roof from the outset. On the main roof, although Row [LRA2-LRB1-LRC3] was closer to the bonfire, significant fire spread was observed along Row [LRA3-LRB2-LRC4], which formed the basis for spread rate calculations.

Using a reference temperature of $300\,^{\circ}\mathrm{C}$, from the temperature data, it is observed that the fire arrived simultaneously at both LRA3 and LRB2. The spread rate between LRB2 and LRC4 was calculated as 0.032725 cm/s over 4,217 s, while the overall spread rate from LRA2 to LRC4 was 0.032779 cm/s over 4,210 s. Given that the thin layer of sticks beneath the turf was the primary fuel, their moisture content, density, and combustion properties likely influenced the fire spread characteristics, contributing to the relatively slow propagation despite the initial proximity to the ignition source.

4.4 Gas Measurements

During each experiment, O_2 concentration measurements were collected a five different heights, and at one of those locations (2.4 m for the laboratory scale and 1.7 m for the door and full scale experiments) CO, CO_2 and UHC were also measured. The results of these measurements are discussed in the following sections.

4.4.1 Laboratory Scale

At the laboratory scale, there was no compartment to collect the combustion gases as the fire spread through the door, resulting in all of the combustion gases quickly exiting from the open back of the hallway. No descending smoke layer was observed visually or from temperature and oxygen measurements. At the back of the hallway concentration of oxygen in the air was measured at varying heights and at all measurement locations except the highest one; the concentration of O_2 remained at ambient (Fig. 51a). This indicates that the smoke never descended below 2.0 m from the floor.

The concentration of CO, CO_2, and UHC were only measured at the sampling location that was 2.4 m from the ground. At this location the behavior of CO and CO_2 mirrors that of O_2 concentration. The concentration of these species remained at ambient until about 200 seconds after ignition. After this point, rapid changes in the gas concentration occurred until the gas sampling was stopped. During this period, the concentration of O_2 decreased from 21% to 5%, while the concentration of CO and CO_2 increased from near zero to 4% or larger. This rapid change in concentration measurements corresponds to the time when sustained burning on the ceiling was observed (Fig. 33). The behavior of the concentration measurements of UHC lagged behind the other measured species. A noticeable rise in the concentration of UHC did not occur until around 300 s post ignition, right before gas sampling was cut off to prevent damage to the sensors. The measured concentration of UHC never exceeded 2% during the first 350 s.

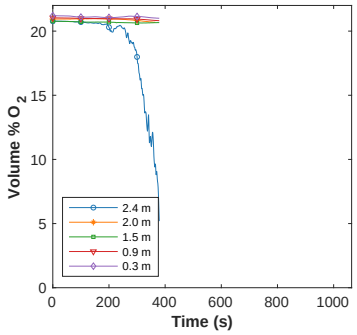

(a) O_2 at varying heights

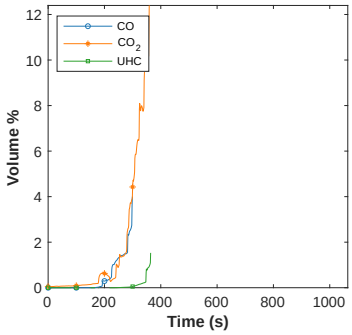

(b) CO, CO_2, and UHC at 2.4 m

Figure 51: Laboratory scale volume percent measurements

4.4.2 Gas Measurement Correction: Door and Full Scale

For the five door scale and the full scale experiments O_2 concentration measurements were collected at various heights. CO, CO_2, and UHC measurements were also measured from 1.7 m sampling location. After returning from the experimental campaign, a leak in the gas sampling setup for the 1.7 m sampling location was discovered. The effect of this leak can be seen clearly by comparing the 1.7 m O_2 measurements to the other vertically distributed sampling locations (Fig. 52a). During the experiments, the measured concentration of the other vertically distributed O_2 measurements were approximately the same (part a of Figs. 53-58). This indicates that a distinct smoke layer did not develop inside the compartment. This behavior was also visually observed during the door experiments. After each burn, when the compartment was opened, the smoke was evenly dispersed inside the compartment. Although the development of a smoke layer was observed during the beginning of the full scale experiment, the O_2 measurements at 0.5, 2.0, and 2.4 m were comparable; therefore, it was assumed that the O_2 measurement at 1.7 m should be as well.

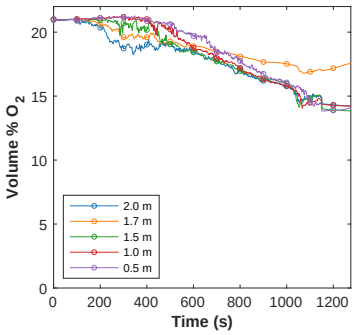

(a) Uncorrected O_2 measurements from a representative test (Burn 4)

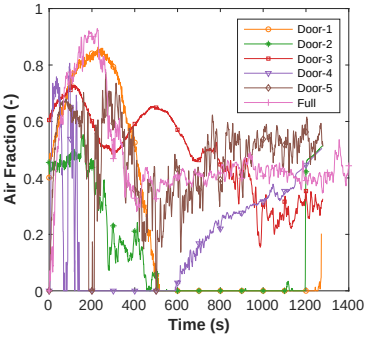

(b) Volume fraction of ambient air included in the gas sample measured

Figure 52: 1.7 m sampling leak correction

With these observations, it was assumed that the actual concentration at the 1.7 m sampling location for the door and full scale experiments was the average of the other vertically distributed

measurements (Door: 0.5, 1.0, 1.5, and 2.0 m and full: 0.5, 2.0, and 2.4 m). Using this corrected O_2 volume fraction measurement the air fraction ($\frac{V_{air}}{V_{sens}}$) or the volume fraction of ambient air included in the gas sample measured by the sensors for 1.7 m sampling location was calculated using Eq. 7, assuming ideal gas behavior.

$$\frac{V_{air}}{V_{sens}} = \frac{X_{O_2,sens} - X_{O_2,samp}}{X_{O_2,air} - X_{O_2,samp}} \tag{7}$$

Where X_{O_2} is the volume fraction of oxygen in the air (21%), the gas mixture measured by the sensors (sens), and at the 1.7 m sampling location (samp). If the measured concentration of O_2 at the 1.7 m location was less than the average of the other measurements, the air fraction for a particular time was assumed to be 0. This is only the case during the door-scale experiments 1, 2, and 4.

For door-scale experiments 1 and 2 the measured O_2 concentration was around ambient throughout the entire experiment and little CO CO_2, and UHC were measured, therefore the effects of the leak of the system should be minimal and assuming an air fraction of zero will have little effect on the tenability analysis. In the case of door-scale Burn 4, the air fraction was specified as zero from 200 s to 600 s. During this period, the O_2 measured at the 1.7 m sampling location was comparable to the other measurement locations, therefore, it seems that leakage was minimal during this period. After this period, the air fraction increased because the filters clogged, resulting in more air being pulled from the leak. The calculated air fraction for all experiments was more variable when the O_2 concentration was around ambient, and then became more constant later in the experiments. This is because at the beginning of each test, the O_2 concentration was around ambient for all locations, and the variability is due to the noise in the measurements. The reduction in this variability is due to the increased difference in O_2 concentration between the ambient air and the structure.

The air fraction for these experiments was used to correct measurements of CO , CO_2, and UHC (species i) (Eq. 8)

$$X_{i,samp} = \frac{X_{i,sens} - X_{i,air}\left(V_{air}/V_{sens}\right)}{1 - \left(V_{air}/V_{sens}\right)} \tag{8}$$

Where $X_{i,air}$ is the concentration of species i in the ambient air: $X_{CO,air} = 0$, $X_{CO_2,air} = 0.04\%$, and $X_{UHC,air} = 0$. These corrected volume fractions are used in the tenability analysis (Section 4.5) and presented in part b of Figs. 53-58.

4.4.3 Door Scale

The gas species measurements of the five door-scale experiments are presented and discussed here.

- **Burn 1:** During the first door-scale experiment, the O_2 concentration measurements at every sampling location remained at ambient during the experiment (Fig. 53a). This is consistent with the fire spread results for this experiment. During this test, the fire did not penetrate the door, and no sustained fire on the roof was observed. Therefore,

little if any combustion gases should have entered the shipping container, resulting in the approximately ambient concentration of O_2 observed.

The concentration measurements of CO, CO_2, and UHC confirm these observations, with all measurements less than 0.25% during the experiment (Fig. 53b). The concentration measurements for CO_2 vary slightly above the ambient concentration of CO_2, indicating a small amount of smoke entering the container. The measured concentrations of CO and UHC also remained near zero. This is consistent with observations during the experiment. No fire spread occurred, but flame impingement on the roof and flame penetration through the gaps in the door were observed. This flame behavior allowed a small amount of combustion gases to enter the storage container, but not enough to create significant amounts of these species inside the container.

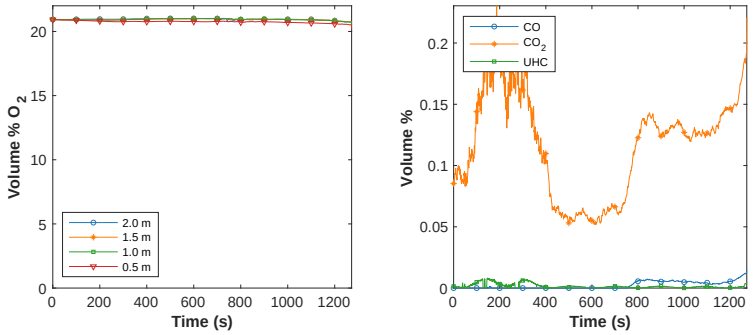

(a) O_2 at varying heights **(b)** Corrected CO, CO_2, and UHC

Figure 53: Door scale Burn 1 volume percent measurements

- **Burn 2:** The O_2 concentration measurements at every sampling location dropped very slowly from ambient for the majority of Burn 2, but dropped more quickly at the end of the experiment (Fig. 54a). The measured volume fraction of UHC remained near zero, but the CO volume fraction rose throughout the experiment (Fig. 54b). The volume fraction of CO_2 increased throughout the experiment but did not exceed 1%. Similarly to Burn 1, the fire did not spread along the roof, but in Burn 2, the flames penetrated the bottom of the door. This means that more combustion gases entered the compartment than in Burn 1, but the fire remained relatively small. This accounts for the slight decrease in volume fraction of O_2, accompanied by a slight increase in combustion products that was observed.

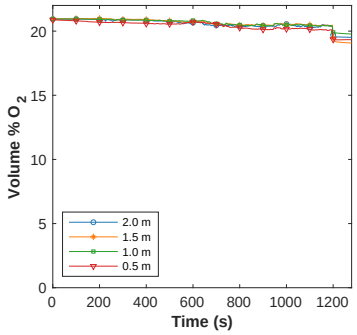

(a) O_2 at varying heights

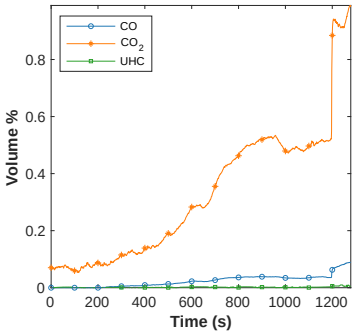

(b) Corrected CO, CO_2, and UHC

Figure 54: Door scale Burn 2 volume percent measurements

- **Burn 3:** The O_2 concentration measurements at every sampling location slowly decreased throughout the burn to around 20% (Fig. 55a). The maximum volume fraction of CO, CO_2, and UHC is similar to Burn 2, but in Burn 3 the volume fraction of the species does not begin to rise until around 700 s after bonfire ignition (Fig. 55b). Based on the species measurements, Burns 2 and 3 are very similar, but the increase in combustion products occurred faster in Burn 3 than in Burn 2. This is probably because in Burn 3, unlike Burns 1 and 2, the fire spread to the roof. This resulted in faster accumulation of CO, CO_2, and UHC just after the roof fire had spread away from the door.

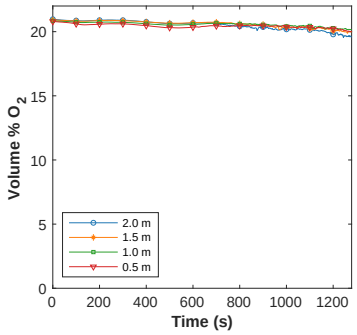

(a) O_2 at varying heights

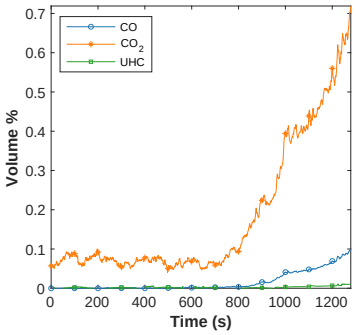

(b) Corrected CO, CO_2, and UHC

Figure 55: Door scale burn 3 volume percent measurements

- **Burn 4:** Burn 4 was the first door scale experiment where the O_2 concentration dropped significantly, reaching less than 15% (Fig. 56a). Similarly, the measured volume fraction of CO and CO_2 rose significantly higher during this burn than the previous three tests (Fig. 56b). This test was the first burn where the door completely failed, resulting in a significant fire inside the compartment. This resulted in higher CO and CO_2 measurements and lower O_2 measurements. Additionally, the rise in CO and CO_2 concentration begins around 200 s, corresponding to the visual observations of fire spread inside the corridor. The volume fraction of CO measured during this experiment exceeded the Acute Exposure Guideline's (AEGL) 10 minute exposure threshold of 0.17% for threatening injury or death [45]. Throughout this experiment, the UHC concentration remained well below that of CO.

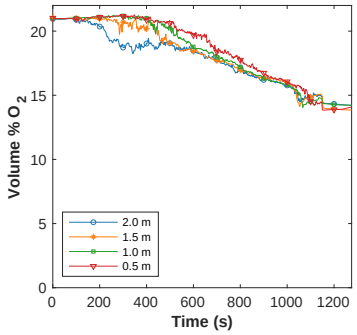

(a) O_2 at varying heights

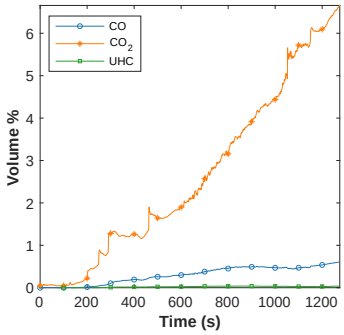

(b) Corrected CO, CO_2, and UHC

Figure 56: Door scale Burn 4 volume percent measurements

- **Burn 5:** The measured species concentration during Burn 5 was most similar to Burn 4. The concentration of O_2 noticeably dropped during the burn (Fig. 57a), but the final O_2 concentration was greater than Burn 4's final concentration. Similarly, the concentrations of CO and CO_2 increased throughout the burn (Fig. 57b), but the concentration of both species at the end of the experiment was less than that of Burn 4. Concerning amounts of CO were measured. This behavior is consistent with the observed flame spread during the experiment. For this burn, the door did not completely fail, and only some areas of the roof had sustained flaming. As a result, fewer combustion gases were produced in the corridor than in Burn 4, leading to lower combustion product concentrations. As was the case for all of the door scale experiments, the concentration of UHC remained near zero for the entirety of the tests.

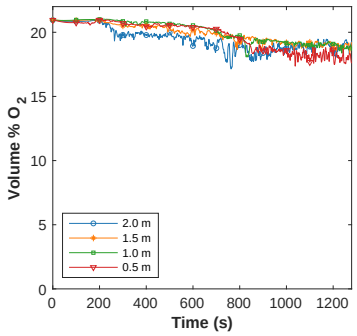

(a) O_2 at varying heights

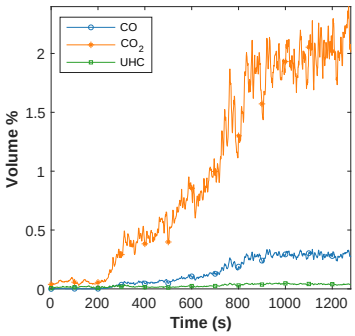

(b) Corrected CO, CO_2, and UHC

Figure 57: Door scale burn 5 volume percent measurements

4.4.4 Full Scale

The full scale experiment persisted for a significantly longer time compared to the laboratory and door scales. The first 1000 s look very similar to the door scale Burn 4 and the laboratory scale, where the oxygen concentration gradually drops to around 15% as shown in Fig. 58a. During this initial period, the CO and CO_2 also increase as shown in Fig. 58b. After this period, the bonfire began to decrease in intensity, and the door began to fall apart and vent the

compartment. This ventilation is as the gas concentrations return to near ambient values during the period of 1000 s to 2000 s. The sharp decrease in oxygen concentration and increase of CO and CO_2 at 2000 s corresponds with a brief flashover observed after refreshing the bonfire with additional fuel. The flashover was surprising at the time and changed the dynamics for the rest of the test.

The remaining portion of the test, 2000 s onward, was not needed for measuring tenability, but rather to monitor for structural collapse. Fuel was periodically added to the bonfire, the fire within the turf house would be reignited again, flashover or near-flashover conditions would be observed briefly, and then the structure would vent again.

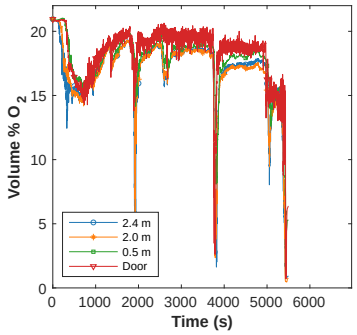

(a) O_2 at varying heights

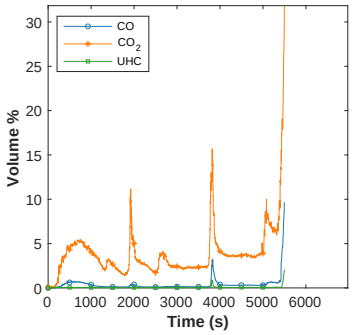

(b) Corrected CO, CO_2, and UHC

Figure 58: Full scale volume percent measurements

4.5 Tenability

The tenability at all three scales was assessed based on the performance based criteria described in Section 2.2.

4.5.1 Temperature

The first two criteria to assess tenability are based on the temperature measurements. If the upper smoke layer reaches 200 °C the compartment is considered untenable, because burns on exposed skin will occur in a matter of seconds due to radiant heat at this temperature [36]. Another tenability consideration is the temperature of the environment surrounding a person's exposed skin. Skin will burn when exposed to temperatures greater than 43 °C, but the damage is rapid at temperatures greater than 70 °C [37]. For this analysis, if the gas temperature 1.7 m or less from the ground inside the compartment reaches 70 °C the compartment is considered untenable.

The smoke layer temperatures inside the compartment for the door and full scale experiments are presented in Fig. 59a. No compartment was included in the experimental design of the laboratory scale experiment; therefore, the gas temperatures at the gas sampling locations are not relevant to tenability analysis for this experiment. The gas temperature located just behind

the door, where a Viking would have stood to prevent entry from the door is the only relevant temperature in terms of tenability of the structure for the laboratory experiment.

The temperature measurements at this location are presented in Fig. 59. The door provided substantial protection from the heat of the fire for the first 200 s after ignition, but by 280 s, the temperature the Viking would have been exposed to exceeded 70 °C, therefore, based on the temperature measurements, the area behind the door was tenable for the first 280 s after the ignition of the fire.

For the door scale experiments, the upper smoke layer temperature never reached 200 °C, but during some of the burns the gas temperature 1.7 m to the floor or lower reached 70 °C. Based on the surrounding gas temperature parameter, the compartment was tenable for the duration of Burns 1 and 2. The Viking's skin would have started to burn from the heat at 1465 s for Burn 3, 487 s for Burn 4, and 711 s for Burn 5. The compartment would have been untenable by 1572 s, 633 s, and 1167 s for Burns 3, 4, and 5, respectively, based on the temperature tenability parameters.

During the full scale experiments, the individuals inside would have experienced burns starting at 441 s, and the turf house would become untenable at 611 s based on the smoke layer temperature (Fig. 59g).

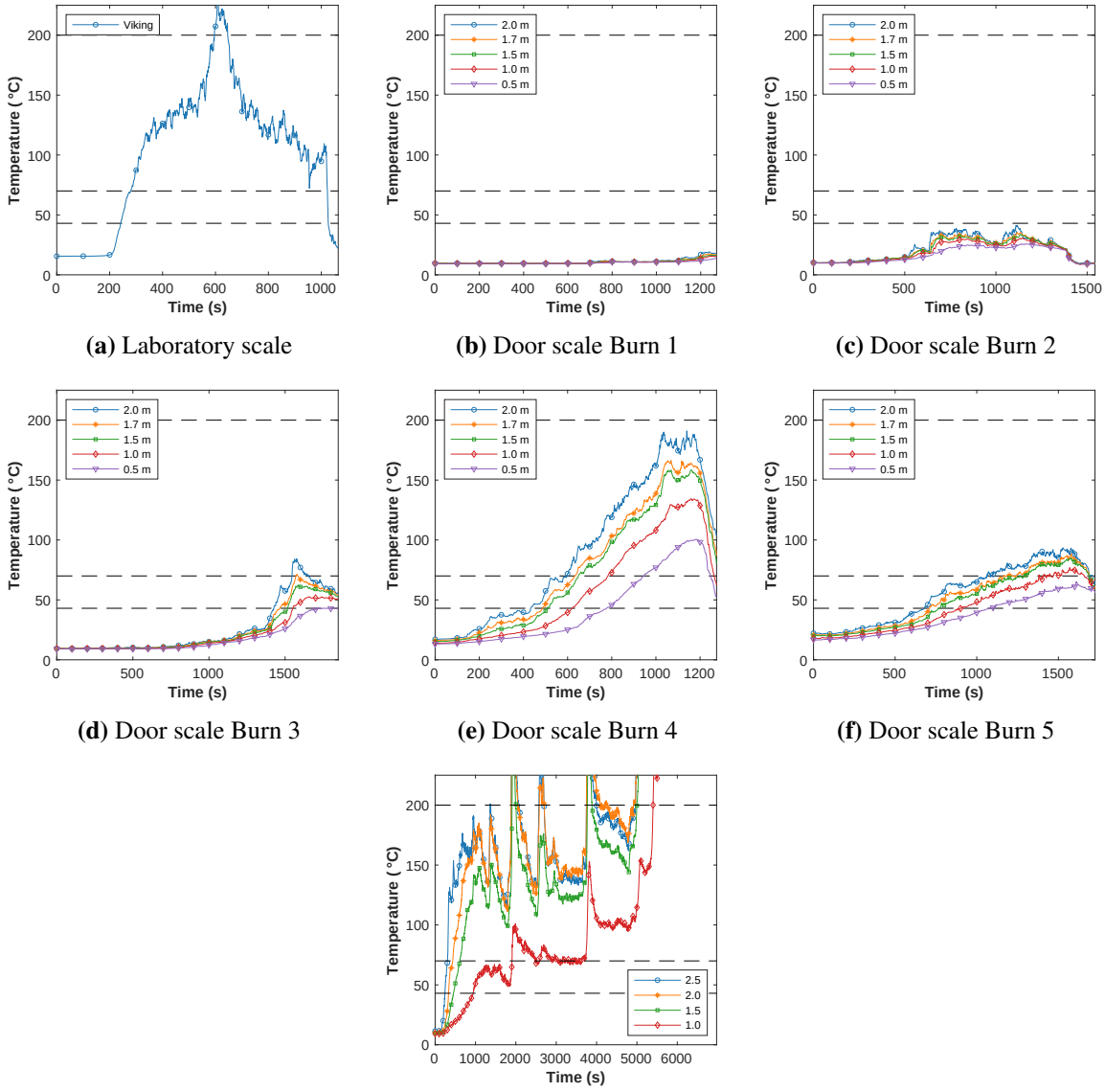

(a) Laboratory scale

(b) Door scale Burn 1

(c) Door scale Burn 2

(d) Door scale Burn 3

(e) Door scale Burn 4

(f) Door scale Burn 5

(g) Full scale

Figure 59: Smoke layer temperature measurements

4.5.2 Fractional Effective Dose

The tenability inside the structure based on the cumulative exposure of toxic gases was assessed using FED. The structure is no longer tenable when the FED reaches 1. Based on this parameter, the structure was always tenable during the Burns 1, 2, and 3 at the door scale (Fig. 60). The lab scale test was no longer tenable at 297 s, and the full scale test at 458 s. The door scale Burns 4 and 5 were no longer tenable at 731 s and 1063 s based on the FED.

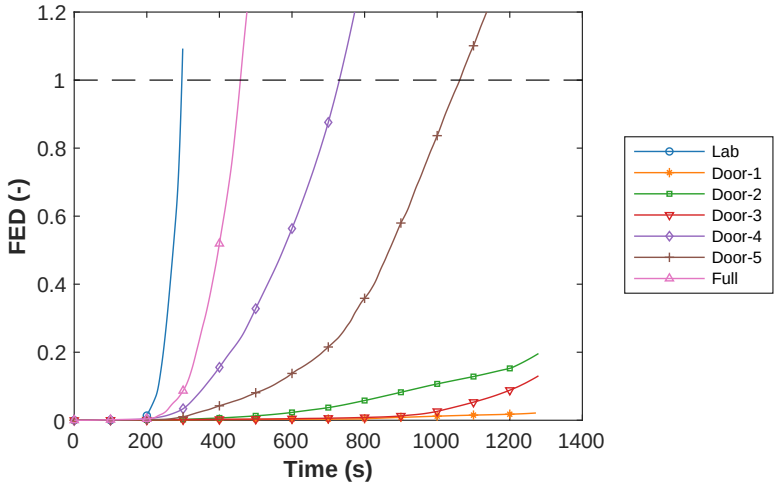

Figure 60: FED results for all three scales

4.5.3 Combined Assessment

During all the experiments, the structure never collapsed, and these criteria were never used for tenability assessment. Referring back to Section 2.2, the time when the structure is no longer tenable is the first time when a temperature or FED threshold is met. Table 4 summarizes how long the structure was tenable based on all the criteria. In the cases where the structure was no longer tenable, the first parameter to reach the threshold was the FED for the full-scale and door-scale Burn 5. In all other cases, the temperature based criteria were first.

Table 4: The duration that each experiment was tenable, based on all of the assessment criteria

Experiment	Duration Tenable (s)
Laboratory Scale	280
Door Scale Burn 1	Full Duration
Door Scale Burn 2	Full Duration
Door Scale Burn 3	1572
Door Scale Burn 4	633
Door Scale Burn 5	1063
Full Scale	458

5 Analysis

5.1 Fire as a Viking-Age War Tactic

Observations from the experiments conducted at different scales show that the Viking-age war tactic was gruesome. The bonfire would have been large, the conditions within the structure would likely have degraded rapidly, and the time to broker an agreement or leave the structure was short.

From the standpoint of creating an untenable environment within the structure, the goal of the bonfire is to degrade the boundary between the inside and outside of the structure, be it the door or the roof structure. The degradation of the boundary increases the ventilation into the structure. The increased ventilation was observed to dramatically increase the fire spread and accelerate the accumulation of the products of combustion within the structure as the bonfire's plume is entrained into the structure. Resulting in an increase in the CO, CO_2, and other combustion products concentrations within the structure while also decreasing the O_2 concentrations. The heat from the bonfire's plume would assist in the pre-drying of the roof structure components. The most dramatic example is in the lab scale test, where the gable fails and the roof structure rapidly transitions to a fully involved fire. Experiments that resulted in untenable conditions were unique in that the roof structures ignited and the fire propagated along the entryway into the compartment. The burning roof structure then greatly accelerated the accumulation of combustion products within the structures. In parallel to the roof ignition, the exterior bonfire would propagate through the base of the door and create gaps for the bonfire's products of combustion to enter the structure. Both of these events require substantially large bonfires and steady burning.

For door or roof failure, the bonfire size must have been large, around 200 kW, based on the door scale results. This fire size is comparable to the peak heat release rate of a burning 42 L trash bin with mixed plastic and paper trash [46]. The fires would have to be even larger if suppression efforts were made by the defenders. Furthermore, this fire would need to be sustained for a significant amount of time.

It is important to remember that the base concept of Viking-age combat with fire on turf houses is to defeat the defenders while minimizing the risk of injury to the combatants attacking the turf house. The defenders would likely be trying to escape the structure or barter an agreement. The defenders would look to maximize the amount of time for either of these activities by suppressing the fire or mitigating the effects of the fire and smoke. The attackers would be trying to prevent the defenders from escaping the structure or attacking them. Time would likely not be a resource for the attackers, and they would have to work quickly. Coupled with the stress of combat and the necessity to source the bonfire fuel locally, the creation, ignition, and subsequent re-loading of the bonfire would have likely been chaotic. The authors of this report note that even with copious planning, prebuilt fires, pre-set fuel packages, and rehearsed movements, the burns were hectic at best.

Even the ignition of an initial small fire may have served as an initial intimidation or negotiation tactic. While the light smoke would initially not be fatal, the associated irritating effects would

likely have caused significant distress among the occupants, pressuring them to surrender. Even with effective firefighting and stuffing of void spaces, it is unlikely that the intrusion of smoke could have been prevented completely. If a small fire was lit at the base of the door for long enough, the smoldering reaction could also penetrate the door and start to create gaps within the door. These gaps would increase the amount of heat and smoke entering the structure and would rapidly increase the rate of spread into the structure if a larger fire were to be built. Exiting the structure from the door would have likely required leaping over an active fire, or at a minimum, a large bed of coals. Any opening of the door would also allow a large amount of products of combustion into the structure, which would further degrade the conditions within the structure.

In the full-scale experiment, the door completely failed, allowing a larger fire to be built in the doorframe and resulting in almost all of the products of combustion entering the structure. If the inside volume was as large as historically anticipated, the method of fully burning down the door may have been the only way of generating enough smoke and heat to create the untenable conditions within the very large structure. It should be noted that the experiments do not account for any fuel loading of the structure, such as wainscoting covering the walls, wooden furniture, or materials stored within the structure. All of these contents have the potential to greatly increase the fire severity while decreasing the amount of fuel needed to support the bonfire.

The Viking-age tactic of burning turf houses must have revolved around creating untenable conditions over inducing structural collapse, which was never observed in the conducted experiments. As the heat from the bonfire or combusting structural components reaches the turf, the turf starts to dry and decrease in weight. While drying would decrease the temperature within the structure, it would also increase the humidity and has the potential to further decrease the tenability. Dried turf also weighs considerably less, which would reduce the structural loads. Coupled with the observation that the structural members across all tests would char, but not fully degrade, the duration and severity of the bonfire would need to be enormous for structural collapse. Even the full scale entryway and nearby structural members, which were subjected to a bonfire for 2 hours, had only just started to deteriorate, but did not fully collapse.

5.2 Fire Protection Reflections

Fires in contemporary turf structures, such as short-term rentals, bring challenges beyond those of regular structural fires that fire departments are familiar with and train for. These experiments investigated a very simplified case of turf structures without any additional interior fuel loading. While the fire threat was historical, an average growth coefficient of 0.0016 kW/s^2 can be calculated by taking a max HRR of 250 kW at 400 s from Fig. 28. This correlates to a very slow fire growth rate and can be used as a planning factor when designing future fire protection systems [47].

Particular areas of concern are the structural integrity of the building, the behavior of the turf under the impingement of fire and water, as well as the lack of feasible escape routes. Due to the massive amount of uncertainty related to the design, construction, materials, and potential fire damage, an aggressive interior attack may only be feasible for the duration of a primary search of the structure and rescue of victims. In non-lifesaving scenarios, the risks of entering the structure due to all of the uncertainty would likely be too high. Further, firefighting operations

may waterlog the turf and increase the load, which may endanger the structural integrity and personal safety of responders. For this reason, the recommendation is made that any non-lifesaving firefighting operations be conducted defensively.

During the suppression of the full scale burn, a piercing nozzle was used to pierce through the turf walls and extinguish the fire in the compartment. This was effective in controlling the bulk of the fire within the structure without placing firefighters in danger. Using the nozzle did require that firefighters climb onto the structure, which does put them at risk for entrapment from a structural collapse. The firefighters slowly assessed and constantly reassessed the structural stability of the turf house before and while climbing on top of the structure. Additionally, the firefighters avoided areas of clear structural decay and instead utilized a hose stream.

Overhaul operations might prove resource-, time- and labor-intensive. Full extinguishment of the structure may require partially or fully disassembling the walls and roof, as well as sufficiently wetting down the turf mats. This process may take many hours and require the use of tanker shuttle operations, especially if a reliable water supply is unavailable. Total suppression of the smoldering turf was also never achieved in any experiments where the roof structure was sufficiently involved. Upon overhaul of these experiments, pockets of smoldering turf were found, often in the central layers of the turf where water was unable to penetrate. Smoldering pockets of turf reignited when exposed to ambient air in several instances, including after the full scale experiment was suppressed and left to sit undisturbed overnight.

The experimental findings of this work indicate that while the turf structures were able to withstand the prescribed fire threat, tenability cannot be assured. This is a significant problem if turf structures are to be used as temporary dwelling units. The following design recommendations were identified during the preparation of this report, in addition to the standard recommendations for dwellings found in the NFPA codes and Standards. While not all-inclusive, they can serve as a start to the performance based design process of any future structures while also maintaining the unique design and historical aspects of turf houses

- Substitute the stick layer between the structural frame and turf for a noncombustible alternative. This will dramatically reduce the fuel loading of the structure and limit the flame spread across the roof.
- Limit the fuel loading and ignition sources within the structure. This can be accomplished by minimizing the amount of furniture, not using wooden wainscoting or combustible wall coverings, preventing the use of open flames or nonstandard heat appliances, and minimizing utilities within the structure.
- Construct the frame of the structure from noncombustible components that will not sufficiently degrade if exposed to heat with the intent of increasing the integrity of the structure.
- Utilize a rapid response fire detection and suppression system, such as smoke detectors and sprinklers, to provide fast detection and notification of a fire event and an initial firefighting effort.
- Provide fire intervention and firefighting training to the caretakers of the structure as well

as local first responders to streamline the fire response process. This process will likely be unique to each structure or location due to the large variety in structure design.

- Ensure that structures are designed with multiple, well-identified, and easily accessible routes of egress.
- Locate any fireplaces or heating sources in the structure on the side opposite the exit.

6 Conclusions

The tenability of Viking-age turf houses exposed to a historically sized bonfire was investigated across three scales. A laboratory scale experiment consisting of a replica door, roof structure, and 1.2 m simulated entryway was conducted in the WPI Fire Protection Engineering Performance Laboratory identified that the bonfire degrades the door and gable materials that form the boundary between the inside and outside of the structure. As this boundary degrades and ventilation is increased, products of combustion from the bonfire enter the structure, preheat the roof structure, and increase the concentration of CO and CO_2 within the structure. Gas concentration and temperature measurements were made throughout the structure to identify the limit of tenability, and heat flux gauges measured the intensity of the bonfire. The limit of tenability occurred at 280 s due to thermal exposures.

Five door scale experiments consisting of a replica door and roof structure attached to a shipping container to simulate the volume of a turf house were conducted at Eiríksstaðir in Búðardalur, Iceland. Gas concentrations, temperatures, and heat fluxes were recorded in a similar manner to the door scale. Bonfire sizes and intensity varied across experiments in order to fully understand the impact of the fire size on tenability outcomes. In two cases, the tenable limit was reached at 633 s and 1063 s from temperature and gas concentrations, respectively. These untenable environments occurred for fire sizes with a maximum sustained HRR of 175 kW and 225 kW. A single full scale turf house replica was also conducted in Iceland with similar instrumentation. The full scale reached untenable conditions at 458 s due to high temperatures when exposed to a fire around 180 kW.

Results of this experimental archaeology study indicate that the Viking-age combat tactic of burning turf houses was an effective way of defeating a defender within their house. Comments based on observations and experimental findings are made on the use of fire as a war tactic, and recommendations are made for protecting contemporary replica turf houses.

7 Acknowledgements

The WPI Hurstwic Team greatly thanks Hurstwic, the Worcester Polytechnic Institute (WPI) Fire Protection Engineering (FPE) Department, Professor Urban, and Professor Simeoni for their support. A special thank you to the Robert W. Fitzgerald Endowed Graduate Support Fund, which allowed the team to travel to and around Iceland and Hurstwic, who covered food and lodging expenses. The WPI Hurstwic Team acknowledges that very rarely are students afforded such a fantastic opportunity to conduct this level of research, especially internationally, and we are grateful for the opportunity.

The WPI Hurstwic Team would like to thank the WPI Laboratory Support Staff, Fritz Brokaw and Mahesh Kottalgi, who assisted with the laboratory experiment and provided support when packing for Iceland. The team would also like to thank Jorge Valdivia who assisted in the laboratory and with the radiometers.

The WPI team would like also to extend their gratitude to Bjarki Sigurðsson, Matt Card, Joe Fonzi, Ívar Örn Þórðarson, Matthew Marino, Reynir A. Óskarson, William R. Short, and the Staff of Eiríksstaðir for their contributions and support throughout this project, especially for their efforts in carrying out much of the construction work for the full-scale setup. Materials were donated by Land og Skógar (Icelandic Forestry Service) and Húsasmiðjan. This project was done in cooperation with Eiríksstaðir, Þjóðminjasafn Íslands (National Museum of Iceland), and Brunavarnir Dala, Reykhóla og Stranda (Fire Department of Dalir, Reykhólar, and Strandir).

Appendices

A Weather Data

During the door and full-scale experiments, the wind direction and velocity were measured using two s-type pitot tubes arranged perpendicular to each other. The differential pressure measurements across each pitot tube were collected with Sensirion SDP800-125Pa pressure transducers at 300 HZ. These differential pressure measurements were condensed to one measurement every three seconds by averaging the differential pressure measurements over the 3 s period. The differential pressure data set was then converted to velocity assuming a constant gas phase temperature of 8 ° C and a probe coefficient of 0.807. The s-type probes were calibrated radially for 6 deflection angles (0, 15, 30, 45, 60, and 75°) and 7 wind speeds (1.8, 4.4, 8, 12.7, 18.5, 25.1, 33.1 m/s) to create a conversion between measured velocity and actual velocity as a function of deflection angle, as shown in Fig. 61. The fit was restricted such that the dimensionless velocity was 1 at an angle of 0° and 0 at 90°. The angular characterization was used to calculate the true magnitude and direction of the wind throughout the experiments, shown in Fig. 62. Due to project constraints, Wind data was unavailable for door scale burn 5.

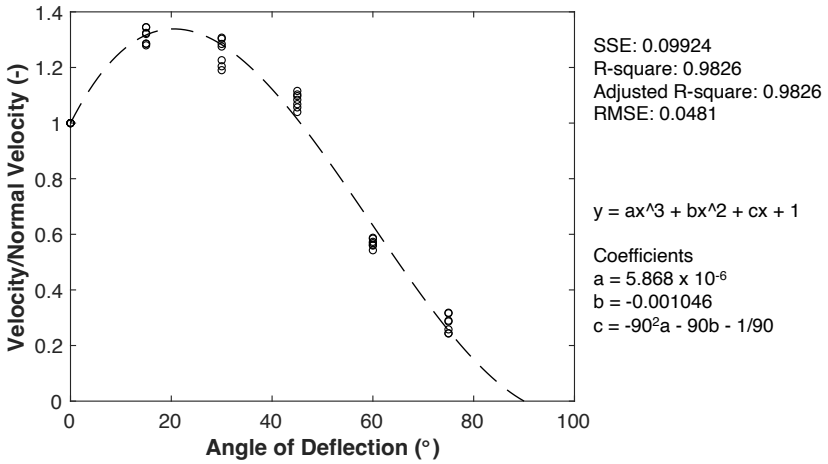

Figure 61: Calibration of s-type pitot tube arrangement.

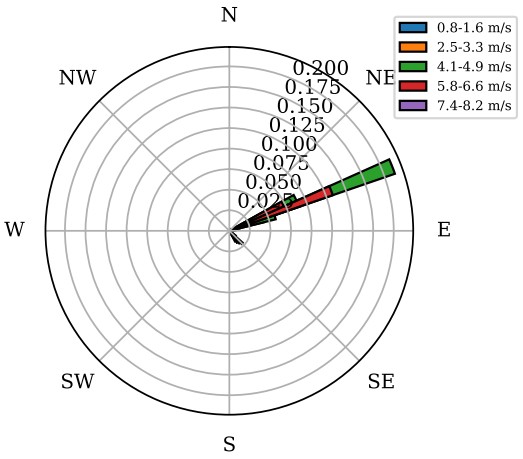

(a) July 5 door scale Burn 1

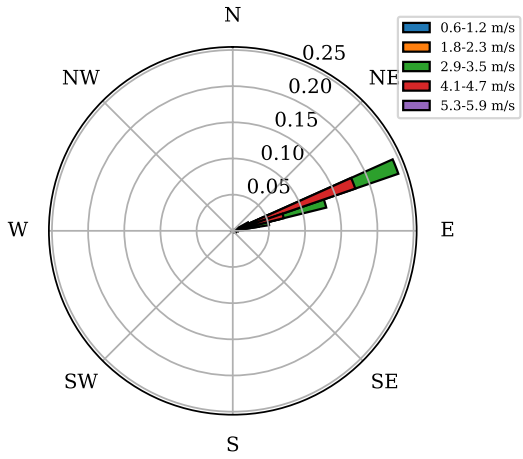

(b) July 5 door scale Burn 2

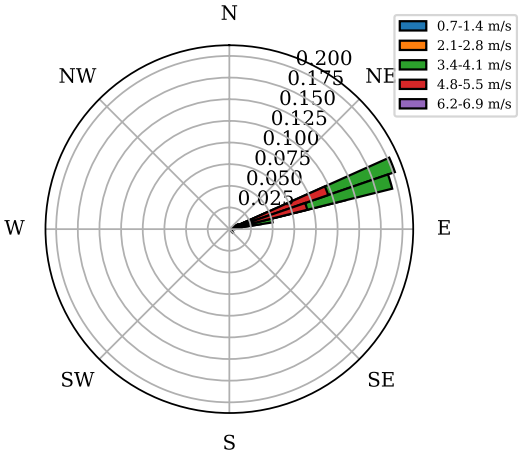

(c) July 6 door scale Burn 3

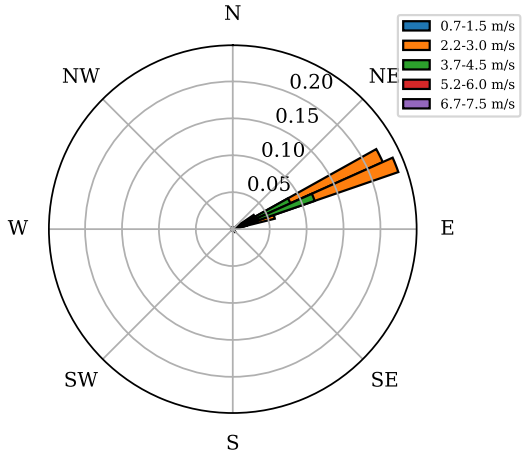

(d) July 6 door scale Burn 4

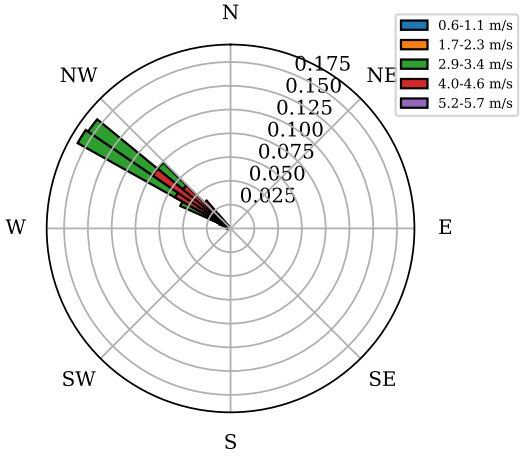

(e) July 7 full scale burn

Figure 62: Wind rose per burn

Table 5: Wind characteristics for different burns

Date	**Burn**	**Magnitude (m/s)**	**Direction** (°)	Cardinal Directions
July 5	Door Scale Burn 1	4.01	80	E
July 5	Door Scale Burn 2	3.00	73	E/NE
July 6	Door Scale Burn 3	3.48	73	E/NE
July 6	Door Scale Burn 4	2.59	70	E/NE
July 7	Full Scale Burn	3.11	305	NW

B Cameras

To obtain a better understanding of the fire dynamics within the compartment, a custom set of sacrificial cameras was developed and refined throughout the project. The cameras were required to be unobtrusive, easy to install and run, robust enough to survive in adverse conditions, and cheap, due to their sacrificial nature. Furthermore, the footage had to be saved remotely to ensure that it was not corrupted as the camera burnt up.

The sacrificial cameras saw two design iterations throughout the project. The first, used exclusively in the laboratory-scale experiment, served as an experimental prototype. The lessons learned from that test were incorporated into the next design iteration to create a more robust camera system.

The cameras used were made by DFRobot (model number: FIT0729). They were chosen due to their simple USB 2.0 connectivity, ability to shoot 1080p video at 30 frames per second, auto focus, and their low cost. In the experimental prototype, the cameras were encapsulated in an enclosure made of 7 mm plywood to prevent accidental short circuiting and allow for better mounting. Connections were made to the computer using several USB 2.0 extension cables. During the burn it was found that the lenses began thermally degrading several minutes before the cameras failed, even if they were not directly exposed to the flames (as in the case of the floor camera). Furthermore, the cables appeared to have failed in the camera that was directly exposed to the flame, along with the enclosure and the board itself. These insights inspired several improvements in the next iteration.

The cameras needed to be modified to survive multiple experiments for the door scale experiments. Considering there were several door-scale experiments planned, it was financially and logistically unfeasible to sacrifice multiple cameras for each burn. The second generation cameras used the same camera board, but significantly improved on the camera enclosure. The exposed electrical connections were secured with non-conductive tape. This allowed for a metal enclosure that would be more robust to mechanical impacts. The backplate was made of a 51x51 mm^2 piece of 1 mm thick sheet metal with a hole drilled into it to pass the cable through. The front of the camera was covered by a 51x51 mm^2, 63.5 mm thick plate of borosilicate glass serving as mechanical protection of the lens as well as a reflector for thermal radiation.

Borosilicate was chosen due to its resistance to thermal shock. Between the back wall and the front glass, glass wool was used as non-conductive thermal insulation. Sidewalls were formed using a layer of glass fiber tape to fasten the sandwiched materials. Then, a layer of reflective aluminum tape was applied to all sides except the lens window to protect the body from thermal radiation. The cable was surrounded by a fire retardant sheath (Flexo 75TB) to protect it from thermal and mechanical damage. Individual interior components visible during a post-fire analysis are shown in Fig. 63c.

Capturing footage from the cameras was done using a custom program written in Python. The program accesses each camera frame and saves it to the disk to ensure that even if the camera footage is interrupted for any reason (thermal damage, becomes unplugged, etc) the previous footage is saved. The program implementation was one of the less reliable aspects of the cameras, leading to several computer crashes. One hypothesis is that these crashes were caused by voltage spikes as the cameras were being damaged. This led to several artifacts in the video metadata, but the footage itself remained usable. An additional limitation was that the frame rate was not constant, due to limitations in disk writing speed. This was especially apparent in the full scale burn. As the cameras failed one by one, the frame rate increased as the load on the computer decreased.

Overall, the cameras outperformed all expectations, at all scales. The cameras in the laboratory-scale burn captured footage that was helpful in determining the mechanism of flame spread, as well as other fire phenomena. One of the cameras survived about 2 minutes of direct flame contact, though the lens had been thermally degraded, making the image cloudy. The cameras in the door and full-scale burns performed even better. Two cameras were used for all of the door-scale burns. One was placed on the floor near the door, and thus exposed a large amount of thermal radiation. Another camera was elevated further back in the compartment and was thus exposed to more convective heating. The elevated camera failed during the 4th burn after compartment air temperatures exceeded 200 °C. The other camera survived all of the door scale experiments (Shown in Fig. 63a).

The full-scale burn featured four cameras recording simultaneously. Three of them were placed on the floor, one was suspended at head height in the compartment. Where possible, the cables were covered by gravel to protect them from the heat. The cables leading to the computer were run directly through the wall. Once again, the camera that was elevated was the first to fail about 23 minutes into the experiment. The next camera failed after being buried under smoldering debris, 26 minutes into the test. The third failed 37 minutes into the test. By happenstance, this camera was knocked over from its original position close to the fire and rotated in time to capture the ceiling of the compartment during flashover. The final camera, located centrally on the floor failed one hour and eight minutes into the burn after capturing two separate flashover events.

Although several of the cameras were recovered after the burn (see Fig. 63b, it was very difficult to say what the exact point of failure (e.g. board, optical sensor, cable) was. From the failure

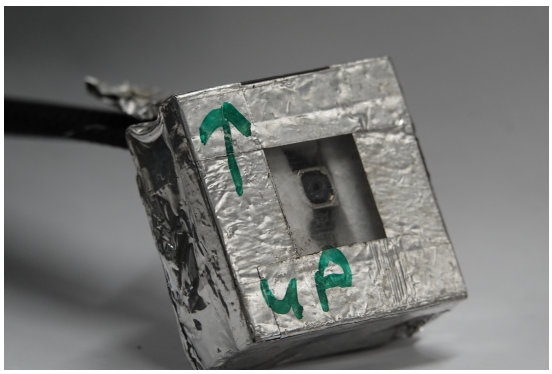

(a) Functioning second-generation camera used in the door-scale burns.

(b) Second-generation camera after the full-scale burn.

(c) Disassembled second-generation camera during the failure analysis.

Figure 63: Second generation cameras

profile, however, it is clear that the cameras that were subjected to higher convective heating failed faster than those that were primarily exposed to thermal radiation. The footage on the failing cameras shows dropped frames (indicated by skipping time), visual artifacts such as colorful pixels and noise, as well as issues with the auto-focus. It was notable that none of the second-generation cameras experienced the clouding of the lens that was characteristic of thermal damage in the laboratory-scale experiments, even under intense thermal radiation. This meant that much more footage was usable for analysis and indicates that the borosilicate glass was effective at shielding the camera module from thermal radiation.

B.1 Camera Recording Software

```
frame_width = 1920
frame_height = 1080
frame_rate = 30
window_name = "Camera " + str(cam_num)
exposure = 166
timestamp_color = (51,255,87)
cap = cv2.VideoCapture(cam_num)

#check if opening the camera was successfull
if (cap.isOpened() == False):
```

```
    print("[ERROR] Unable to open camera feed for camera number
     ↪  ", cam_num)

cap.set(cv2.CAP_PROP_FOURCC, cv2.VideoWriter.fourcc(*"MJPG"))
cap.set(cv2.CAP_PROP_FRAME_WIDTH, frame_width)
cap.set(cv2.CAP_PROP_FRAME_HEIGHT, frame_height)
cap.set(cv2.CAP_PROP_FPS, frame_rate)
out = cv2.VideoWriter(outFile, cv2.VideoWriter.fourcc(*"MJPG"),
 ↪  frame_rate, (frame_width, frame_height))

try:
    while True:
        ret, frame = cap.read()
        if ret == True:
            #Add the watermark
            frame_height , frame_width, _ = frame.shape
            #add a FPS Counter
            new_frame_time = datetime.now()
            #add the timestamp to the image
            font = cv2.FONT_HERSHEY_PLAIN
            cv2.putText(frame, "WPI FPE", (frame_width - 200,
             ↪  frame_height - 20), font, 2, (255,255,255), 2,
             ↪  cv2.LINE_AA)
            cv2.putText(frame, str(datetime.now()), (20,
             ↪  frame_height - 20), font, 2, timestamp_color,
             ↪  2, cv2.LINE_AA)
            #write the frame to the output video -> fps wont be
             ↪  displayed
            out.write(frame)
            #optionally display the FPS, image only, wont be
             ↪  saved
            if disp_fps == True:
                time_dif = new_frame_time - prev_frame_time
                fps = 1 / (time_dif.microseconds / 1000000)
                fps = str(int(fps))
                cv2.putText(frame, fps, (20, 50),
                 ↪  cv2.FONT_HERSHEY_SIMPLEX, 2,
                 ↪  timestamp_color, 2, cv2.LINE_AA)
                prev_frame_time = new_frame_time

            cv2.namedWindow(window_name,cv2.WINDOW_NORMAL)
            cv2.imshow(window_name, frame)
            if cv2.waitKey(1) & 0xFF == ord('q'):
                break
        else:
            print("[ERROR] Camera Failure.")
            break
```

```
        print("[SYSTEM] Saving Video")
        cap.release()
        out.release()
        cv2.destroyAllWindows()

    except Exception as e:
        print("[ERROR] something went wrong")
        print(e)
        cap.release()
        out.release()

    except KeyboardInterrupt:
        print("[SYSTEM] Detected Keyboard Interrupt. Saving
         ↪  Video.")
        cap.release()
        out.release()
        cv2.destroyAllWindows()

    #uncomment below to make sure the video is saved if an error
     ↪  occurs
    except:
        print("[ERROR] Camera Capture Failed. Saving Video.")
        cap.release()
        out.release()
        cv2.destroyAllWindows()
```

C Burn Timelines

C.1 Laboratory Scale

Table 6: Timeline of the laboratory scale burn.

Seconds	Phenomenon	Observed By
0	Ignition	LabView, Cameras 2 and 4
49	Light smoke exiting rear of corridor	sac cam 1
155	Firebrands enter above the door	sac cam 1
185	Gable experiences flame contact	Camera 2
195	Intermittent Flame intrusion above the door	sac cam 1, Camera 3
203	Sustained fire in the corridor ceiling	sac cam 0 and 1
215	Heavy smoke from the rear of the corridor	Camera 4
217	Flames rolling along the corridor ceiling	sac cam 0
230	Development of Ceiling Jet	sac cam 1
238	Gable is fully involved	Camera 2
241	Intermittent flames from the rear of the compartment	Camera 4
256	Transition from ceiling jet to rollover	Camera 3
267	Sac cam 0 is immersed in flames	sac cam 0
273	Sustained fire exiting the rear of the corridor	Camera 2
371	Sac cam 0 fails	sac cam 0
468	Framing members on the right ext. wall are involved	Camera 2
543	Bonfire dies down slightly	Camera 2
583	Sac cam 1 begins taking thermal damage	sac cam 1
592	Heavy fire from all visible sides of the roof	Camera 4
594	Sudden ignition of the doors cross beam	Camera 3
629	Sac cam 1 fails	sac cam 1

Seconds	Phenomenon	Observed By
639	Gable appears to have vented	Camera 3
648	Debris fall from the Gable	Camera 3
788	Debris fall from the Gable	Camera 2
809	Debris falls from the ceiling	Camera 3
939	Start of suppression	Cameras 1, 2, 3, and 4, LabView

C.2 Door Scale Burn 1

Table 7: Timeline for door scale Burn 1

Seconds	Phenomenon	Observed By
-836	sac cam 2 started	sac cam 2
-804	sac cam 0 started	sac cam 0
-451	Camera 1 start	LabView
-451	Camera 1 clip 1 starts	Camera 1
-432	Camera 2 start	LabView
-117	Camera 1 shot goes out of focus	Camera 1
-48	"ignition"	Camera 1
-42	Ignition	LabView
-2	Second Ignition announced	Camera 1
0	Second ignition	LabView
89	Flames seen in the base of the bonfire	Camera 1
131	Camera 1 refocuses	Camera 1
265	Camera 1 clip 1 ends	Camera 1
265	Camera 2 starts	Camera 2
273	Camera 1 clip 2 starts	Camera 1
273	Wind screen is placed upwind of the fire	Camera 1
301	Camera 1 clip 2 ends	Camera 1
547	Several Fire brands visible	sac cam 0
619	First ignition	Camera 2
640	Sudden intrusion of smoke from bottom left corner	sac cam 0
642	Short flame intrusion on bottom left corner	sac cam 0
643	Ceiling ignition (short flareup, then smoldering) center right	sac cam 0

Seconds	Phenomenon	Observed By
653	Intermittent fire in the ceiling	sac cam 0
656	intermittent flames on the bottom left corner of the door	sac cam 0
660	Ceiling ignition on the left	sac cam 0
663	Ceiling ignition on the left subsides	sac cam 0
679	Sustained fire in the ceiling, both sides near the door	sac cam 0
698	Notable smoke layer	sac cam 2
704	Ignition	Camera 2
719	Flame in the bonfire	Camera 2
733	Visibility is reduced	sac cam 2
868	Fire dies down	Camera 2
974	Windshield is placed upwind	Camera 2
1038	Camera 1 clip 3 ends	Camera 2
1079	Fire nearly self-extinguishes	Camera 2
1113	Camera 1 clip 3 starts	Camera 1
1113	Wind screen is moved away	Camera 1
1116	Fire grows dramatically	Camera 1
1140	Fire intensifies	Camera 2
1142	Windscreen is moved away	Camera 2
1143	Fire dies down	Camera 2
1152	Fire dies down again	Camera 1
1155	Flames reach the gable	Camera 2
1266	Bonfire is manually compressed	Camera 1
1293	New Kindling is added	Camera 1
1295	New Kindling is added	Camera 2
1313	Fire grows dramatically	Camera 1
1323	Flame contact in the gable	Camera 1
1340	Fire grows dramatically	Camera 2
1384	Fire dies down a bit	Camera 1
1430	More kindling is added through the following minute	Camera 1
1489	Fire grows a little bit	Camera 1
1516	New Kindling is added through the next minutes	Camera 2
1557	Fire grows again	Camera 2
1607	Bonfire is manually rearranged	Camera 1
1631	Bonfire is manually rearranged	Camera 2

Seconds	Phenomenon	Observed By
1694	Jackson Crawford attempts to light a cigar	Camera 1
1720	Flames visible from the base of the scale	Camera 1
1828	Fire has mostly died down	Camera 1
1878	Bonfire is moved away from door by FFs	Camera 1
1918	Suppression	Camera 2
1918	Camera 2 clip ends	Camera 2

C.3 Door Scale Burn 2

Table 8: Timeline for door scale Burn 2

Seconds	Phenomenon	Observed By
-836	sac cam 2 started	sac cam 2
-804	sac cam 0 started	sac cam 0
-451	Camera 1 start	LabView
-451	Camera 1 clip 1 starts	Camera 1
-432	Camera 2 start	LabView
-117	Camera 1 shot goes out of focus	Camera 1
-48	"Ignition"	Camera 1
-42	Ignition	LabView
-2	Second ignition announced	Camera 1
0	Second ignition	LabView
89	Flames seen in the base of the bonfire	Camera 1
131	Camera 1 refocuses	Camera 1
265	Camera 1 clip 1 ends	Camera 1
265	Camera 2 starts	Camera 2
273	Camera 1 clip 2 starts	Camera 1
273	Wind screen is placed upwind of the fire	Camera 1
301	Camera 1 clip 2 ends	Camera 1
547	Several firebrands visible	sac cam 0
619	First ignition	Camera 2
640	Sudden intrusion of smoke from bottom left corner	sac cam 0
642	Short flame intrusion on bottom left corner	sac cam 0
643	Ceiling ignition (short flare-up, then smoldering) center right	sac cam 0

Seconds	Phenomenon	Observed By
653	Intermittent fire in the ceiling	sac cam 0
656	Intermittent flames on the bottom left corner of the door	sac cam 0
660	Ceiling ignition on the left	sac cam 0
663	Ceiling ignition on the left subsides	sac cam 0
679	Sustained fire in the ceiling, both sides near the door	sac cam 0
698	Notable smoke layer	sac cam 2
704	Ignition	Camera 2
719	Flame in the bonfire	Camera 2
733	Visibility is reduced	sac cam 2
868	Fire dies down	Camera 2
974	Windshield is placed upwind	Camera 2
1038	Camera 1 clip 3 ends	Camera 2
1079	Fire nearly self-extinguishes	Camera 2
1113	Camera 1 clip 3 starts	Camera 1
1113	Wind screen is moved away	Camera 1
1116	Fire grows dramatically	Camera 1
1140	Fire intensifies	Camera 2
1142	Windscreen is moved away	Camera 2
1143	Fire dies down	Camera 2
1152	Fire dies down again	Camera 1
1155	Flames reach the gable	Camera 2
1266	Bonfire is manually compressed	Camera 1
1293	New kindling is added	Camera 1
1295	New kindling is added	Camera 2
1313	Fire grows dramatically	Camera 1
1323	Flame contact in the gable	Camera 1
1340	Fire grows dramatically	Camera 2
1384	Fire dies down a bit	Camera 1
1430	More kindling is added through the following minute	Camera 1
1489	Fire grows a little bit	Camera 1
1516	New kindling is added through the next minutes	Camera 2
1557	Fire grows again	Camera 2
1607	Bonfire is manually rearranged	Camera 1
1631	Bonfire is manually rearranged	Camera 2

Seconds	Phenomenon	Observed By
1694	Jackson Crawford attempts to light a cigar	Camera 1
1720	Flames visible from the base of the scale	Camera 1
1828	Fire has mostly died down	Camera 1
1878	Bonfire is moved away from door by FFs	Camera 1
1918	Suppression	Camera 2
1918	Camera 2 clip ends	Camera 2

C.4 Door Scale Burn 3

Table 9: Timeline for door scale Burn 3

Seconds	Phenomenon	Observed By
-1127	sac cam 0 starts	sac cam 0
-1118	sac_cam_2 starts	sac_cam_2
-807	Camera 1 On	LabView
-799	Camera 2 on	LabView
-799	Camera 2 starts	Camera 2
-486	Camera 2 on 2	LabView
-386	ignition attempt	Camera 2
-382	First ignition attempt	Camera 1
-257	Second ignition attempt	Camera 1
-244	First Ignition	LabView
-234	Smoke visible	Cam2
-221	Smoke visible	Camera 1
-184	small flames visible	Camera 2
-117	Fire is inspected	Camera 1
-108	Fire is inspected	Camera 2
-75	Additional newspaper is inserted	Camera 1
-75	More newspaper is added	Camera 2
-49	Second Ignition attempt	Camera 2
0	Main Ignition	LabView
12	Smoke visible	Camera 2
18	Flames visible in the bonfire	Camera 1
56	Flames visible in the bonfire	Camera 2

Seconds	Phenomenon	Observed By
128	Fire is being pushed by the wind	Camera 1
167	Fire is pushed by the wind	Camera 2
232	Windshield is installed	Camera 1
236	Windshield is installed	Camera 2
273	Windshield is removed	Camera 2
276	Fire grows	Camera 1
278	Windshield is removed	Camera 1
284	Fire grows	Camera 2
300	First firebrands visible	sac cam 0
344	Flames reach the gable intermittently	Camera 2
351	Flame rises into the ceiling, intermittently	Camera 1
440	first flame intrusion around the left side of the door, midway up	sac cam 0
448	Top of door is on fire	Camera 1
478	Smoke visible from the eaves	Camera 1
503	flames die down a little bit	Camera 2
538	Fire is rearranged	Camera 2
548	Fire is rearranged	Camera 1
550	ignition of the right ceiling and left top door, then spreads to the left ceiling	sac cam 0
566	Fire grows, smoke through the roof	Camera 2
569	flames in the ceiling die down, but smoldering is still visible	sac cam 0
581	flames in left ceiling intensify	sac cam 0
641	ceiling fire dies down, small flames visible	sac cam 0
643	puffing visible at the bottom of the door	sac cam 0
648	Smoke indicates significant fire in the corridor	Camera 1
663	ceiling fire has spread away from the door on the right side	sac cam 0
684	Fire emanating from the soffit	Camera 1
693	Fire in the left eave	Camera 2
713	Fire in the eaves grows significantly	Camera 1
716	fire on the ceiling has grown	sac cam 0
717	Fire in the eaves grows significantly	Camera 2
726	New fuel is added	Camera 1
734	New fuel is added throughout next minutes	Camera 2

Seconds	Phenomenon	Observed By
743	Fire is rearranged	Camera 2
744	Fire is piled with shovel	Camera 1
762	More fuel	Camera 1
801	smoke layer occludes the ceiling.	sac cam 1
855	Camera 1 clip 2 starts	Camera 1
856	Heavy fire in the gable	Camera 1
886	fire in eves dies down	Camera 2
909	Turf falls from the left side of the roof	Camera 1
930	Heavy white smoke from left side of roof	Camera 1
943	Fire is piled with shovel	Camera 2
955	Fire is rearranged	Camera 1
961	smoke layer has reached the floor	sac cam 1
969	Fire in eves re-intensifies	Camera 2
975	Fire in the eaves returns	Camera 1
983	Camera 1 clip 1 ends	Camera 1
1003	More fuel is added	Camera 2
1056	Fire in the gable extends to the right side	Camera 1
1064	Heavy fire in the gable	Camera 2
1144	Heavy smoke from the roof	Camera 2
1259	Left soffit panel falls off	Camera 1
1259	Panel on the left soffit falls off	Camera 2
1263	Turf mat falls of the left roof	Camera 2
1304	Camera 2 clip 1 ends	Camera 2
1346	Camera 2 clip 2 starts	Camera 2
1466	Turf mat falls off the left roof	Camera 1
1706	the ceiling is still fully involved	sac cam 0
1979	Start of suppression	Camera 1
2509	Camera 1 clip 2 ends	Camera 1

C.5 Door Scale Burn 4

Table 10: Timeline for door scale Burn 4

Seconds	Phenomenon	Observed By
-540	sac cam 0 starts	sac cam 0
-533	sac cam 2 starts	sac cam 1
-370	Camera 1 on	LabView
-370	Camera 1 starts	Camera 1
-358	Camera 2 on	LabView
-358	Camera 2 footage starts	Camera 2
-15	Ignition	Camera 1
-7	Smoke visible	Camera 1
0	Ignition	LabView
27	Windscreen is removed	Camera 1
45	First firebrands visible	sac cam 0
73	flames visible in the bonfire	Camera 1
98	Intermittent flame contact of the eaves	Camera 1
103	Door Ignition	LabView
111	flame intrusion in the center of the door. Flame visible at the top left ceiling	sac cam 0
119	puffing flames at the center and bottom right of the door.	sac cam 0
128	repeated fire at the left ceiling, flame intrusion along the left edge of the door.	sac cam 0
163	fire at left edge of door intensifies	sac cam 0
175	Smoke visible from the eaves	Camera 1
176	sustained burning in the left ceiling near the door	sac cam 0
196	Fire in the gable	Camera 1
209	continuous flames along left edge, center and bottom right of door	sac cam 0
233	fire in ceiling intensifies, fire in the right corner of ceiling.	sac cam 0
243	Door and gable fully involved	Camera 1
256	fire dies down	Camera 1
284	Fire in the eaves is out	Camera 1
301	fire in the eaves reappears	Camera 1

Seconds	Phenomenon	Observed By
328	smoke condition intensifies and occludes ceiling. flames visible through smoke	sac cam 0
370	Fire on the left roof	Camera 1
490	fire is rearranged	Camera 1
499	sac cam 0 fully occluded	sac cam 0
507	Fire in the eaves grows, more smoke	Camera 1
765	increased smoke from the eaves	Camera 1
771	fire is rearranged	Camera 1
853	Fire in the eaves has died down, intermittent flames	Camera 1
915	shows intense fire all along the ceiling	sac cam 2
994	possible ceiling jet in the compartment	sac cam 2
1000	fire in the gable reappears	Camera 1
1014	rapid intensification of fire in ceiling, development of ceiling jet	sac cam 2
1026	all structural members in the ceiling are fully involved	sac cam 0
1056	ceiling jet burns out	sac cam 0
1106	heavy smoke from the eaves	Camera 1
1146	Camera 1 footage ends	Camera 1
1171	ceiling fire dramatically intensifies	sac cam 0
1180	Piece of turf falls from the ceiling	sac cam 0

C.6 Door Scale Burn 5

Table 11: Timeline for door scale Burn 5

Seconds	Phenomenon	Observed By
-540	sac cam 0 starts	sac cam 0
-533	sac cam 2 starts	sac cam 1
-370	Camera 1 on	LabView
-370	Camera 1 starts	Camera 1
-358	Camera 2 on	LabView
-358	Camera 2 footage starts	Camera 2
-15	Ignition	Camera 1
-7	Smoke visible	Camera 1
0	Ignition	LabView

Seconds	Phenomenon	Observed By
27	Windscreen is removed	Camera 1
45	First firebrands visible	sac cam 0
73	flames visible in the bonfire	Camera 1
98	Intermittent flame contact of the eaves	Camera 1
103	Door Ignition	LabView
111	flame intrusion in the center of the door. Flames at the top left ceiling	sac cam 0
119	puffing flames at the center and bottom right of the door.	sac cam 0
128	repeated fire at the left ceiling, flame intrusion left edge of the door.	sac cam 0
163	fire at left edge of door intensifies	sac cam 0
175	Smoke visible from the eaves	Camera 1
176	sustained burning in the left ceiling near the door	sac cam 0
196	Fire in the gable	Camera 1
209	continuous flames along left edge, center and bottom right of door	sac cam 0
233	fire in ceiling intensifies, fire in the right corner of ceiling.	sac cam 0
243	Door and gable fully involved	Camera 1
256	fire dies down	Camera 1
284	Fire in the eaves is out	Camera 1
301	fire in the eaves reappears	Camera 1
328	smoke intensifies and occludes ceiling. flames visible through smoke	sac cam 0
370	Fire on the left roof	Camera 1
490	fire is rearranged	Camera 1
499	sac cam 0 fully occluded	sac cam 0
507	Fire in the eaves grows, more smoke	Camera 1
765	increased smoke from the eaves	Camera 1
771	fire is rearranged	Camera 1
853	Fire in the eaves has died down, intermittent flames	Camera 1
915	shows intense fire all along the ceiling	sac cam 2
994	possible ceiling jet in the compartment	sac cam 2
1000	fire in the gable reappears	Camera 1

Seconds	Phenomenon	Observed By
1014	rapid intensification of fire in ceiling, development of ceiling jet	sac cam 2
1026	all structural members in the ceiling are fully involved	sac cam 0
1056	ceiling jet burns out	sac cam 0
1106	heavy smoke from the eaves	Camera 1
1146	Camera 1 footage ends	Camera 1
1171	ceiling fire dramatically intensifies	sac cam 0
1180	Piece of turf falls from the ceiling	sac cam 0

C.7 Full Scale Burn

Table 12: Timeline for full scale burn, * denotes times that could not be verified

Seconds	Phenomenon	Observed By
-792	sac cam 2 started	sac cam 2
-777	sac cam 4 started	sac_cam_4
-763	sac cam 6 started	sac cam 6
-742	sac cam 8 started	sac cam 8
-625	Camera 1 start	LabView
-625	Camera 1 clip 1 starts	Camera 1
-620	Camera 2 start	Lab_view
-620	Camera 2 clip 1 starts	Camera 2
-172	Light smoke visible in the compartment	sac cam 8
-30	Tinder bundle is lit	Camera 2
-29	Tinder bundle is ignited	Camera 1
-11	Tinder bundle is inserted into the bonfire	Camera 1
-7	Ignition	Camera 2
-4	Ignition	Camera 1
0	Ignition	LabView
9	Smoke from the bonfire	Camera 1
20	Light smoke visible in the compartment	sac cam 4, sac cam 6
21	Smoke visible in the bonfire	Camera 2
26	small flames visible in the bonfire	Camera 1
86	No more flames visible in the bonfire	Camera 1

Seconds	Phenomenon	Observed By
104	Smoke can be seen entering the compartment above the door	sac cam 2, sac cam 8
113	Smoke production increases, small flames reappear	Camera 1
122	flames can be seen at the top of the door	sac cam 2, sac cam 8
124	Fire grows, flames at door height	Camera 1
127	Flames visible above the bonfire	Camera 2
136	Intermittent flame contact in the eaves	Camera 2
141	Eaves experience intermittent flame contact	Camera 1
169	Sustained flame contact in the eaves	Camera 2
170	intermittent fire spread in the corridor ceiling	sac cam 8
171	Smoke emanating from the turf of the main roof	Camera 1
174	Gable experiences sustained flame contact	Camera 1
179	sustained fire in the ceiling	sac cam 2
183	fire spreads along the corridor ceiling	sac cam 8
194	Smoke visible from the corridor roof	Camera 2
197	sac cam 6 view of ceiling is occluded by smoke	sac cam 6
204	fire spreading rapidly along the ceiling	sac cam 6
205	Flames spreading from corridor to the compartment	sac cam 8
206	Flames grow, smoke lightens	Camera 1
207	Significant Fire in front of the door	Camera 2
207	flames puffing from the bottom of the door	sac cam 2
217	Smoke condition rapidly deteriorates, smoldering visible on the ceiling	sac cam 8
220	sac cam 4's view of compartment is obstructed by smoke, fire glow visible	sac cam 4
245	Significant seeping smoke through the turf	Camera 1
248	Puffing and intermittent fire at the bottom of the door	sac cam 8
252	Smoke seeping from the main roof	Camera 2
280	Sustained fire at the bottom of the door	sac cam 2
298	Minor flame spread in the grass of the turf to the left of the door	Camera 1
302	smoke condition deteriorates	sac cam 2
312	sac cam 6 is completely occluded by smoke	sac cam 6
316	Sustained fire emanating from the eaves above the door	Camera 1

Seconds	Phenomenon	Observed By
316	fire spreading up the door, glow indicates significant fire in the ceiling	sac cam 2
325	Smoke seeping on the B-side roof	Camera 2
335	sac cam 8 view is occluded by smoke, fire glow is visible	sac cam 8
337	ceiling is occluded by smoke	sac cam 2
467	zero visibility conditions	sac cam 2
513	sac cam 8 is mostly occluded by debris	sac cam 8
529	Fire emanating from the gable	Camera 2
556	Turf on the AB corner flares up briefly	Camera 2
569	The bonfire has compressed and the flame heights are lower	Camera 1
610	sac cam 2 footage interrupted	sac cam 2
704	smoke condition improves in the compartment	sac cam 4
707	possible fire glow visible on the compartment ceiling	sac cam 4
735	Door shows significant gaps between boards	Camera 2
771	Sudden ignition of the turf on the bottom AB corner of the hut, short lived	Camera 1
772	Brief flare up of the AB corner turf	Camera 2
791	People going to the DAQ table	Camera 1
850	Door is still in place, but is mostly charred through	Camera 1
851	Smoke clears up, but sac cam 6 view is obstructed by debris	sac cam 6
882	Right panel above the door comes lose, still attached though	Camera 2
903	Fire from the eaves above the door intensifies	Camera 1
912	Right panel above the door comes lose, still attached though	Camera 1
927	Fire in the gable increases significantly	Camera 2
928	Fire spread/ceiling jet visible along the ceiling	sac cam 6
930	A bottom section of the door fails, leaving a hole	Camera 1
931	Right panel falls off, into the bonfire,	Camera 1
932	Right panel falls into the fire	Camera 2
935	Visible fire spread on the compartment ceiling towards the vent opening	sac cam 4
943	Smoke from the main roof seems to have gotten thicker	Camera 1

Seconds	Phenomenon	Observed By
948	Smoke conditions increases	Camera 2
950	Ceiling jet subsides	sac cam 6
955	Fire intensity in the section above the door decreases after panel falls	Camera 1
1007	Left panel above the door falls into the fire	Camera 2
1086	sac cam 8 view is cleared, door is fully involved	sac cam 8
1114	sac cam 4 footage interrupted	sac cam 4
1119	sac cam 6 footage interrupted	sac cam 6
1121	sac cam 8 footage is interrupted	sac cam 8
1131	Brief flame appears in the turf on the AB corner of the hut	Camera 1
1148	Bottom 1/3 of the door is completely burnt out	Camera 2
1153	Most of the bottom of the door has smoldered through by now	Camera 1
1165	Camera 1 clip 1 ends	Camera 1
1165	Camera 1 clip 2 starts	Camera 1
1170	Camera 2 clip 1 ends	Camera 2
1175	Smoke from the main roof and chimney has lightened significantly	Camera 1
1186	sac cam 2 footage resumes, door and sofit have failed and vented	sac cam 2
1187	Camera 2 clip 2 starts	Camera 2
1192	sac cam 4 footage resumes	sac cam 4
1196	Bottom 1/3 of the door is completely burnt out	Camera 1
1200	sac cam 6 footage resumes, conditions are clear	sac cam 6
1200	Bottom of door is on fire, smoldering in the ceiling, but no flames	sac cam 2
1207	sac cam 8 footage resumes, smoldering visible in the corridor ceiling	sac cam 8
1214	sac cam 4 fails	sac cam 4
1248	Fire is piled by FF	Camera 1
1256	Turf on the bottom layer of the AB corner ignites, shortlived	Camera 1
1273	Fire is piled with shovel by FF	Camera 2
1285	New fuel is added	Camera 1
1297	new kindling is added to the fire by FF	sac cam 2

Seconds	Phenomenon	Observed By
1305	FF knocks out bottom half of the door while adding fuel	Camera 1
1309	More fuel is added	Camera 2
1337	sac cam 8 is buried by kindling	sac cam 8
1339	Part of the door is knocked out while fuel is added	Camera 2
1340	Bonfire grows significantly	Camera 1
1347	Fire spread along the B side wall	sac cam 6
1352	Minor Fire spread along the left corridor wall	sac cam 2
1372	Sections of the gable have vented, left panel is missing	Camera 1
1381	Light smoke seeping through the turf	Camera 1
1421	sac cam 8 fails	sac cam 8
1706	Fire appears to have died down a lot	Camera 1
1753	New fuel is added, The entire door is knocked out in the process	Camera 1
1777	More fuel is added	Camera 2
1795	What is left of the door collapses when FF adds fuel to the fire	sac cam 2
1821	Rest of the door is broken as FF adds fuel	Camera 2
1856	Significant fire growth in the door way	Camera 1
1861	Camera 2 is knocked over and now faces the ceiling of the main compartment	sac cam 2
1871	Smoke seeping from the ceiling increases significantly	Camera 1
1871	Pine branch is shoved into the corridor	Camera 2
1873	Flames visible in the corridor ceiling through the gable	Camera 1
1876	Onset of flashover	sac cam 2
1878	fire spread on the ceiling	sac cam 6
1880	fire spread rapidly accelerates	sac cam 6
1883	All fuel in the corridor is fully involved	Camera 1
1887	Autoignition of C-side ceiling	sac cam 6
1891	Thick yellowish smoke emanating from the roof, indicating pos. flashover	Camera 1
1891	Rapid fire spread on the ceiling	sac cam 2
1896	Heavy fire extending out of the top of the corridor	Camera 1
1898	Ceiling is fully involved	sac cam 6

Seconds	Phenomenon	Observed By
1899	Smoke increases	Camera 2
1901	Fire spread along B-side wall	sac cam 6
1905	Flames visible in the corridor ceiling	Camera 2
1908	Minor fire spread down the far wall	sac cam 2
1909	Fire intensity decreases a little bit	Camera 1
1914	Flames push out of the gable	Camera 2
1927	Corridor roof appears to sag.	Camera 1
1932	Flashover subsides	sac cam 2
1935	Flashover subsides, fire and smoldering are visible on the C-side wall and ceiling	sac cam 6
1943	Fire intensity appears to decrease, bad visibility due to smoke	Camera 2
1943	some flames and widespread smoldering visible on the ceiling	sac cam 6
1958	Smoke condition lightens, fire intensity has decreased significantly	Camera 1
2010	Ceiling flames subside, smoldering continues all over the ceiling	sac cam 6
2052	sac cam 2 fails	sac cam 2
2233	Some flames visible in the corridor ceiling	Camera 1
2420	Low intensity fire	Camera 2
2423	More fuel is added	Camera 1
2450	New fuel is added	Camera 2
2494	No more smoldering visible on the ceiling	sac cam 6
2515	Large pine bundle is added	Camera 1
2576	Bonfire intensity increases slowly, but not by much	Camera 1
2604	Fire intensity increases somewhat	Camera 2
2955	Camera 1 clip 2 ends	Camera 1
2977	Camera 2 clip 2 ends	Camera 2
2987*	Camera 1 clip 3 starts, low intensity bonfire, corridor ceiling sagging a lot	Camera 1
2987	Camera 2 clip 3 starts	Camera 2
2993*	Last support from the corridor gable collapses	Camera 1
2995	Last support from the corridor gable collapses	Camera 2
3219*	Fire continues to burn at low intensity	Camera 1
3355*	Turf on the bottom AB corner auto ignites briefly	Camera 1

Seconds	Phenomenon	Observed By
3418	Camera 2 clip 3 ends	Camera 2
3451*	Seeping smoke through the roof has more or less ceased	Camera 1
3615*	FFs Get picture taken	Camera 1
3651*	More fuel is added (Thick logs)	Camera 1
3738*	Pine branches are added	Camera 1
3757*	Bonfire grows significantly	Camera 1
3758	Ceiling jet develops, onset of second flashover	sac cam 6
3776*	Doorway is fully involved	Camera 1
3778*	Increased smoke production, yellowish smoke seeping through turf	Camera 1
3788	Ignition 2	LabView
3791*	Heavy fire in the corridor	Camera 1
3808*	Possible minor flame spread on the roof, centrally located	Camera 1
3816	flashover subsides	sac cam 6
3821*	heavy fire subsides	Camera 1
3829	intermittent flames visible on the ceiling	sac cam 6
3846*	Heavy smoke envelopes the structure, decreasing visibility significantly	Camera 1
3896*	Less smoke. Low intensity bonfire visible.	Camera 1
3928	sac cam 6 fails	sac cam 6
4727*	Camera 2 clip 4 starts, fuel is in the doorway	Camera 2
4777*	Camera 1 clip 3 ends	Camera 1
4809*	FF stuffs the doorway with a shovel, fire continues to be rearranged	Camera 2
4851*	Heavy fire in the corridor	Camera 2
5027*	Camera 1 clip 4 starts	Camera 1
5028*	Camera 1 clip 4 ends	Camera 1
5207*	More fuel is added	Camera 2
5299*	Heavy smoke develops	Camera 2
5327*	Camera 1 clip 5 starts	Camera 1
5353*	Fire growing in the fuel	Camera 1
5368*	FF stuffs the doorway with a shovel, fire continues to be rearranged	Camera 1
5393*	Doorway is stuffed to the brim	Camera 2

Seconds	Phenomenon	Observed By
5489*	Fire grows taller than the doorway	Camera 1
5588*	FFs stop adding fuel	Camera 2
5607*	More fuel is added	Camera 1
5757*	People throw fuel at the fire	Camera 2
5789*	FF rearange fire, wearing SCBA, adding fuel continuously	Camera 1
5875*	Intense fire in the doorway	Camera 1
6022*	Camera 2 clip 4 ends	Camera 2
6062*	Increased smoke production	Camera 1
6601*	Camera 1 clip 4 ends	Camera 1

References

[1] S. B. Hafsteinsson, "Museum politics and turf-house heritage," *Journal of Cultural Preservation*, vol. 12, no. 3, pp. 78–88, 2010.

[2] S. B. Hafsteinsson and M. G. Jóhannesdóttir, "dirt hovels and cultural heritage: The eradication and inheritance of the icelandic turf house," *Vernacular Architecture*, vol. 54, no. 1, pp. 70–87, 2023.

[3] C. Zhang, "Review of structural fire hazards, challenges, and prevention strategies," *Fire*, vol. 6, p. 137, 2023. [Online]. Available: https://doi.org/10.3390/fire6040137

[4] B. Chorlton and J. Gales, "Fire performance of cultural heritage and contemporary timbers," *Engineering Structures*, vol. 201, p. 109739, 2019.

[5] A. Otto *et al.*, "Mass heritage timber performance in fire," *6th International Structural Specialty Conference at CSCE Annual Conference*, 2017.

[6] L. Yang *et al.*, "Full-scale fire experiment of timber buildings in rural areas of southwest china," *International Journal of Architectural Heritage*, vol. 17, no. 9, pp. 1505–1524, 2023.

[7] P. Wei *et al.*, "Full scale test on fire spread and control of wooden buildings," *Procedia Engineering*, vol. 11, pp. 355–359, 2011.

[8] Q. Dong *et al.*, "Investigation of fire protections status for nanjing representative historical buildings and future managements measures," *Procedia Engineering*, vol. 71, pp. 377–359, 2014.

[9] A. Garcia-Castillo *et al.*, "Fire in heritage and historical buildings, a major challenge for the 21st century," *Developments in the Built Environment*, vol. 13, p. 100102, 2023.

[10] W. R. Short, "Personal communication with the author," 2025, private conversation. Not publicly available.

[11] P. Pulsiano, *Medieval Scandinavia: an encyclopedia*. Taylor & Francis, 1993, vol. 1.

[12] W. R. Short, *Icelanders in the Viking Age*. McFarland, 2010.

[13] W. R. Short and R. A. Óskarson, *Men of Terror: A Comprehensive Analysis of Viking Combat*. Westholme Publishing, LLC, 2021.

[14] A. Wawn, "The saga of the people of vatnsdal," *The Complete Sagas of Icelanders Including 49 Tales: IV Regional Feuds*, p. 60, 1997.

[15] P. Acker, *The Saga of the People of Floi*. unknown, unknown, vol. 3, chronicles the history and legends of the Floi region and its people.

[16] A. Maxwell, *The Saga of the People of Reykjadal and of Killer-Skuta*. unknown, unknown, vol. 4, a detailed account of the people of Reykjadal and the infamous Killer-Skuta.

[17] “Brennu-njáls saga, chapter 129,” a climactic chapter in one of Icelands most famous sagas.

[18] “Eyrbyggja saga, chapter 31,” describes the history and legends of the inhabitants of Eyr and the surrounding area.

[19] “Hænsna-Þóris saga, chapter 9,” a tale centered on the disputes and trials of Hænsna-Þórir in medieval Iceland.

[20] “Króka-refs saga, chapter 10,” the story of Króka-Ref and his cunning strategies and adventures.

[21] “Brennu-njáls saga, chapter 19,” a prominent Icelandic saga detailing the feuds and legal disputes in medieval Iceland.

[22] “Gull-Þóris saga, chapter 18,” a saga exploring the life and exploits of Gull-Þórir.

[23] L. M. Larson, *The earliest Norwegian laws: being the Gulathing law and the Frostathing law*. New York: Columbia University Press, Ltd., 1935.

[24] G. Karlsson, K. Sveinsson, and M. Árason, *Grágás: lagasafn íslenska þjóðveldisins*. unknown: unknown, 1992, a compilation of Icelandic laws from the era of the Icelandic Commonwealth.

[25] N. F. P. Association *et al.*, *NFPA® 909, Code for the Protection of Cultural Resource Properties–museums, Libraries, and Places of Worship*. NFPA, 2013.

[26] NFPA, “Nfpa 914: Code for fire protection of historic structures,” 2001.

[27] M. Green, *Building Codes for Existing and Historic Buildings*. John Wiley & Sons, 2011.

[28] Althingi, *Cultural Heritage Act*. Althingi, 2012.

[29] National Fire Protection Association, NFPA 909: Code for the Protection of Cultural Resource Properties–museums, Libraries, and Places of Worship 2021 Edition, Online; Accessed though National Fire Codes.

[30] National Fire Protection Association, NFPA 909: Code for the Protection of Cultural Resource Properties–museums, Libraries, and Places of Worship 2021 Edition, Online; Accessed though National Fire Codes.

[31] International Existing Building Code 2021 Edition, Online.

[32] M. J. Hurley, D. T. Gottuk, J. R. H. Jr., K. Harada, E. D. Kuligowski, M. Puchovsky, J. L. Torero, J. M. W. Jr., and C. J. WIECZOREK, “Sfpe handbook of fire protection engineering,” 2016.

[33] V. Hreinsson, R. Cook, and P. L. Acker, *The complete sagas of Icelanders: including 49 tales*. Leifur Eiríksson Reykjavík:, 1997, vol. 5.

[34] “Brennu-njáls saga, chapter 119,” another pivotal moment in the saga of Brennu-Njál.

[35] “Gísla saga, chapter 3,” a tragic tale of the outlaw Gísli Súrsson.

[36] D. A. Purser and J. L. McAllister, "Assessment of hazards to occupants from smoke, toxic gases, and heat," *SFPE handbook of fire protection engineering*, pp. 2308–2428, 2016.

[37] N. A. Martin and S. Falder, "A review of the evidence for threshold of burn injury," *Burns*, vol. 43, no. 8, pp. 1624–1639, May 2017.

[38] G. Ólafsson, "Eiríksstaðir í haukadalur fornleifarannsókn á skálarúst (archaeological investigation of a hut ruin)," 1998.

[39] R. Gardon, "An instrument for the direct measurement of intense thermal radiation," *Review of Scientific Instruments*, vol. 24, no. 5, pp. 366–370, 1953.

[40] R. A. Miller and H. S. Alpert, "Temperature dependent performance of schmidt–boelter heat flux sensors," *Review of Scientific Instruments*, vol. 94, no. 2, 2023.

[41] B. B. Bohara and A. K. Batra, "Development of multi-functional nano-paint for energy harvesting applications," *Progress in Natural Science: Materials International*, 2018.

[42] C. Fang, "Design and testing of a thin film thermocouple calibrator for aerospace applications," Ph.D. dissertation, Shandong Agricultural University, 2023.

[43] P. Pinto, M. Littin, J. Rivera, G. Severino, J. Cruz, and A. Fuentes, "A simpler tractable contour technique to model thermal radiation from buoyant diffusion flames," *Experimental Thermal and Fluid Science*, vol. 149, p. 111027, 2023.

[44] E. V. Mueller, N. Skowronski, J. C. Thomas, K. Clark, M. R. Gallagher, R. Hadden, W. Mell, and A. Simeoni, "Local measurements of wildland fire dynamics in a field-scale experiment," *Combustion and Flame*, vol. 194, pp. 452–463, 2018.

[45] N. R. Council, *Acute Exposure Guideline Levels for Selected Airborne Chemicals: Volume 8*. Washington, DC: The National Academies Press, 2010.

[46] National Fire Protection Association, NFPA 921: Guide for Fire and Explosion Investigations 2024 Edition, Online; Accessed though National Fire Codes.

[47] National Fire Protection Association, NFPA 72: National Fire Alarm and Signaling Code 2025 Edition, Online; Accessed though National Fire Codes.